

Radiation induced degradation of elastomers.

ADDY, S. W.

Available from Sheffield Hallam University Research Archive (SHURA) at:

<http://shura.shu.ac.uk/19200/>

This document is the author deposited version. You are advised to consult the publisher's version if you wish to cite from it.

Published version

ADDY, S. W. (1987). Radiation induced degradation of elastomers. Doctoral, Sheffield Hallam University (United Kingdom)..

Copyright and re-use policy

See <http://shura.shu.ac.uk/information.html>

ProQuest Number: 10694080

All rights reserved

INFORMATION TO ALL USERS

The quality of this reproduction is dependent upon the quality of the copy submitted.

In the unlikely event that the author did not send a complete manuscript and there are missing pages, these will be noted. Also, if material had to be removed, a note will indicate the deletion.

uest

ProQuest 10694080

Published by ProQuest LLC(2017). Copyright of the Dissertation is held by the Author.

All rights reserved.

This work is protected against unauthorized copying under Title 17, United States Code
Microform Edition © ProQuest LLC.

ProQuest LLC.
789 East Eisenhower Parkway
P.O. Box 1346
Ann Arbor, MI 48106- 1346

RADIATION INDUCED DEGRADATION
OF ELASTOMERS

by

S.W.ADDY.

A thesis submitted to the
council for national Academic
Awards in partial fulfilment
of the Requirements
for the Degree of
Doctor of philosophy

Collaborating Establishment:-

Central Electricity Generating Board
Bedminster Down
Bristol
England

Sponsoring Establishment:-

Department of Metals and
Materials Engineering
Sheffield City Polytechnic

December 1987

Radiation Induced Degradation of Elastomers

by

s.W.Addy

Abstract

An attempt has been made to evaluate the kinetics of the thermal and combined thermal/radiative degradation of a peroxide cured polydimethylsiloxane elastomer (PDMS), and a vinylidene fluoride-hexafluoropropylene elastomer (Viton E60-C), by chemical stress relaxation measurements.

It was observed that the PDMS elastomer degraded thermally by hydrolytic scission of the main chain and chain reformation by condensation of the silanol chain end groups. However, predominant chain reformation was observed during thermal degradation studies and it was believed that this was a consequence of the reformation of chains cut during the test, and also the reformation of chains cut prior to the test in the post cure operation. These two components of the observed chain reformation response were subsequently rationalized by a model.

Thermal degradation of the Viton E60-C elastomer appeared to take place by hydrolytic scission of the amine crosslinkages, and subsequent crosslink reformation by condensation, indicating that the material had not been subjected to a suitable post cure treatment in order to remove water generated by the vulcanization reaction. At temperatures above 200°C predominant crosslinking was observed and this was attributed to the presence of a concurrent reaction which leads to the formation of ring structures.

Thermal/radiative degradation studies indicated that temperature and radiation had a synergistic effect on the overall rate of induced chain scission in the PDMS elastomer but the mechanisms responsible for this phenomenon have yet to be established.

Acknowledgements.

I would like to thank Dr D.W.Clegg and Dr A.T.Collyer for their encouragement and support throughout the project, and Dr G.C.Corfield for his guidance during the early stages of the research programme. I am also indebted to J.Best for his permission to use the γ -irradiation facility at Berkely and P.Crum for her assistance with the irradiation studies.

The assistance of the technical staff of the Department of Metals and Materials Engineering at Sheffield City Polytechnic was essential to the project, especially in those areas concerned with the construction of the stress relaxation rig and the modification of the instron testing equipment.

Contents.

	page no
1. Introduction	1
1.1. Polymers in Nuclear Engineering Applications	2
1.2. The Nuclear Environment	2
1.2.1. Normal Reactor Operation	3
1.2.2. Accident Situation	3
2. Degradation of Polymers Upon Exposure to the Nuclear Environment.	4
2.1. Introduction	5
2.2. Degradation by γ -Radiation	5
2.2.1. General Effects	5
2.2.2. Effects of Molecular Structure on Degradation Mode	8
2.2.3. Factors Influencing Radiative Stability	10
2.2.3.1. Effects of Chemical Structure	10
2.2.3.2. Effects of Additives (Antirads) on Stability	10
2.2.3.3. Effects of Physical Structure	13
2.3. Thermal Degradation	15
2.3.1. General Classification of Reactions	15
2.3.2. Factors Influencing Thermal Stability	20
2.3.2.1. Effects of Chemical Structure on Physical and Chemical Stability	20
2.4. Oxidative Degradation	26
2.4.1. Concept of Autoxidation	26
2.4.2. Factors Influencing Oxidative Stability	29
2.4.2.1. Effects of Chemical Structure	29
2.4.2.2. Effects of Physical Structure	31
2.4.2.3. Effects of Antioxidants or Stabilisers	32

2.5	Hydrolytic Degradation	36
2.6	Degradation of Specific Materials	37
2.6.1.	Degradation of Silicone Elastomers	37
2.6.1.1.	Radiative Degradation Mechanisms	37
2.6.1.1.1.	Effects of Incorporating Aromatic Groups into the Chemical Structure	39
2.6.1.1.2.	Effects of Copolymerisation with Diphenylsiloxane	40
2.6.1.1.3.	Effects of Blending with Polystyrene	40
2.6.1.2.	Thermal Degradation Mechanisms	43
2.6.1.3.	Hydrolytic Degradation Mechanisms	43
2.6.2.	Degradation of Fluorocarbon Elastomers (with reference to vinylidene fluoride - hexafluoropropylene elastomers)	45
2.6.2.1.	Radiative Degradation Mechanisms	45
2.6.2.2.	Thermal Degradation Mechanisms	47
2.6.2.3.	Hydrolytic Degradation Mechanisms	48
3.	Techniques for the Evaluation of Crosslinking and Scission Kinetics in Polymers	49
3.1.	Measurement of Molecular Weight	49
3.2.	Sol / Gel Fraction Measurements	50
3.3.	Equilibrium Stress - Strain Measurements	52
3.4.	Equilibrium Swelling Measurements	56
3.5.	Chemical Stress Relaxation Measurements	57
3.5.1.	Evaluation of Kinetics in Elastomers Degrading by Irreversible Main Chain Scission Reactions.	57
3.5.2.	Evaluation of Kinetics in Elastomers Degrading by Irreversible Scission of the Crosslinkages.	62

3.5.3.	Determination of the Site of the Scission Reaction in Degrading Elastomers.	63
3.5.3.1.	Technique Proposed by Tobolsky	63
3.5.3.2.	Empirical Technique Proposed by Osthoff et al	64
3.5.4.	Evaluation of Degradation Kinetics of Elastomers undergoing Simultaneous Scission and Crosslinking Reactions	66
3.6.	Sol / Gel Fraction Measurements in Conjunction with Chemical Stress Relaxation Measurements	69
4.	Aspects of Irradiation Studies on Polymers	71
4.1.	Basic Definition of Absorbed Dose and Units of Measurement	71
4.2.	Radiation Sources	72
4.3.	Dosimetry	73
4.4.	The Concept of Radiation Yield	73
5.	Experimental	74
5.1.	Materials	74
5.1.1.	Materials Selection	74
5.1.2.	Materials Preparation	75
5.1.2.1.	Preparation of Peroxide - Cured PDMS elastomer	75
5.1.2.2.	Preparation of Viton E60-C Elastomer	77
5.1.2.3.	Preparation of PDMS Elastomer Containing Entrapped PS	79
5.1.3.	Materials Characterisation	79
5.1.3.1.	Characterisation of PDMS and Viton E-60C Elastomers	79
5.1.3.2.	Characterisation of PDMS Elastomer Containing Entrapped PS	80
5.2.	Experimental Procedure	81
5.2.1.	Physical Stress Relaxation Studies on PDMS and Viton E-60C Elastomers	81

5.2.2.	Thermal Degradation Studies	82
5.2.2.1.	Chemical Stress Relaxation Studies on PDMS and Viton E60-C Elastomers	82
5.2.2.2.	Cure / Post Cure Trials on PDMS Elastomer	83
5.2.3.	Combined Thermal / Radiative Degradation Studies	84
5.2.3.1.	Chemical Stress Relaxation Studies on PDMS and Viton E60-C Elastomers	84
6	Results	87
6.1.	Characterisation of PDMS and Viton E60-C Elastomers	87
6.2.	Characterisation of PDMS elastomer Containing Entrapped PS	88
6.3.	Physical Stress Relaxation Studies on PDMS and Viton E60-C Elastomers	88
6.4.	Thermal Degradation Studies	90
6.4.1.	Chemical Stress Relaxation Studies on PDMS Elastomer	90
6.4.2.	Chemical Stress Relaxation Studies on Viton E60-C Elastomer	95
6.4.3.	Cure / Post Cure Trials on PDMS Elastomer	96
6.5.	Combined Thermal / Radiative Degradation Studies	96
6.5.1.	Chemical Stress Relaxation Studies on PDMS Elastomer	96
6.5.2.	Chemical Stress Relaxation Studies on Viton E60-C Elastomer	97
7.	Discussion	98
7.1.	Characterisation of PDMS and Viton E60-C Elastomers	98
7.2.	Characterisation of PDMS Elastomer Containing Entrapped PS	103
7.3.	Physical Stress Relaxation Studies	105
7.4.	Thermal Degradation Studies	108
7.4.1.	PDMS Elastomer	108

7.4.2.	Viton E60-C Elastomer	1
7.5.	Combined Thermal / Radiative Studies	1
7.5.1.	PDMS Elastomer	1
7.5.2.	Viton E60-C Elastomer	1
8.	Concluding Remarks	1
9.	Recommendations for Further Work	1
	References	1
	Tables	1
	Figures	1
	Plates	2

1. Introduction.

The degradation of polymers by various stresses, ie temperature, γ -radiation, oxygen, H₂O, etc, have received considerable attention with the result that the degradation mechanisms of a wide variety of polymers are well documented. Consequently, the relationships between the chemical and physical structures of polymers and their stability towards a particular stress have been well established, together with methods of enhancing stability. These intensive investigations have also led to the development of a host of techniques for the evaluation of the degradation kinetics of polymers.

In view of the above it is surprising to discover that studies of the degradation kinetics of polymers during service in nuclear reactor installations has received relatively little attention, in spite of the fact that the stresses which are operative under these conditions are known.

The aims of the present investigation are to investigate the degradation mechanisms which are operative in specific elastomers when they are subjected to the combined stresses of temperature and γ -radiation. It is believed that such an approach will lead to a more accurate prediction of the performance of polymer components during service in a nuclear reactor, and also lead to the development of more suitable materials.

1. Polymers in Nuclear Engineering Applications.

Nuclear reactor installations contain a surprisingly large number of components which utilise the peculiar electrical and mechanical properties of polymers. Their variety can be appreciated by reference to Table 1.1. which lists the components to be found in a typical water-cooled fission reactor. These components are essential not only for the successful routine operation of the reactor but also for the provision of emergency shutdown procedures in the event of a nuclear incident⁽¹⁾. Under such conditions components must remain functional, monitoring and containing the radioactive species, until the radiation has fallen to an acceptable level.

Safe reactor operation is dependent on the accurate prediction of component performance during service. It is now appreciated that such information can only be obtained from a knowledge of the degradation reactions taking place in the materials and their subsequent effects on the relevant properties. The degradation kinetics are governed by the environment in which the components function.

1.2. The Nuclear Environment.

In the active zone of the reactor the absorbed dose rate of the radiation is in the region of 10^{12} rad hr⁻¹ and prohibits the use of polymeric materials in close proximity to the reactor core. Consequently polymer components are restricted to the containment area of the reactor complex.

1.2.1. Normal Reactor Operation.

During normal operation the radiation environment in the containment area consists of γ -rays and neutrons which escape through the wall of the reactor core. The γ -ray energy spectrum may be in the region of a few KeV to about 8 MeV depending on the specific design of the reactor. The absorbed dose rate ranges from 10 to 100 rad hr⁻¹ having an average value of 50 rad hr⁻¹. Taking a design value of 40 years for the operational lifetime of the reactor components will receive an estimated integrated dose of approximately 2×10^7 rad. Throughout this period the temperature is ambient ($\approx 50^\circ\text{C}$) and the relative humidity maintains a value of approximately 90%.

1.2.2. Accident Situation.

Accidents of various degrees could occur during reactor operation the worst possible being a loss of coolant accident (LOCA)⁽¹⁾. This would result in complete vaporization of the core. Under these extreme conditions the release of fission products would occur and continue until the system is cooled down by the emergency cooling facility. The dose rate would vary with time during this period but could reach a maximum of about 10^7 rad hr⁻¹ after a few seconds.

In addition to the radiation, the environment will consist of steam at high pressure, and a continuous spray of chemical solutions, such as boric acid and sodium hydroxide. After 'shut down' the dose rate would gradually decay over a period of about 1 year. During this time the integrated absorbed dose could reach levels as high as 5×10^8 rad.

2. The Degradation of Polymers Upon Exposure to the Nuclear Environment.

2.1. Introduction.

It is apparent from the description of the nuclear environment presented in the previous section that the degradation of polymer components during service is highly complex. Both thermal and radiative degradation may occur simultaneously, and the kinetics of these reactions may be influenced by the presence of oxygen. There is also the possibility of concurrent hydrolytic degradation. The occurrence of any of these mechanisms, and their contribution to the overall degradation kinetics is dependent on the chemical structure of the polymer and its physical state.

2.2. Degradation by γ -Radiation.

2.2.1. General Effects.

γ -radiation is regarded as a form of high energy radiation as a consequence of the energies of its photons, which lie in the region of 1 MeV. By comparison the energies of photons associated with visible and UV radiation, those responsible for the photodegradation of polymers, are far lower having values of 4-5 eV. These energies are comparable with bond energies found in typical polymer structures. For example, the strengths of C-C and C-H bonds are approximately 420 and 340 KJ mol⁻¹ respectively.

The effects of γ -radiation and low energy radiation (visible and UV) on polymers are significantly different. Photodegradation is highly selective. The photons are absorbed only at appropriate chromophoric groups in the structure. The energy which is imparted by the photons is redistributed according to well defined rules, and the bonds which are finally broken are usually in the vicinity of the site of absorption.

By contrast, the most significant effects of high energy radiation arise from the interaction of incident photons with the orbital electrons of the polymer molecule in a more or less random fashion. The possible subsequent reactions which may take place are presented in Fig 2.1. (2a).

In losing its energy in a succession of interactions each photon excites a number of electrons as in reaction 1. If the excitation energy is less than the ionisation energy, the excited molecule may dissociate into radicals (reaction 2), otherwise ionisation will occur

(reaction 3). The positive ion radicals may subsequently react with a free electron to reform an excited molecule (reaction 4) or they may decompose to form a radical and a positive ion (reaction 5). The electrons may react with polymer molecules to form negative ion radicals (reaction 6) which decompose to form a radical and a negative ion (reaction 7).

In reality, the overall picture is very much more complex than indicated in Fig 2.1. For example, charge and energy transfer processes occur and ions are destroyed in ion-ion and ion-electron interactions. Ionic degradation mechanisms have been detected in several systems and are characterised by a temperature dependence of the relevant reaction kinetics^(3a-5). However, it is now generally accepted that the predominant mechanisms which are operative during the radiative degradation of polymers are radical in nature⁽⁶⁾.

The possible radical reactions which may take place upon exposure to γ -irradiation can be classified as follows:-

- (i) A polymer radical may be formed by cleavage of a bond in the pendant groups attached to the main chain. Usually a hydrogen atom is split off which leads to the formation of a hydrogen radical. However it is also possible for low molecular weight radicals to be generated in some cases. Further cleavage of a bond in an adjacent pendant group leads to the formation of a lateral bond or crosslink, and in the case of hydrogen radical generation, the formation of a hydrogen molecule by the following steps (P and P' denote respectively the polymer and polymer radical):-





The interaction of low molecular weight radicals, if present, with each other, or with available hydrogen radicals results in the formation of volatile low molecular weight products

- (ii) A polymer radical may be formed by cleavage of the main chain by the following mechanism :-



Subsequent interaction of these radicals with any of those generated by the previous mechanism leads to the formation of a trifunctional crosslink. Stabilisation of the radicals is also possible by interaction with hydrogen radicals or other low molecular weight radicals that may be present.

- (iii) Radicals may be formed by the action of radiation on other components present in the system excluding the main polymer. These may be additives or impurities, etc. Such reactions are termed indirect reactions.
- (iv) If irradiation is carried out in the presence of oxygen peroxide radicals may be formed. (The formation of these radicals and their participation in degradation reactions is discussed in Section 2.4.).

As a consequence of these reactions polymers undergo significant physical changes during irradiation. Changes in physical and mechanical properties, such as viscosity and shear modulus are observed, and extreme effects may induce phase changes in the polymer.

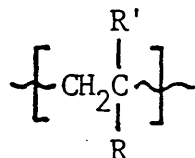
The results of numerous early studies of the radiation induced changes in the physical properties of a wide range of polymers have been collated independently by Charlesby⁽⁷⁾ and Lauton et al⁽⁸⁾. It was discovered that the majority of polymers fall into one of two categories depending on their response to γ -radiation. Some undergo predominant scission reactions and are characterised by a reduction in the number average molecular weight. Others crosslink with little, if any, accompanying scission reactions. These polymers are characterised by a progressive increase in the number average molecular weight, and ultimately develop into an insoluble three dimensional network or gel. The responses of some of the more common polymers reported in the above reviews are given in Table 2.1. A notable exception to this classification is polyvinylchloride since it has been reported to undergo crosslinking, and scission reactions by various authors.

It must be stressed that this grouping is not absolute as the response of a given polymer depends upon the specific conditions employed during irradiation. For example, the presence of oxygen may promote the scission reaction in some polymers. (The influence of oxygen on degradation kinetics is considered in Section 2.4.).

2.2.2. Effects of Molecular Structure on Degradation Mode.

From studies to date it has become apparent that particular features of the molecular structure determine whether degradation takes place by scission or crosslinking reactions. The general observations may be summarised as follows:-

- (i) All vinyl polymers in which chain scission predominates have the following structure⁽⁹⁾:-



There is no hydrogen atom on the side group R but an α -substituent such as CH_3 , Cl, F, etc. It has been proposed that this substituent induces a steric strain which weakens the C-C bond of the main chain making it susceptible to scission.

- (ii) In branched chain hydrocarbon polymers scission appears to be predominant.
- (iii) If the polymer chain is predominantly a C-O repeating group, as in the case of polyacetal, then degradation takes place by rapid chain scission.
- (iv) The presence of C-O linkages in a group which bridges the main polymer chain, as in polyvinylbutyral and polyvinylformal, appears to induce rapid main chain scission.
- (v) Some degree of correlation between bond energies and mode of degradation has been observed by Wall⁽¹⁰⁾ who found a tentative relationship between heats of polymerisation and the tendency to undergo scission or crosslinking reactions. Generally, it was observed that those polymers with high heats of polymerisation crosslink, and those with low values undergo chain scission. It should be noted that there are many exceptions to this rule, polystyrene and polyisobutylene being two examples. This is not surprising as an explanation solely

relying on bond energies as a criterion is an oversimplification. The reactivity of the radicals generated in the polymer during irradiation and their subsequent mobility must also be considered.

2.2.3. Factors Influencing Radiative stability.

2.2.3.1. Effects of Chemical Structure.

Many attempts have been made to correlate the molecular structure of polymers with their radiative stability. The most comprehensive review of work in this area has been carried out by Sisman and Bopp⁽¹¹⁾. The results of their findings are presented in Table 2.2. in which the polymers are ranked in order of decreasing radiative stability. It was discovered that the most resistant structures are those that incorporate high concentrations of aromatic groups.

This phenomenon is due to the fact that the aromatic ring structures act as 'energy sinks'. During irradiation the incident energy is preferentially absorbed by the groups and as a result they are transformed to higher energy vibration modes. Subsequently this energy is dissipated as harmless heat energy. Thus the formation of an excited polymer molecule and any subsequent degradation reactions are prevented.

2.2.3.2. Effects of Additives (Antirads) on Stability.

The preceding section suggests that there may be a possibility of enhancing the radiative stability of a polymer by the introduction of compounds of high conjugation. One of the first workers to demonstrate experimentally that the use of certain aromatic additives prevent, to a large extent, the structural and property changes encountered in polymers

during exposure to γ -radiation was Wundrich⁽¹²⁾. The protection of polymethylmethacrylate by a series of compounds with a range of resonance energies (conjugation energies) was evaluated. The dependence of the degradation yield* on the content of benzene, naphthalene, phenanthrene, anthracene, pyrene, and benz- (α) -anthracene in the polymer in the polymer is shown in Fig 2.2. It was observed, as can be seen by reference to Table 2.3⁽¹³⁾ that the degradation yield for a given concentration of additive decreases with increasing resonance energy of the compound. Furthermore, it was found that the quantities $G_0/(G - 1)$ and % mole of additive present are linearly related (with the exception of phenanthrene).

Similar conclusions have been drawn from an examination of the protective action of polystyrene, naphthalene, anthracene, and phenanthrene on polyethylene. Radiation yields in these investigations were estimated from the volume of hydrogen evolved, and are presented in Fig 2.3.⁽¹⁴⁾ Again the effectiveness of the additives appears to be proportional to their conjugation.

The incorporation of aromatic compounds results in moderate increases in stability. Far greater resistance can be imparted to a polymer by the addition of substances that preferentially react with any radicals generated during irradiation before they can participate in subsequent degradation reactions.

* the radiation yield is defined in Section 4.4.

These additives inhibit degradation by acting in one of the following ways:-

- (i) Restoring the initial polymer molecule, from which the free radical was formed.
- (ii) De-activating free radicals by the formation of a new stable compound.
- or (iii) Forming new radicals which have a lower reactivity.

The introduction of compounds having effective donor and acceptor properties with respect to hydrogen atoms are particularly successful in increasing stability. Compounds which possess these properties are in effect a continuously working store of hydrogen. Hydrogen atoms are transferred to newly formed radicals resulting in protection by either of conditions (i) or (ii) described above. Simultaneously, the ability of the additive to accept hydrogen leads to the capture of the hydrogen atom that has been split off resulting in its replenishment so that it can offer further protection. A typical example of additives with these properties are sulphhydryl compounds^(3b).

Evidence of protection by hydrogen donation has been provided by Geymer⁽¹⁴⁾. He studied the influence of a wide range of compounds, distinguished by the lability of their hydrogen atoms, on the radiation induced crosslinking of polypropylene. The results, consisting of intrinsic viscosity and gel fraction measurements, are presented in Table 2.4.

It can be seen that there is a general trend between the effectiveness of these compounds and the bond strength of their most labile hydrogen atom. For example, isopropyl alcohol is an effective crosslink inhibitor, but tert-butyl alcohol, which contains strongly bound hydrogen

atoms, does not show any protective action.

Special reference must be made to the successful utilisation of certain sulphur and nitrogen containing compounds as radiation stabilisers. These include amino-alkane thiols and amino-alkyl thiols, thiourea and guanidine derivatives, dithio-carbamates, thiazolidines, and amino-disulphides.

Significant levels of radiation protection can be attained by the addition of compounds which are highly effective free radical acceptors. Various compounds of sulphur and free sulphur have been found to be highly effective in some polymers⁽¹⁵⁻²¹⁾. Garret and Ormerod⁽¹⁹⁾ demonstrated that the addition of colloidal sulphur to a polyvinylsiloxane led to a marked decrease in the free radical concentration during irradiation and an increase in the absorbed dose required to give incipient gelation. Increases in the radiation stability of other polysiloxanes and butadiene rubbers in the presence of sulphur has been observed⁽¹⁷⁾.

2.2.3.3. Effects of Physical Structure.

Early investigations by many authors have established that the initial physical state of the polymer has a significant influence on chemical and physical changes incurred during γ - irradiation⁽²²⁻³⁰⁾. These phenomena have been explained in terms of the mobility of induced radicals as this factor governs the rate of subsequent radical interaction.

A sharp decrease in the crosslink formation yield has been observed in a wide range of materials when irradiation is carried out at temperatures below the glass transition⁽³¹⁻³⁴⁾. It is believed

that this reduction is due to severe restrictions imposed upon radicals in the glassy state thus preventing possible crosslink formation. This hypothesis is substantiated by experimental evidence⁽³⁵⁻³⁷⁾ of the build up of unreacted radicals in polymers irradiated in the vitreous and crystalline states. Once generated these frozen in radicals can become mobile and participate in degradation reactions after irradiation, if the polymer undergoes a transformation to a state of greater radical mobility. For example, such a change may be induced by a subsequent increase in temperature.

These post irradiation effects are most pronounced in the case of materials that are prone to oxidation if they are heated in air after being irradiated in vacuum^(3c). This is because degradation is enhanced not only by increased radical mobility but also by an increase in the rate of oxygen diffusion into the material (Section 2.4.1.2.).

2.3. Thermal Degradation.

2.3.1. General Classification of Reactions.

Although there are a large variety of degradation reactions which may be thermally induced in polymers Grassie⁽³⁸⁾ demonstrated that they may be categorised into two general types, namely, depolymerisation, and substituent reactions.

All depolymerisation reactions have an underlying feature, irrespective of the detailed reaction mechanism, in that degradation results in progressive cleavage of the main backbone chain. At any intermediate stage in such a reaction the products will consist of the same monomer units as the parent material.

It has been observed that thermal degradation takes place by radical depolymerisation reactions in a large variety of addition polymers. However, detailed studies, especially those of Shima and Wall,⁽³⁹⁻⁵⁵⁾ suggested that more than one radical mechanism was operative. The materials investigated exhibited widely different degradation kinetics and yielded a variety of degradation products. For example, the degradation of polymethylmethacrylate results in almost quantitative conversion to monomer and is accompanied by a slow decrease in molecular weight. Conversely, the molecular weight of polyethylene decreases rapidly and the products consist of long chain olefinic fragments.

It was established that both these extreme cases and all intermediate behaviours can be described by the single depolymerisation mechanism presented below⁽⁵⁶⁻⁵⁹⁾:-

- (i) Initiation. This involves the splitting of the chain to form radicals, and may occur at the chain ends, at the impurities in the chain structure, or randomly along the main chain.

random initiation



terminal initiation

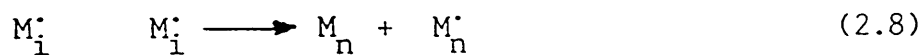


- (ii) Depropagation. The process in which monomer is produced. It is the exact reverse of propagation in the polymerisation reaction.



- (iii) Transfer reactions. Reactions in which a long-chain radical attacks another chain (intermolecular) or itself (intramolecular) resulting in fragments larger than monomer, and subsequent main chain scission.

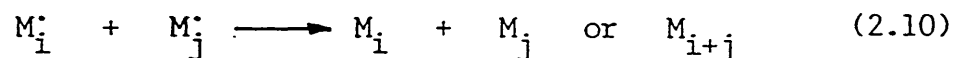
transfer



scission



(iv) Termination. Here radicals are destroyed. It is believed to be analogous to the mutual termination process which occurs in radical polymerisation, although there is no definite evidence whether combination or disproportionation takes place.



In the above reactions n is the chain length of the starting material, and $M_i, M_j, \text{etc.}$, and $M_i^{\cdot}, M_j^{\cdot}, \text{etc.}$, represent respectively 'dead' polymer molecules, and long chain radicals that are $i, j, \text{etc.}$ monomer units in length.

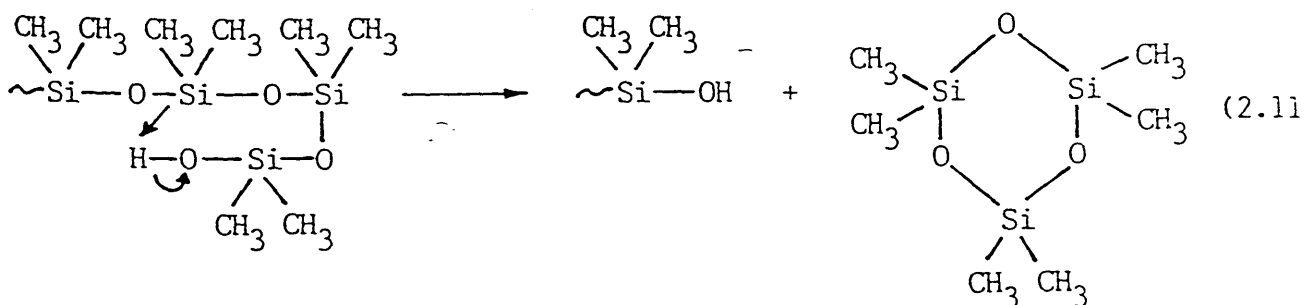
These extensive investigations⁽³⁹⁻⁵⁵⁾ led to some quantitative correlations between the chemical structure of the polymer and the nature of the depolymerisation reactions that take place. In general, the relative importance of depropagation and transfer reactions to the overall reaction mechanism depends, principally, on two factors, the reactivity of the degrading polymer radical, and the lability of reactive pendant atoms (usually hydrogen) in the polymer structure.

Low lability of reactive atoms, and low radical reactivity favour depropagation, which is characterised by systematic cleavage of the backbone or 'unzipping' to yield monomer. Conversely, conditions of high radical reactivity and weakly bonded substituent atoms promote random scission of the main chain by transfer reactions, resulting in high molecular weight decomposition products.

It is now apparent that the stabilising effect of carboxy unsaturation is responsible for the complete predominance of the depropagation reaction in polymethylmethacrylate. The benzene ring present in polystyrene offers less stability resulting in competing depropagation and transfer reactions. The influence of radical stability may be emphasised further by a comparison of the behaviours of polyethylene and polypropylene with the polydienes. The hydrogen atom availability of the two groups of polymers is comparable, but the overwhelming transfer observed in the former, due to the high radical activity, gives way in the latter to a significant proportion of depropagation, as a result of the increased radical stability conferred by the α -unsaturation.

The far greater strength of the C-F bond over the C-H bond is reflected in the fact that the transfer process, which dominates the polyethylene degradation reaction, is totally absent in the thermal decomposition of polytetrafluoroethylene.

Depolymerisation may take place in some systems by non-radical reactions. A notable example is the high temperature (+300°C) degradation of polysiloxanes. Recent studies by Grassie⁽⁶⁰⁾ revealed that the terminal hydroxyl groups in these structures played a key role in thermal degradation. The following transfer process resulting in the formation of a range of cyclic structures is now generally accepted:-



Reaction of the hydroxyl group at a point further from the chain end will lead to a higher oligomer product by this mechanism.

Other examples of non-radical depolymerisation which are of technological importance are the initial stage in the degradation of polyesters, involving an alkyl-oxygen scission reaction^(2b), and the initial depolycondensation of polyurethanes.^(2c)

Substituent reactions cover the broad range of reactions in which the pendant groups that are attached to the main chain are involved. These reactions will occur in any given system only if they can be initiated at temperatures lower than those at which main chain bonds are broken. Hence, such reactions are observed at relatively low temperatures. In contrast, thermal depolymerisation reactions seldom take place below 200°C even if the conditions are favourable.

Particular systems of interest include the decomposition of the ester group in polyvinylacetate and the higher polymethylmethacrylates, for example iso-propyl, sec-butyl, and tert-butyl, and the thermal degradation of polyvinylchloride.

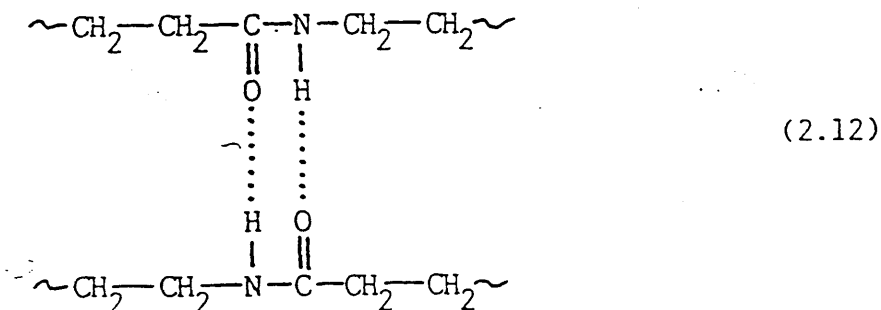
Some polymers undergo a particular type of substituent reaction termed cyclization and elimination. These reactions, which take place in materials such as poly-N-methylmethacrylamide, polymethylvinylketone, polymethylisopropenylketone, and polymethacrylic acid, involve cyclization reactions between adjacent substituents on the main chain with the elimination of a small molecule.

3.2. Factors Influencing Thermal Stability.

2.1. Effects of Chemical Structure on Physical and Chemical Stability.

The criterion for the thermal stability of a polymer is usually defined in terms of the retention of its mechanical properties. Deleterious property changes may be brought about by reversible or irreversible processes. Reversible processes include softening, melting, and other phase transformations such as T_g , etc. Irreversible processes are those which involve chemical degradation reactions, such as chain scission, crosslinking, etc.

Increased thermal stability may be realised to a limited extent by the prevention or retardation of irreversible processes. This can be achieved by modifying the chemical structure of the polymer to promote stronger intra-, and inter-molecular attractions. An example of promoting chain interaction is by the introduction of polar groups. A comparison of the structures of polyethylene and the nylons reveals that the nylons may be regarded as polyethylene with regularly distributed pendant polar groups. Strong chain interaction occurs at these groups through the following hydrogen bonding mechanism:-



This factor is responsible for the superior properties of nylon 6,6 and has led to its application as an engineering material at much higher temperatures than polyethylene. (T_m and T_g are respectively, 540K and 333K for nylon, and 410K and 188K for polyethylene.).

Far greater improvements in thermal stability are attained by modification of the chemical structure in order to prevent or retard possible thermal degradation reactions. This can be achieved by the elimination of weakly bonded pendant groups (especially hydrogen atoms) or by the introduction of stabilising aromatic structures into the polymer molecule.

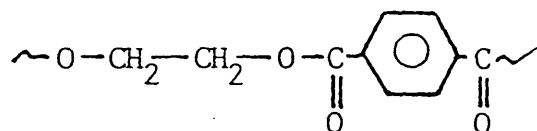
Substitution of the labile hydrogen atoms by fluorine atoms has resulted in the development of more thermally stable structures. This is a consequence of the relatively high dissociation energy of the C-F bond in comparison to the C-H bond. In fact fluorine atoms are so strongly bound that there is no known method for the controlled replacement of fluorine in a fluorocarbon polymer by any other group.

Complete substitution by fluorine results in polytetrafluoroethylene, the most stable structure that can be obtained by this approach. However, the adverse physical properties of this material severely restrict its application as a high temperature material. A compromise has to be made in which improved processing properties are imparted to the material at the expense of less effective protection. This is achieved by partial fluorine substitution and has led to the development of several commercially available high temperature materials such as, polychlorotrifluoroethylene, polyvinylidene-

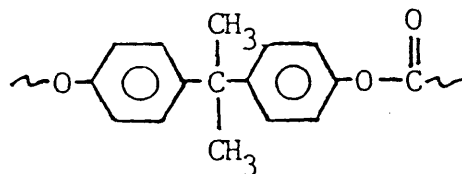
-fluoride, tetrafluoroethylene-hexafluoropropylene copolymers, and vinylidene fluoride-hexafluoropropylene copolymers.

Although the elimination of labile pendant groups is successful in enhancing thermal stability more significant advances in the development of high temperature materials have been realised by the incorporation of aromatic groups into the polymer structure. These groups act as energy sinks preferentially absorbing any incident energy in a manner comparable to that previously described for γ -radiation and exert short range protection of bonds in the structure. The presence of these structures also increases chain stiffness and this can have the added advantage of preventing the onset of any undesirable reversible processes.

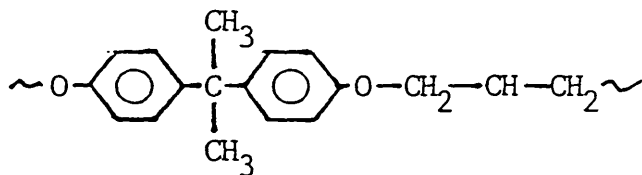
Using the above criterion the linear polymer possessing optimum stability will be polyphenylene. This polymer is, in fact, stable to at least 500°C but the extreme stiffness of the chains results in an insoluble, infusible, quite intractable material, metaphorically described as brick dust. An improvement in physical properties at the expense of stability is achieved by the insertion of interatomic linking groups of a variety of types. This has given rise to many well established commercial engineering materials, such as polyethyleneterephthalate,



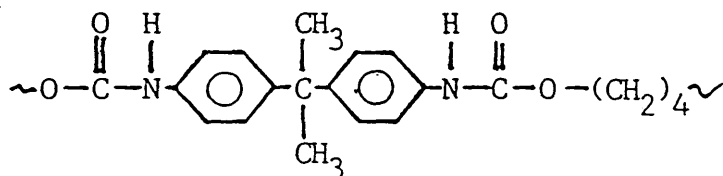
polycarbonates,



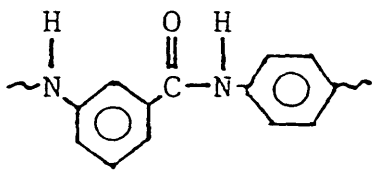
epoxy resins, for example, like the structure below,



polyurethanes, with the typical structure,

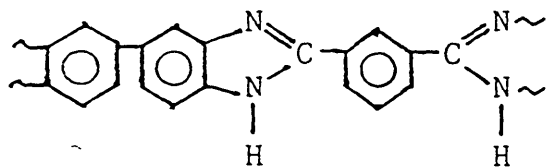


and the so called aromatic nylon, which has the following structure,

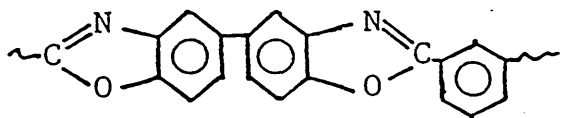


As a consequence of the aliphatic main chain groups these materials possess limited thermal stability and cannot be used in long term applications at temperatures above $\approx 250^{\circ}\text{C}$.

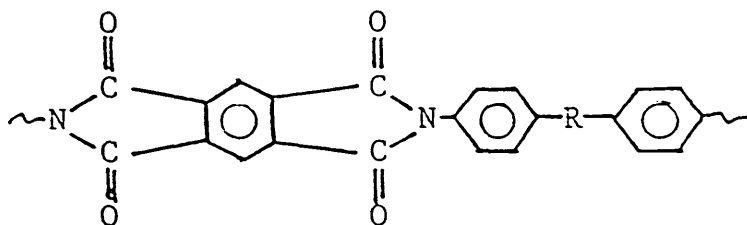
Further progress toward high temperature materials has depended on the elimination of these 'weak links' from the polymer structure and has been achieved by the incorporation of more stable links. A large number of polymers of this kind have been synthesised and several are being manufactured commercially. These include the benzimidazoles, which have the structure below,



the benzoxazoles, with the following structure,

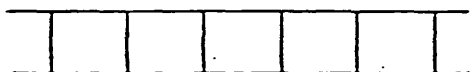


and the polyimides, which have the general structure,



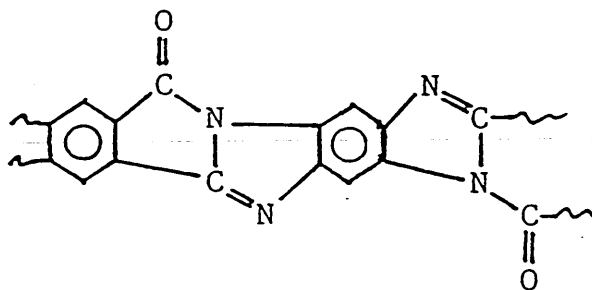
All of these materials possess excellent thermal stability and retain their mechanical properties indefinitely at temperatures of the order of 500°C.

It was assumed that any further advances in polymer stability might be achieved by the synthesis of ladder polymers, so called because their general structure can be represented by the following schematic:-

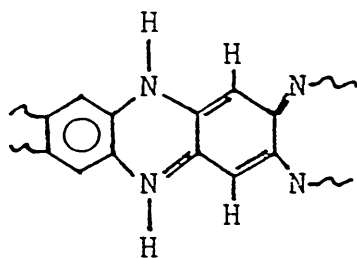


Being linear the polymer should be tractable, but as a consequence of being two-stranded the polymer should be highly stable. This is because chain scission would involve the cleavage of at least two bonds within a particular cycle of atoms. Tessler⁽⁶¹⁾ has demonstrated that this would be a rare event if thermal degradation were to take place by random bond scission throughout the structure.

Structures that have been prepared include those of the polybenzimidazopyrrolones, which have the following general structure:-



and the polyquinoxalines, which have the general structure:-



Unfortunately the performance of these materials has been disappointing as they appear to offer no significant increase in thermal stability. The reasons for this are not clear at present but it has been proposed that this may be due the difficulty of synthesising perfect ladder structures, or to the fact that degradation may involve localised scission within a cycle of the structure.

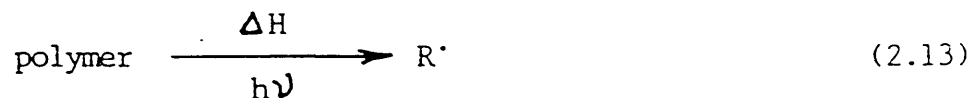
2.4. Oxidative Degradation.

2.4.1. Concept of Autoxidation.

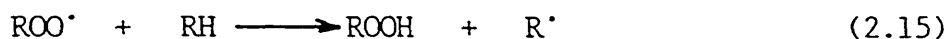
The presence of oxygen can have a significant influence on both the thermal and radiative degradation kinetics of hydrocarbon polymers. One of the most important is the main chain scission reaction induced by the breakdown of alkoxy radicals. These reactions are infrequent, for example, the molar ratio of number of chain scissions : number of molecules of oxygen absorbed during the oxidative degradation of poly-ethylene has been reported at 0.002 at 25°C rising to a value of 0.01 at 100°C⁽⁶²⁾, demonstrating the minor contribution of this mechanism to the overall oxidation process. However, such reactions have far reaching effects, as a relatively small number of main chain scissions in a polymer can result in a considerable deterioration of mechanical properties.

The various mechanisms which are responsible for the oxidation of hydrocarbon polymers are now well established. A major contribution to the understanding of these mechanisms arose from the pioneering work of Bolland and Bateman^(63,64) on the oxidative degradation of low molecular weight model compounds of natural rubber. The overall process is made up of the following stages:-

- (i) Initiation. Essentially the production of polymer radicals. This may be induced thermally or by exposure to γ -radiation:-

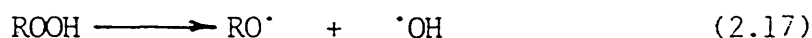
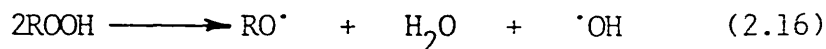


(ii) Propagation. Oxygen, which usually exists in the ground state as a diradical, participates in a radical chain reaction leading to the formation of a hydroperoxide:-

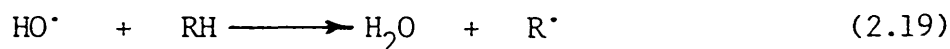
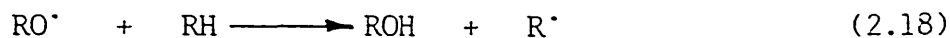


Reaction 2.14. is a radical pairing process, which has a low activation energy and occurs with high frequency. On the other hand the second step (reaction 2.15.) involves the breaking of a C-H bond and consequently has a higher activation energy. Hence, reaction 2.15. is the rate determining step in the oxidation process and alkylperoxyl radicals are the dominant radical species present.

(iii) Hydroperoxide decomposition. Once generated hydroperoxide may decompose by the action of heat or radiation resulting in the formation of alkoxy and hydroxyl radicals:-

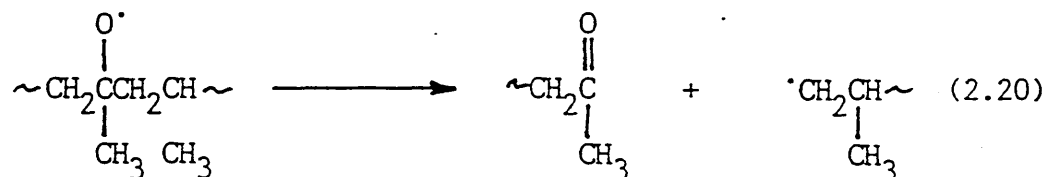


These radicals then react with labile pendant atoms (usually hydrogen) by the following mechanisms:-

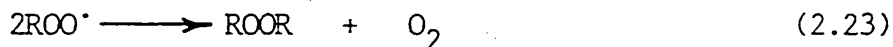


Main Chain Scission. Although the majority of radicals formed

abstract hydrogen, the alkoxy radicals may undergo α, β -bond scission resulting in cleavage of the backbone chain. A typical example of this is the mechanism operative during the oxidation of polyethylene given below:-



Termination. The following radical annihilation reactions are possible depending on the availability of oxygen:-



As alkyl radicals are the dominant radical species termination occurs primarily by reaction 2.23.

An interesting feature of reactions 2.18. and 2.19. is that they effectively inject new radicals into reaction 2.14. resulting in the formation of more hydroperoxide. Hence, the oxidative degradation reaction is an auto-accelerating process, and is usually referred to as auto-oxidation. These reactions are characterised by a very low initial reaction rate which gradually accelerates, often to some constant value.

the consequences or the relative efficiencies of reactions 2.14.

and 2.15. lead to the following rate equation for the autoxidation of hydrocarbon polymers:-

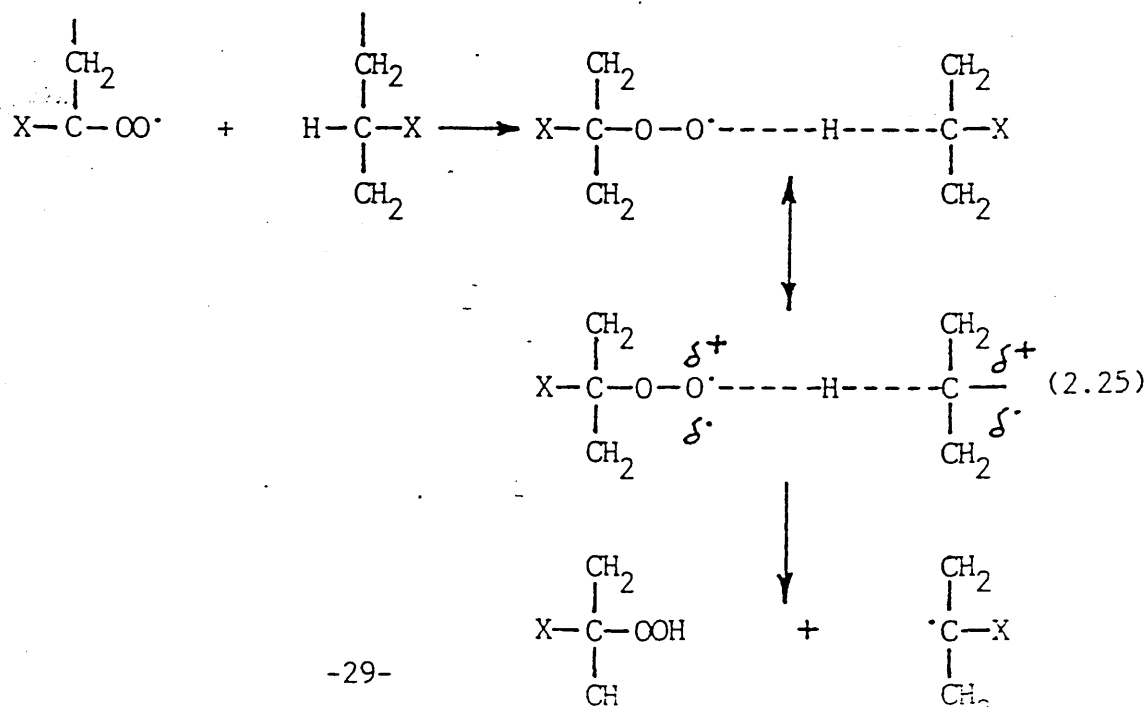
$$\frac{d[O_2]}{dt} = k_{(2.15)} k_{(2.23)}^{-0.5} r_i^{0.5} [RH] \quad (2.24)$$

where r_i is the rate of initiation of the autoxidation reaction and $k_{(2.15)}$ and $k_{(2.23)}$ are the respective rate constants of reactions (2.15) and (2.23). The above relationship specifically applies to oxidative degradation under conditions of unrestricted oxygen supply to the polymer.

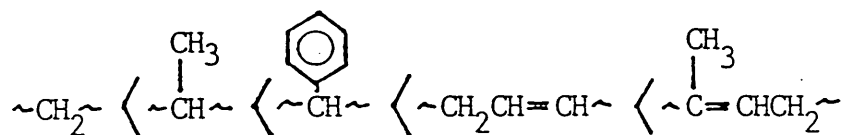
2.4.2. Factors Influencing Oxidative Stability.

4.2.1. Effect of Chemical Structure.

The effect of chemical structure on the susceptibility of a polymer to oxidise can be discussed in the light of equation 2.24. After radical initiation has taken place the oxidation rate is dependent on the rate constant $k_{(2.15)}$ for hydroperoxide formation. This is dependent on the energy of the transition state in the hydrogen abstraction reaction for the particular polymer in question. Consider the following transition state in the autoxidation of a hydrocarbon polymer:-

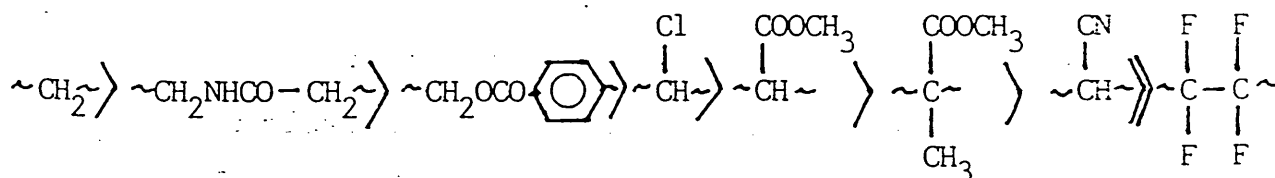


In the transition state the carbon atom to which the labile hydrogen atom is attached may assume a partial electron delocalisation (δ^-), partial ionic charge (δ^+ , δ^-) or a combination of both depending on the nature of X. The results of studies of the rate of oxidation of a range of hydrocarbon polymer molecules in solution has been reported by Grassie et al^(2d). It was discovered that the oxidation rate increased in the following series:-



These responses are primarily due to the delocalising effect of the attached group but polar effects are also superimposed (CH_3 is electron releasing).

In polymers containing hetero-atoms, polarity normally predominates and it has been observed that the oxidation rate of the following polymer structures decreases in the order:-



Polytetrafluoroethylene, which is included in the ranking, possesses outstanding thermal stability. This is because autoxidation cannot occur in structures that have no labile hydrogen atom.

2.4.2.2. Effects of Physical Structure.

It is well documented that the oxidation kinetics of bulk hydrocarbon polymers are governed, to a large extent, by their physical state and not by their particular chemical structure. This is a consequence of the differences in the degradation kinetics of bulk materials compared with those of polymer molecules in isolation.

Under these conditions of restricted oxygen supply the rate of the overall oxidation process is dependent on the rate of alkyl radical production (reaction 2.14). The controlling step in this reaction is the rate at which molecular oxygen can migrate through the material to sites of interaction with the polymer radicals. As the diffusion of oxygen or any other molecular species through a polymer is related to the degree of chain mobility it becomes apparent that the oxidation rate of a material is significantly influenced by its physical state.

Hence, in the liquid state, where chain mobility is high, the radicals are easily accessible to molecular oxygen, and if the chemical structure of the polymer is favourable (section 2.4.2.1.), it will readily be oxidised. Conversely, the severe restrictions imposed on chain mobility in the glassy or crystalline state inhibits penetration by oxygen and the rate of oxidation is retarded, even in the case of highly oxidisable polymer structures. Under these conditions any oxidative degradation reactions are confined to the immediate vicinity of the surface of the material^(65,66).

An interesting aspect of the effect of physical structure on the oxidative stability of polymers is provided by semi-crystalline materials. These polymers are essentially two phase systems consisting of spherulitic clusters of crystals embedded in an amorphous matrix. Oxygen can diffuse easily through the amorphous regions in these materials but cannot

penetrate the crystalline regions. Maximum oxidation damage occurs in these materials when oxidation reactions take place at the spherulite boundaries as this gives rise to loss of cohesion with the matrix and results in a drastic deterioration in mechanical properties. A consequence of this is that the same amount of oxidation creates much more damage in a highly crystalline polymer than it does in a less crystalline polymer of similar chemical structure. Thus although high density polyethylene oxidises less readily than low density polyethylene it undergoes physical degradation far more rapidly.

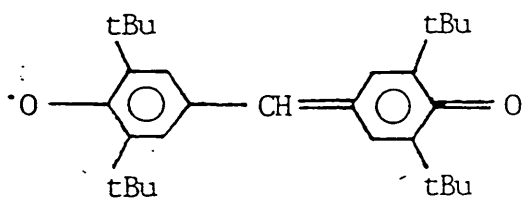
Similar problems are encountered in other two-phase polymers. A typical example is provided by rubber modified polystyrene. In this material the polystyrene phase contains occluded domains of polystyrene surrounded by a rubber-styrene graft copolymer, which acts as a solid phase dispersant for the rubber in the polystyrene matrix. However, the rubber blocks possess far lower oxidative stability than the polystyrene homopolymer and this leads to a rapid loss of the energy absorbing properties of the 'adhesive' between the polystyrene domains. Consequently, although the initial impact resistance of high impact polystyrene is higher than polystyrene itself, the reverse is true within a short time after exposure to an oxygen containing environment, due to the degradation of the rubber phase.

2.3. Effects of Antioxidants or Stabilisers.

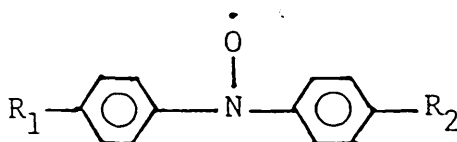
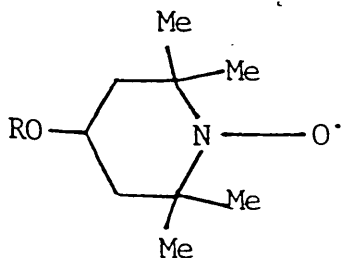
Significant improvements in the oxidative stability of polymers may be achieved by the addition of certain compounds known as stabilisers or antioxidants. All these agents interfere with the radical reactions that lead to the incorporation of oxygen into the chemical structure of the polymer. The autoxidation mechanism discussed in Section 2.4.1. is

presented in Fig 2.4. The mechanism can be envisaged as two interacting cyclical processes. The first cycle is the alkyl-alkylperoxyl chain reaction, and the second involves the homolysis of hydroperoxides, which feeds the chain reaction with new radicals. When steady state conditions are attained, the rate of formation of hydroperoxides by cycle A is equal to their rate of decomposition by cycle B, and the rate of oxidation is constant. The purpose of adding an inhibitor is to prevent this stage being reached by inhibiting or retarding the formation of hydroperoxides as long as possible, or by initiating the decomposition of hydroperoxides to non-radical products.

Antioxidants which act by oxidising the alkyl radical to give a carbonium ion and subsequent inert reaction products, such as olefins, are electron acceptors and are known collectively as chain breaking acceptors (CB-A). The stage at which these agents act in the reaction are illustrated in the above scheme. Benzoquinone and aromatic nitro-compounds fall into this category. However, by far the most important are the 'stable' free radicals, of which galvinoxyl has the structure:-

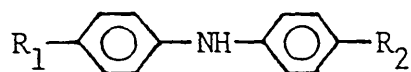


and nitroxyls, which have the following general structures:-



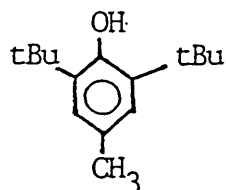
Chain-breaking donor (CB-D) antioxidants are reducing agents or electron donors. They exert their protective influence by reducing the alkylperoxyl radical to a number of products which are inert or act as antioxidants themselves. ^(2e). The earliest antioxidants to be investigated fall into this class.

During the early development of rubber, it was observed that some vulcanising agents led to superior ageing performance of the finished product. These agents were subsequently identified as the arylamines, which have the general structure:-



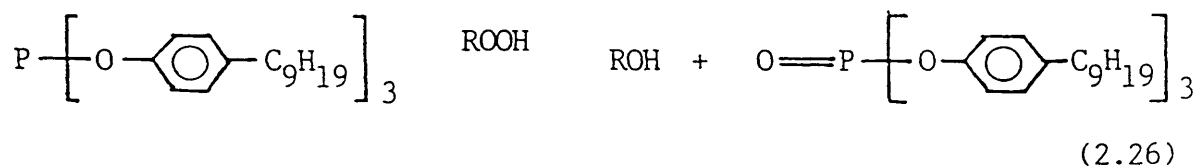
Of these, diphenylamine ($R_1 = R_2 = H$) was one of the earliest antioxidants to be developed commercially. However, this compound is too volatile to be used in modern rubber technology, and higher molecular weight alkylated derivatives, such as octylated diphenylamine ($R_1 = R_2 = tOct$) are employed for stability at high temperatures. The 4-aminodiphenylamines, for example, N-isopropyl-N'-phenyl-p-phenylenediamine ($R_1 = H$, $R_2 = NH$ iso Pr) and diphenyl-p-phenylenediamine ($R_1 = H$, $R_2 = NH$ Ph) are important antidegradants that are used extensively in tyres.

A disadvantage of the arylamines is that they cause considerable discolouration of the polymers to which they are added. This has been attributed to the formation of extensively conjugated quinonoid oxidation products. Non-staining antioxidants have been developed which are based on substituted phenols. The simplest, most important member of this class, which is used as an antioxidant in other technologies (eg, foodstuffs) is the hindered phenol 2,6-di-tert-butyl phenol, usually referred to as butylated hydroxytoluene, whose structure is given overleaf.



This additive is relatively volatile, and is therefore not used in polymers destined for use at high temperatures, due to its rapid physical loss. This problem has been overcome by the development of a variety of higher molecular weight hindered phenols.

High molecular weight phosphite esters have been used for many years as gel-stabilisers for synthetic rubbers. These additives fall into the category of stoichiometric peroxide decomposers (PD-S) as they reduce hydroperoxides stoichiometrically by a non-radical mechanism to inert products, thus preventing the generation of alkoxy radicals. A notable example of one such compound is trinonylphenylphosphite, which reduces hydroperoxides to alcohols by the following mechanism:-



Of much more general applicability are a class of sulphur compounds which destroy hydroperoxides by a catalytic mechanism, and are hence known as catalytic peroxide decomposers (PD-C). Acidic species, such as sulphur acids are very effective antioxidants but normally cannot be used in polymers. This is due to their insolubility in organic materials and their corrosive tendencies. However, a number of soluble sulphur compounds give acidic species on oxidation with

hydroperoxides and therefore act as reservoirs for any peroxidolytic
species.

A particularly important group of (PD-C) compounds, which form the basis of thermal antioxidant systems for a wide range of thermoplastic hydrocarbon polymers are the dialkylthiodipropionates. Also worthy of mention are the metal thiolates, which are employed extensively in hydrocarbon rubbers.

2.5. Hydrolytic Degradation.

Hydrolysis may be regarded as a particular type of solvolysis reaction in which water is the reactive agent. Other solvolysis agents include alcohols, ammonia, hydrazine, etc. Many polymers are subject to this mode of degradation if their chemical structure contains any hydrolysable linkages. Examples of common polymers, which are prone to hydrolytic degradation, and their associated scission mechanisms are presented in Table 2.3. It can be seen that the susceptible linkages invariably form part of the main chain structure, and consequently degradation results in cleavage of the main chain.

Polymers are generally much more resistant to hydrolysis than might be predicted from the behaviour of polymer molecules in isolation⁽⁶⁷⁾. This is not due to any difference in the stability of the hydrolysable linkages under these conditions, but is a consequence of the properties of bulk polymers. Attack is usually confined to the surface of the material because of the hydrophobic nature of most organic polymers (an exception are the majority of polysaccharides, which are water soluble).

In the bulk state, the kinetics of hydrolytic degradation are analogous to those of oxidative degradation, and the effects of physical structure on degradation kinetics can be explained by the same arguments put forward in Section 2.4.2.2.

Degradation of Specific Materials.

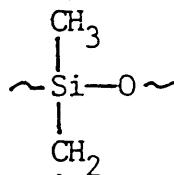
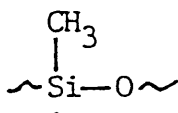
It is appropriate that the degradation mechanisms operative in silicone and fluorocarbon elastomers are reviewed in detail, as materials from these categories have been selected for study in the present investigation. The references cited in this section appear to be the most recent available.

Degradation of Silicone Elastomers.

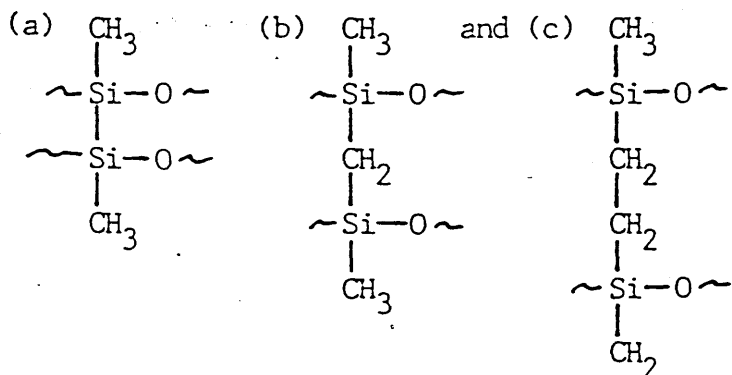
Radiative Degradation Mechanisms.

It is well established that the polysiloxanes undergo predominant crosslinking when they are exposed to γ -radiation.^(68-77.) This response has led to the rising popularity of radiation curing as a processing route for silicone elastomers.^(77-81.)

One of the earliest and most comprehensive studies of the relevant crosslink formation mechanisms was by Miller⁽⁸²⁾ who irradiated a series of linear polysiloxanes in air, oxygen, and nitrogen. It was discovered that irradiation led to the cleavage of Si-CH₃, and SiCH₂-H bonds resulting in the generation of the following radicals:-



Subsequent interaction of these radicals may lead to the possible formation of the three types of crosslink structure given below:-



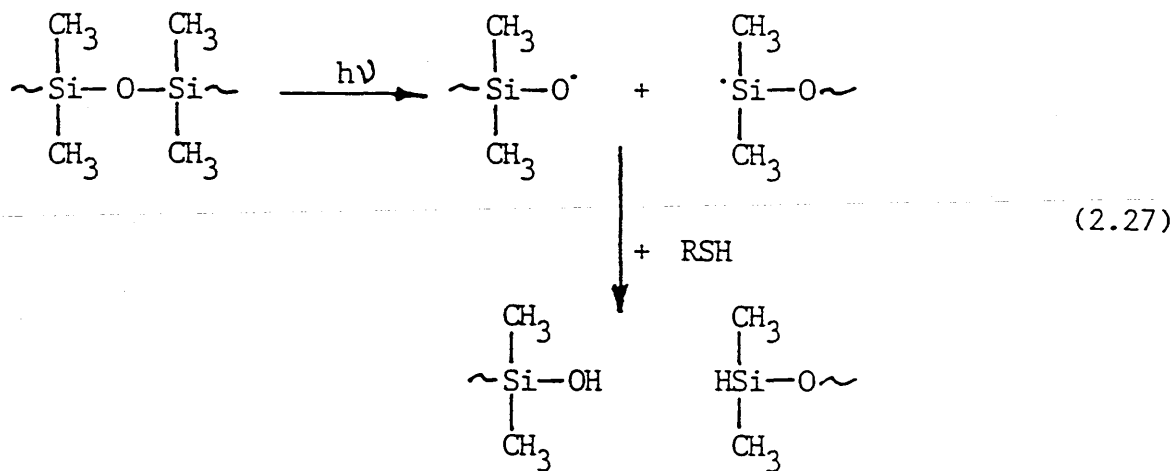
The analysis of gaseous products evolved during irradiation indicated that these crosslinks were formed in the ratio (a):(b):(c) = 1.1:1.8:0.5.

With increasing irradiation temperature Charlesby⁽⁷⁾ reported that crosslink formation rates in polysiloxanes increase. The effect has been verified by Fischer⁽⁸³⁾ who found, under conditions of identical absorbed dose rate and exposure time, that samples irradiated at 200°C contained approximately twice the number of crosslinks as those irradiated at 40°C.

The effects of various atmospheres on crosslinking kinetics have been explored by Jenkins^(84,85). The results of these studies revealed that the crosslinking rate was at its highest value when irradiation was performed in vacuum. Less intense crosslinking was experienced in helium, even less in nitrous oxide, and crosslink formation was at a minimum when irradiation was carried out in air.

Experiments on thin films (\approx 1mm) of liquid polysiloxanes has established that irradiation under oxygen at increased pressure (\approx 1 Atm) results in a decrease in the crosslink yield. It has been proposed that this effect may be due to the oxidation of peroxy radicals generated during irradiation, thus preventing them from participating in subsequent crosslinking reactions⁽⁸²⁾.

Although the radiative degradation of polysiloxanes takes place primarily by crosslinking reactions, a significant amount of induced scission has been detected by several workers^(73,86,87). A technique utilising the radical scavenging properties of the mercaptans was used by Miller⁽⁸⁷⁾ to establish the crosslinking mechanism. He reasoned that if scission of the main chain took place then H and OH groups should be incorporated onto the cleaved chain ends by the following mechanism:-



The presence of these groups were detected by IR analysis, and their number suggested that polysiloxanes exhibit a crosslinking:scission ratio of approximately 10:1.

1.1.1. Effects of Incorporating Aromatic groups into the Chemical Structure.

The substitution of aromatic groups, for example phenyl for methyl in the polydimethyl structure has been found to impart greater resistance to radiation induced crosslinking^(7,88,72). It has been demonstrated by Miller⁽⁸⁸⁾ that the position of the methyl group with respect to the aromatic substituent has a pronounced effect on radiative stability. It has already been demonstrated that this group is most susceptible to crosslink formation via C-H bond rupture. The methyl group which receives the greatest protection has been identified as the one which is directly opposed to the phenyl group in the structure.

In silicone polymers the ease of crosslink formation decreases with increasing phenyl substitution. The relative crosslink yields in a series of siloxane polymers of comparable molecular weight were reported as:-

$\sim\text{Si}(\text{Me})_2-\phi\sim$	20
$\sim\text{Si}(\text{O})(\text{Me})-\phi\sim$	2
$\sim\text{Si}(\text{O})-\phi\sim$	1

When groups of increased conjugation, such as biphenyl and naphthyl are substituted even greater radiative stability is observed. The degree of radiation protection appears to be related to the extent of conjugation of the aromatic pendant group.

1.2. Effects of Copolymerisation with Diphenylsiloxane.

An alternative method of conferring increased radiation stability to a polysiloxane is by the incorporation of diphenylsiloxane blocks into the backbone chain. Warrick^(69,72) reported that the absorbed dose required to induce the same degree of crosslinking was 20 times greater for a dimethylsiloxane-diphenylsiloxane block copolymer than for a comparable dimethylsiloxane polymer, furthermore, the efficiency of crosslink formation was found to be dependent on the number of diphenylsiloxane blocks incorporated into the main chain. Using calculations developed by Alexander and Charlesby⁽⁸⁹⁾, Kioke and Danno⁽⁹⁰⁾ determined the extent of the protective effect offered by the phenyl section in such copolymers. It was discovered that the protection of a single phenylsiloxane unit extended over 5-6 adjacent monomer units of dimethylsiloxane in the polymer. The range of this protective action has been the subject of much disagreement, however more recent studies by Delides⁽⁹¹⁾ has substantiated these findings.

1.3. Effects of Blending with Polystyrene.

When blending polymers, the criterion for miscibility is the accompanying free energy change. In the case of equilibrium processes this quantity may be expressed by the following relationship:-

$$\Delta G_{\text{mix}} = \Delta H_{\text{mix}} - T \Delta S_{\text{mix}} \quad (2.28)$$

where:-

ΔH_{mix} = enthalpy change on mixing

and ΔS_{mix} = entropy change on mixing

Although, strictly speaking, the mixing of two polymers is not considered to be an equilibrium process, the above treatment, which may be applied to solutions, can be extended and used for the quantitative analysis of polymer blends. The entropy change encountered on mixing polymers of very high molecular weight, like those encountered in blends, is negligible, and may be considered as essentially zero. Therefore, the enthalpy change on mixing becomes the overriding factor in determining miscibility.

The enthalpy of mixing, which depends on the energy changes encountered when two dissimilar species come into contact, is, to an approximation, independent of molecular chain length, and can be represented by the following relationship proposed by Hildebrand⁽⁹²⁾:-

$$\Delta H_{\text{mix}} = V(\delta_1 - \delta_2)^2 \phi_1 \phi_2 \quad (2.29)$$

Where V is the total volume of the mixture, and δ_1, δ_2 , and ϕ_1, ϕ_2 , are, respectively, the solubility parameters and the volume fractions, of the two components. Conditions of maximum solubility will exist when $\delta_1 = \delta_2$ and $\Delta H_{\text{mix}} = 0$. Otherwise ΔH is always positive and only partial miscibility is attained.

Substitution of the relevant solubility parameters for polydimethylsiloxane and polystyrene, $18.2 (\text{MJ}^{-3})^{\frac{1}{2}}$ and $14.6 (\text{MJ}^{-3})^{\frac{1}{2}}$, respectively⁽⁹³⁻⁹⁸⁾ in equation 2.29. results in a high enthalpy of mixing, indicating that such a blend would exhibit low miscibility.

These predictions have been confirmed experimentally by Galin and Rupprecht⁽⁹⁹⁾. It was observed that the morphology of a polydimethylsiloxane-polystyrene blend is made up of two distinct macrophases, one styrene, and the other dimethylsiloxane. Any degree of miscibility of the components was not reported in these studies.

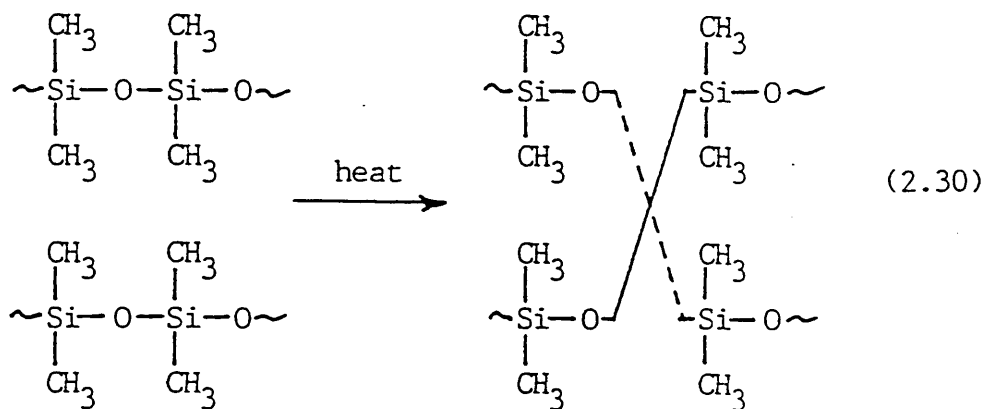
Recently, the effects of γ -irradiation on an extensive range of polydimethylsiloxane-polystyrene blends has been assessed by Astill⁽¹⁰⁰⁾. A selection of the results of these investigations, which were carried out at various dose rates under vacuum, are presented in Fig 2.5. It can be seen that there is a significant decrease in the gel fraction of irradiated blends in the low % styrene region irrespective of the dose rate employed. The author established that the doses employed in the studies were not sufficient to induce crosslinking of the polystyrene, and therefore the effects were attributed to a reduction in the radiation induced crosslinking of the polydimethylsiloxane. Bearing in mind the morphology of these blends, and the limited range of protection afforded to dimethylsiloxane by diphenylsiloxane in copolymers it seemed unlikely that any significant level of protection was afforded to the polydimethylsiloxane by the discrete polystyrene phase.

It was proposed that these effects may be due to the limited solubility of polystyrene in the polydimethylsiloxane phase, and corroborative evidence has been provided by DSC studies of the blends⁽¹⁰¹⁾. The glass transition associated with the polydimethylsiloxane phase in the blends occurred at a slightly higher temperature than that of pure polydimethylsiloxane. Also a broadening of the transition range was observed. Both these effects are characteristics of blends which exhibit partial miscibility. The concentration of polystyrene, if present, in the polydimethylsiloxane phase, and its distribution, has yet to be resolved.

Thermal Degradation Mechanisms.

Initial studies of the thermal degradation of silicone elastomers appeared to yield contradictory evidence. Although significant main chain scission was detected during degradation the crosslink density of the elastomers remained unchanged. It is now generally accepted that these effects are the result of chain interchange reactions, in which cleaved chains are subsequently reformed by interaction of the newly formed chain ends.

The relevant degradation mechanisms that have been proposed for these materials have been reviewed by Thomas⁽¹⁰²⁾. Under inert atmospheres, such as dry air, or nitrogen, degradation is believed to take place by a simple siloxane bond interchange mechanism, as illustrated below:-

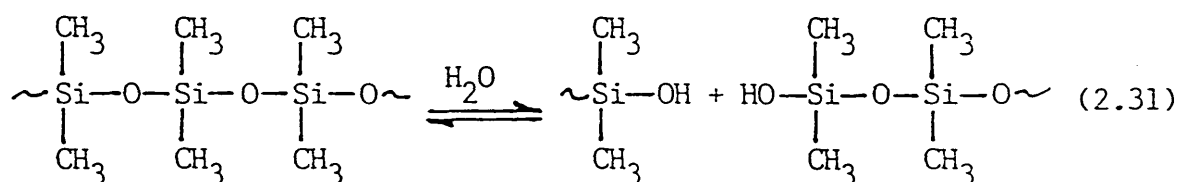


It has been demonstrated that the reaction is catalysed by various acidic species, and bases, such as potassium hydroxide, which arise from the initial polymerisation process.

3. Hydrolytic Degradation Mechanisms.

Osthoff et al⁽¹⁰³⁾ revealed that the stress relaxation response of a benzoyl peroxide cured polydimethylsiloxane elastomer was greatly enhanced by the introduction of water vapour into the reaction chamber. This increase

was attributed to a rapid increase in the rate of main chain scission. However, the crosslink density of the elastomer still maintained its original value, and it was apparent that a consequent increase in the rate of chain reformation was taking place. A new mechanism was proposed to account for the change in degradation kinetics. Cleavage of the chains was explained in terms of a hydrolytic scission reaction (the siloxane bond is known to be susceptible to hydrolytic scission (Section 2.5.)), and chain reformation by the subsequent condensation of the silanol groups, as indicated in the following scheme:-



It was established that the scission reaction was catalysed by benzoic acid, which is a decomposition product of the curing agent employed (benzoyl peroxide). Identical studies on comparable elastomers vulcanized by γ -irradiation revealed that they possessed superior thermal stability in water vapour atmospheres, and this was attributed to the absence of any peroxide residuals in these materials.

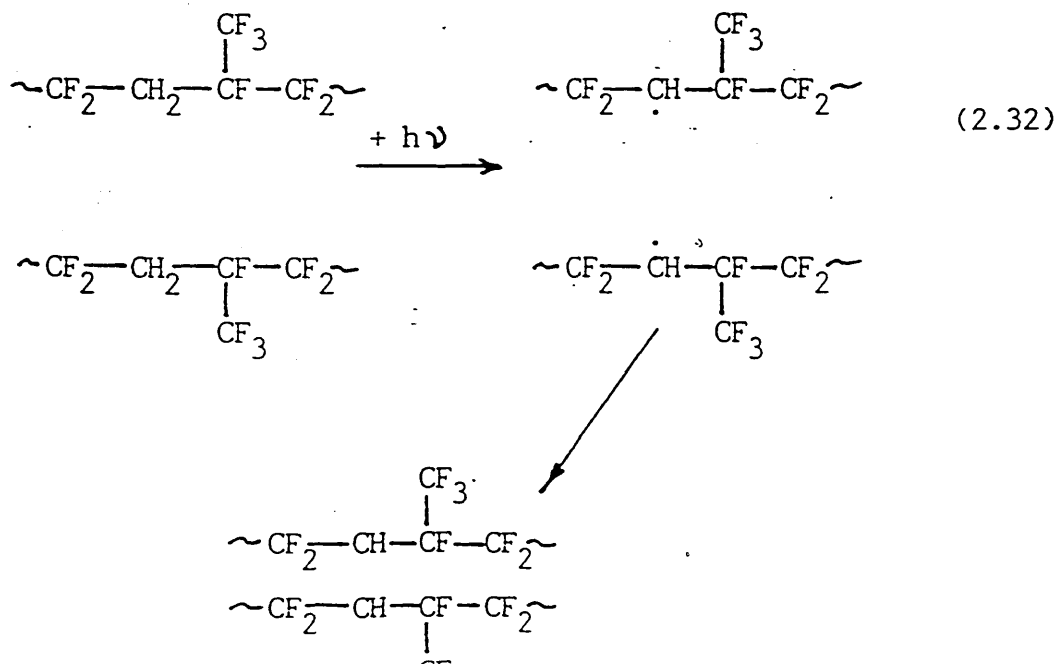
More recent investigations have shown that predominant hydrolytic scission can take place in silicone elastomers during storage for long periods prior to use⁽¹⁰⁴⁾. Apart from moisture, the scission reaction rate appeared to be enhanced by the presence of ammonia.

2.6.2. Degradation of Fluorocarbon Elastomers.

2.6.2.1. Radiative Degradation Mechanisms.

Early studies of the radiative degradation of fluorocarbon polymers resulted in several general observations regarding the mode of degradation and chemical structure^(105,106). It appears that polymers which are completely halocarbon, for example polytetrafluoroethylene and polychlorotrifluoroethylene, undergo predominant scission with little accompanying crosslinking. Conversely, predominant crosslinking is exhibited by those polymers which contain pendant hydrogen atoms. This effect has led to the widespread application of radiation curing to the two major families of fluorocarbon rubbers, the Viton elastomers ($C_3F_6 + CF_2CH_2$), and the closely related Kel-F elastomers ($CF_2CFCl + CF_2CH_2$). Consequently, the radiation induced crosslinking of these materials has received considerable attention^(107,114).

The crosslink formation mechanism, which is now generally accepted, was first proposed by Dixon et al⁽¹⁰⁷⁾. It is believed that the initial stage of the process involves the cleavage of relatively weak CH_2-H bonds, and that crosslink formation takes place by the interaction of resultant radicals, as described below:-



It has been discovered that this reaction has several interesting features. Studies of radiation cured Viton A elastomers revealed that the crosslink density of the material continued to increase during the post cure treatment, and furthermore, that the rate of this retarded crosslinking reaction increased with increasing temperature. These post-irradiation effects have been attributed to the existence of radiation induced radicals, which do not participate in immediate crosslink formation, but react later at higher temperatures^(107,115,116). As a consequence of these effects, it is now standard procedure to subject this material to a thermal treatment, after exposure, in order to develop the maximum degree of crosslink formation, and hence realise optimum mechanical properties.

The above investigations also revealed that although this crosslink possesses greater thermal stability than its traditional peroxide, or amine cured counterpart, it too becomes unstable at sufficiently high temperatures.

Crosslink and scission yields for Kel-F and Viton elastomers have been reported to lie in the ranges $G_C = 0.62$ to 1.35 , and $G_S = 0.78$ to 4.5 ^(107,116). The reasons for these discrepancies have not been established, but they are probably due to differences in material preparation conditions and testing procedures. Studies by Kryukova et al⁽¹¹⁴⁾ revealed that the presence of oxygen can result in substantial changes in both crosslinking and scission kinetics. However, his findings were inconclusive as they yielded contradictory results.

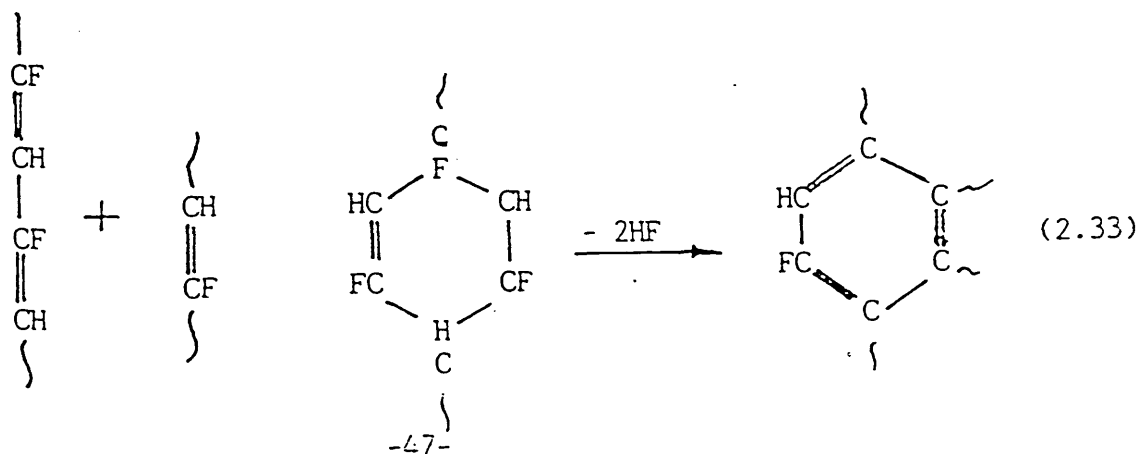
Despite these variations it is apparent that a substantial amount of scission is taking place during the degradation of these materials. A review of the pertinent literature reveals no instances of a reported

scission mechanism for these materials but it is believed that they undergo a random main chain scission reaction, when exposed to γ -radiation.

2.2. Thermal Degradation Mechanisms.

As a consequence of their highly fluorinated structures these elastomers possess outstanding thermal stability. They can usually be subjected to temperatures as high as 250 - 300°C without degrading or losing their mechanical properties⁽¹¹⁷⁾. At higher temperatures rapid degradation of fluorocarbon polymers takes place by thermal decomposition of the polymer. The associated mechanisms are complex and have yet to be resolved but it is apparent that C-C bond rupture, associated with a reduction in molecular weight, the evolution of HF and crosslinking reactions are taking place. As a consequence of these reactions the elastomers are transformed to low molecular weight hydrocarbons.

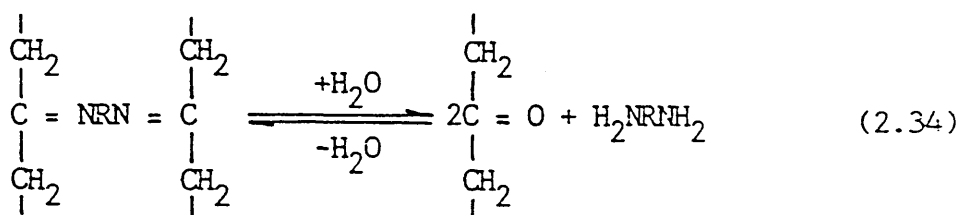
Numerous studies have indicated that some vinylidene fluoride-hexafluoropropylene elastomer predominantly crosslink at temperatures in excess of 200°C. However there is still a great deal of controversy over the mechanisms that are operative. The most feasible, is the one in which further dehydrofluorination is believed to occur, either by amine, or directly by the base present (MgO), resulting in unsaturation which then leads to the formation of ring structures, as shown below⁽¹¹⁸⁾:-



2.3. Hydrolytic Degradation Mechanisms.

It has been observed, in the special case of elastomers cured with amine derivatives, that thermal stability can be drastically reduced, and consequently thermal degradation may take place at far lower temperatures.

In the presence of water, a reversion reaction involving hydrolysis of the amine crosslinkages, has been reported. It is believed that the reaction takes place by the following mechanism:-



The occurrence of such a reaction is an indication that the elastomer has not received a suitable post cure treatment. The importance of post curing these materials has been highlighted by Smith⁽¹¹⁹⁾. By hydrolysis he was able to recover approximately 70% of the amine present in a Viton A elastomer. From his results it was evident that all cross-links of the above type which were present in the material would have been hydrolysed if sufficient water had been present.

3. Techniques for the Evaluation of Crosslinking and Scission Kinetics in Degrading Polymers.

A variety of techniques are available for evaluating the rates of cross-linking and scission reactions, induced in polymers by γ -irradiation. In the following sections these techniques will be discussed together with their specific applications and limitations. Reference will also be made to associated, underlying, theoretical concepts, when appropriate.

1. Measurement of Molecular Weight.

The degradation kinetics of linear polymers, which undergo chain scission in the absence of crosslinking reactions, may be determined from molecular weight measurements.

Detailed studies of the degradation of polyisobutylene (Fig 3.1), polymethylmethacrylate, and poly- α -methylstyrene indicated that the number of induced cleavages, encountered in these materials, was proportional to the absorbed dose, and virtually independent of dose rate, when irradiation was performed under vacuum^(3d). Under these conditions it was shown that the rate of the degradation reaction may be evaluated from the following relationship⁽¹²⁰⁾:-

$$1/\bar{M}_{nd} - 1/\bar{M}_{no} = kD = G_d D / 100 N \quad (3.1)$$

where:-

\bar{M}_{no} = number average molecular weight of polymer before irradiation.

\bar{M}_{nd} = number average molecular weight of polymer after irradiation.

D = absorbed dose (eV.g⁻¹).

G_d = degradation (scission yield)

N = Avagadro's constant.

and k = rate constant of the scission reaction.

2. Sol / Gel Fraction Measurements.

In the special case of linear polymers which degrade solely by crosslinking reactions, the degradation yield may be determined from a knowledge of the gel formation dose, and the initial weight average molecular weight of the polymer by application of the following relationship^(3e):-

$$G_c = n \cdot 10^5 / D_g M_{w0} \quad (3.2)$$

where:-

G_c = crosslinking yield.

D_g = gel formation dose (Mrad).

M_{w0} = weight average molecular weight of the polymer.

and $n = 4.8$

The gel formation dose is the absorbed dose required to induce incipient gelation of the polymer. This quantity may be evaluated by extrapolation of the line of the dependence of the gel fraction on the absorbed dose, to the intersection with the abscissa, i.e. to zero gel content. An alternative approach is to monitor the change in weight average molecular weight during irradiation. If the reciprocal of this quantity is plotted along the ordinate, and the absorbed dose along the abscissa, then the extrapolation of this dependence to $1/M_w$ equal to zero, will give the value of D_g .

Equation 3.2 is only applicable under conditions of random crosslink formation, and also when there is no change in the molecular weight distribution of the polymer during degradation⁽¹²¹⁾.

When irradiation induces simultaneous crosslinking and scission reactions in polymers, the respective yields for each reaction may be determined from the well known Charlesby - Pinner relationship, given below⁽¹²²⁾:-

$$S + \sqrt{S} = \frac{50N}{\bar{M}_{n0} G_c} \cdot \frac{1}{D} + G_d / G_c \quad (3.3)$$

where:-

S = sol fraction of irradiated polymer.

M_{n0} = number average molecular weight of polymer prior to irradiation.

D = absorbed dose (Mrad)

G_d = degradation (scission) yield.

and G_c = crosslinking yield.

Reliable kinetic data may be obtained by application of the above relationship

only if the following conditions are fulfilled:-

- (i) The polymer has the 'most probable molecular weight distribution.
- (ii) There is a random distribution of crosslinking and scission reactions during irradiation.
- iii) The polymer is subjected a sufficiently high dose, ie well above that required for incipient gelation.
- (iv) The crosslinking and scission yields are independent of the absorbed dose.

Under these conditions a linear relationship between $S + \sqrt{S}$ and the reciprocal of the absorbed dose should be obtained, from which both the crosslinking and scission yields can be determined. If the initial molecular weight distribution of the polymer is significantly different from the 'most probable' distribution the resulting curves become non-linear and the above relationship cannot strictly be applied. However, a reliable estimate of the ratio G_d / G_c may still be established for these materials from solubility data obtained at high absorbed doses. This is because a significant amount of scission will have taken place under these conditions, and this will result in the molecular weight distribution of the polymer approximating to the 'most probable' distribution.

3.3. Equilibrium Stress - Strain Measurements.

Under special conditions, when physical relaxation processes are absent and the material has attained a time - independent modulus (absence of viscous flow), then the degradation of elastomer network structures may be evaluated from stress - strain measurements. This is achieved by application of rubber elasticity theory, which is valid for ideal elastomer networks under equilibrium conditions.

The relevant equation was derived independently by James and Guth⁽¹²³⁾ Wall⁽¹²⁴⁾, and Flory⁽¹²⁵⁾, and although their treatments differ slightly, they are in fact analogous. An exact treatment of these theories is beyond the scope of this work. However, it is hoped that the following considerations, although oversimplified, will demonstrate the underlying concepts behind their reasoning.

If an elastomer undergoing some deformation dL (in this case a tensile deformation) is considered, then the resultant internal energy change associated with this process may be evaluated from the following relationship:-

$$dU = T dS - dW \quad (3.4)$$

where dS and dW are the change in entropy, and the work done by the system respectively. The work done by the system is made up of two components, pressure-volume work, and the restraining force $f dL$, and can be represented by the following expression:-

$$dW = P dV - f dL \quad (3.5)$$

where P and dV are the respective pressure, and volume change encountered. Substituting equation 3.5 into equation 3.4. leads to the expression:-

$$dU = T dS - P dV + f dL \quad (3.6)$$

Differentiating with respect to L at constant temperature and volume, and subsequent re-arrangement, yields the following relationship for the force exerted by the elastomer upon deformation:-

$$f = \left[\frac{\partial U}{\partial L} \right]_{T,V} - T \left[\frac{\partial S}{\partial L} \right]_{T,V} \quad (3.7)$$

In elastomers, the change in internal energy which is experienced upon deformation is negligible, and consequently the major contribution to the force arises from the change in entropy. This decrease in entropy is due to changes in network chain conformation.

The above treatment has assumed that the internal energy is independent of the conformations of the network chains, i.e. $(\partial U / \partial L)_{T,V} = 0$, and the elastomer is said to be ideal. It is apparent that the derivation of the final equation essentially involves the evaluation of the entropy change which accompanies deformation of the elastomer network. This is achieved by the following procedure:-

- (i) Initially, the number of possible conformations of a freely jointed, volumeless, network chain which obeys Gaussian statistics, is evaluated.
- (ii) The total number of conformations of an isotropic network of such Gaussian chains is evaluated by assuming that this is the product of the individual chains comprising the network.
- (iii) The total entropy of the network is evaluated by application of the well known Boltzmann relationship, given below:-

$$S = k \ln \Omega \quad (3.8)$$

where:-

k = Boltzmann's constant.

and Ω = total number of chain conformations available to the network.

- (iv) The total entropy of the network in the deformed state is evaluated and hence the entropy change encountered upon deformation of the network can be determined. In the treatment it is assumed that affine deformation has taken place, and that the crosslink junctions in the network transform in the same ratio as the macroscopic deformation ratio of the sample.
- (v) The entropy change, which is expressed in terms of dimensional changes encountered in the elastomer, is related to the force exerted by the network.

The final equation may be expressed in the following simplified form:-

$$f / A_0 = \sigma = G (\lambda - \lambda^{-2}) \quad (3.9)$$

where:-

f = force.

A_0 = original cross-sectional area of the sample.

σ = uniaxial stress (based on A_0)

G = shear modulus.

λ = extension ratio.

In the above expression, which is valid under conditions of uniaxial stress, the shear modulus may be expressed by the relationship:-

$$G = N_c RT = \rho RT / \bar{M}_{nc} \quad (3.10)$$

where:-

N_c = number of network chains per unit volume of elastomer (moles / unit vol).

R = gas constant.

T = absolute temperature.

ρ = density of the elastomer.

\bar{M}_{nc} = number average molecular weight of the network chains.

The equation is only valid for the case of perfect networks. These consist of chains which are terminated at both ends by crosslinkages. Thus all the polymer chains are incorporated into the network. However, real elastomer networks, unlike their ideal counterparts, contain defects, as depicted schematically in Fig 3.2. Although there is no available treatment for the occurrence of chain loops, or chain entanglements, which act as quasi-crosslinkages, an empirical modification to equation 3.9. for free chain ends has been proposed by Flory⁽¹²⁶⁾, and is given below:-

$$f / A_0 = N_c RT (\lambda - \lambda^{-2}) (1 - \alpha [M_{nc} / M_n]) \quad (3.11)$$

where:-

M_n = number average molecular weight of uncrosslinked polymer.

and α = constant (usually 2.0).

This technique is severely restricted in its application and can only be applied successfully to elastomers which degrade solely by crosslinking reactions. Under these conditions, the following relationship reported by Makhlis^(3f) may be used for the determination of the relevant kinetics.

$$\frac{\sigma}{(\lambda - \lambda^{-2})} = \frac{RTG_c D}{0.48 \times 10^{-6}} - \frac{2\rho RT}{\bar{M}_n} \quad (3.12)$$

where G_c is the crosslink yield, and D is expressed in Mrad.

In practice, if the experimental dependence of the value of $\sigma / (\lambda - \lambda^{-2})$ on the absorbed dose is represented graphically, the radiation yield can be calculated from the gradient of the curve, which has a value of $\rho RTG_c / 0.48 \times 10^{-6}$.

4. Equilibrium Swelling Measurements.

The number of network chains in a crosslinked polymer structure may be determined from the degree of swelling which is encountered when the material is immersed in a suitable solvent (ie, one of similar solubility parameter to the polymer). Under equilibrium conditions, when the polymer has absorbed the solvent and attained constant weight, Flory and Rehner⁽¹²⁷⁻¹²⁹⁾ have proposed the following relationship, from which the crosslink density of the material can be estimated. (the Flory correction for free chain ends has been included in this treatment.):-

$$\ln(1 - \psi) + \psi + \mu\psi^2 + \nu_o \rho_p \left[\left(1 - 2\bar{M}_{nc} / \bar{M}_{no}\right) \right] \left[\psi^{1/3} - 2\psi / f \right] = 0 \quad (3.13)$$

in which:-

$$\nu = 1 / M_{nc} \quad (3.14)$$

$$\psi = 1 / (Q + 1) \quad (3.15)$$

$$Q = \frac{\rho_p}{\rho_s} \left[\frac{P - P_o}{P_o} \right] \quad (3.16)$$

where:-

ψ = volume fraction of polymer in the swollen material.

μ = polymer - solvent interaction parameter (Huggins constant).

ρ_p, ρ_s = density of the polymer and solvent, respectively.

M_{nc} = number average molecular weight of the network chains,

M_{no} = number average molecular weight of uncrosslinked polymer.

f = lattice functionality constant (the number of chains issuing from a lattice point).

ν = number of network chains per unit mass of polymer.

Q = equilibrium degree of swelling of the material.

P_o, P = mass of the sample before and after swelling, respectively.

It is apparent that this technique can be utilised for the evaluation of degradation kinetics in crosslinked materials however it is restricted to those materials which degrade solely by crosslinking reactions, as is the case with equilibrium stress-strain measurements.

3.5. Chemical Stress Relaxation Measurements.

It was first shown by Tobolsky⁽¹³⁰⁾ that stress relaxation of elastomers can occur as a consequence of chemical reactions resulting in a breakdown of the network structure. The importance of these early findings were highly significant, as they revealed that the chemical relaxation responses exhibited by these elastomers were intimately related to the kinetics of the prevailing degradation reactions.

Since these early findings, network degradation theories have been developed, and chemical stress relaxation studies have been undertaken on a vast range of elastomers in order to attempt to resolve their thermal degradation mechanisms. Consequently, the chemical stress relaxation technique is now highly developed, and can be used for the evaluation of a variety of degradation mechanisms, as will become apparent from the proceeding sections.

.1. Evaluation of Kinetics in Elastomers Degrading by Irreversible Main Chain Scission Reactions.

The theories of network degradation by irreversible main chain scission all employ the basic chemorheological relationship developed by Tobolsky as their basis. An understanding of this relationship can be grasped by considering a chemical stress relaxation test on an elastomer which degrades by the above mechanism.

At the outset of a stress relaxation test, the stress at $t = 0$ may be expressed by the following relationship by application of the kinetic theory of rubber elasticity:-

$$\sigma(0) = N_c(0)RT(\lambda - \lambda^{-2}) \quad (3.17)$$

where $N_c(0)$ is the initial number of moles of network chain/unit volume of elastomer. Hereafter this quantity will be referred to as the initial network chain density.

Suppose that after time t the network has degraded and there has $q_m(t)$ main chain cleavages/unit volume of elastomer. There are now $N_c(t)$ network chains/unit volume supporting the stress, which may be given by the relationship:-

$$\sigma(t) = N_c(t)RT(\lambda - \lambda^{-2}) \quad (3.18)$$

where $N_c(t)$ is the network chain density at time t . Combining equations 3.17. and 3.18. results in the expression which is the fundamental equation of chemorheology:-

$$\sigma(t)/\sigma(0) = N_c(t)/N_c(0) \quad (3.19)$$

Hence the stress ratio at a particular time gives the fraction of load bearing chains remaining in the network. However, the total number of scissions which has taken place during this period $q_m(t)$ will be greater than the number of scissions of load bearing chains, as shown in Fig 3.3.

As equation 3.19 only records the cleavages of load bearing chains it cannot be used in the above form for determining the true rate of the scission reaction. This problem is resolved by reference to the theories of network degradation. All the theories are based on the initial proposition that the elastically effective chains in the network have a distribution of chain lengths which may be expressed by the most probable distribution^(131,132) The population of such a relationship is given by the expression:-

$$N_{c_x}(0) = N_c(0)P(1 - P)^{x-1} \quad (3.20)$$

where:-

$N_{c_x}(0)$ = initial number of moles of chains/unit volume
of elastomer of length x .

P = reciprocal of the average chain length.

Berry and Watson⁽¹³³⁾ pictured a network chain as being composed of a number of repeat units, each of which is equally capable of undergoing cleavage, and hence reasoned that the probability of a chain being cut was related to its length (the number of repeat units comprising the chain). Applying this treatment to equation 3.20 yields the following relationship:-

$$N_{c_x}(\tau) = N_c(0)(1 - \beta(\tau))^x \quad (3.21)$$

where $\beta(\tau)$ is the probability that a repeat unit in a network chain has undergone a scission in time τ .

Combining equations 3.21 and 3.20 gives the expression:-

$$N_c(\tau)/N_c(0) = P(1 - \beta(\tau))/(P + \beta(\tau)(1 - P)) \quad (3.22)$$

As all repeat units are equally susceptible to undergo scission irrespective of the length of the chain in which they are contained, $\beta(\tau)$ may be expressed by the equation:-

$$\beta(\tau) = q_m(\tau)/M_0 \quad (3.23)$$

where M_0 is the number of moles of repeat units/unit volume of elastomer capable of undergoing scission. Substitution of equation 3.23 into equation 3.22 leads to the final Berry - Watson relationship between the stress ratio and the number of main chain scissions:-

$$\sigma(\tau)/\sigma(0) = N_c(\tau)/N_c(0) = \frac{P(1 - q_m(\tau)/M_0)}{P + (q_m(\tau)/M_0)(1 - P)} \quad (3.24)$$

Yu⁽¹³⁴⁾ developed an expression based on the assumption that the probability that a particular chain is cut is not dependent on the length of the chain but, ^{depends} on the number of chains of this length in this network. Thus the number of moles of scissions/unit volume of chains of length x is given by the relationship:-

$$q_{m_x}(\tau) = q_m(\tau) \cdot x N_{c_x}(0) / \sum_{x=1}^{\infty} x N_{c_x}(0) \quad (3.25)$$

The number of moles of uncut chains of length x /unit volume at time τ is then given by the expression:-

$$N_{c_x}(\tau) = N_{c_x}(0) (1 - 1/N_{c_x}(0))^{q_{m_x}(\tau)} \quad (3.26)$$

Substitution of equation 3.20 into equation 3.26 and summing over all possible chain lengths leads to the final equation:-

$$\sigma(\tau)/\sigma(0) = N_c(\tau)/N_c(0) = P / (\exp(Pq_m(\tau)/N_c(0)) + P - 1) \quad (3.27)$$

Tobolsky⁽¹³⁵⁾ developed a much simpler theory by assuming that the network was composed of chains of uniform chain length. We now have the conditions:-

$$N_{c_x}(\tau) = N_c(\tau) \quad (3.28)$$

and
$$N_{c_x}(0) = N_c(0) \quad (3.29)$$

Substituting the above relationships into equation 3.21 and employing equation 3.27. leads to the relationship:-

$$\sigma(\tau)/\sigma(0) = N_c(\tau)/N_c(0) = (1 - q_m(\tau)/M_0)^X \quad (3.30)$$

If the average chain length is very large, as is the case in elastomers, the above equation may be approximated to give the simplified relationship:-

$$\sigma(\tau)/\sigma(0) = N_c(\tau)/N_c(0) = \exp(-q_m(\tau)/N_c(0)) \quad (3.31)$$

These three models of irreversible main chain scission have been compared by Murakami and Ono⁽¹³⁰⁾. They investigated the variation of the stress ratio with the number of main chain scissions/unit volume for elastomers with different average chain lengths. It was discovered that as $1/P$ approached 100 (a typical value for elastomers),^{all} the above treatments were equivalent.

These findings imply that the degradation kinetics of elastomers undergoing random scission of the main chain can be evaluated by application of the simplified Tobolsky relationship (equation 3.31.) to chemical stress relaxation data.

Evaluation of Kinetics in Elastomers Degrading by Irreversible Scission of the Crosslinkages.

Murakami and Ono⁽¹³⁰⁾ have proposed that the degradation Kinetics of an elastomer network structure undergoing random degradation of the crosslinkages can be represented by the following relationship:-

$$dq_c(\tau)/d\tau = K(N_{cr}(0) - q_c(\tau)) \quad (3.32)$$

where:-

$N_{cr}(0)$ = initial number of moles of crosslinks/unit volume of elastomer.

$q_c(\tau)$ = number of moles of crosslink scissions/unit volume of elastomer in time τ .

K = constant proportional to the crosslink scission rate.

The above relationship can readily be solved to give ~~the expression below:-~~

$$q_c(\tau) = N_{cr}(0)(1 - \exp(-K\tau)) \quad (3.33)$$

~~Subsequent~~ ~~be~~ - arrangement of the above expression leads to the following ~~relationship~~ which may be utilised for the evaluation of the relevant degradation kinetics from chemical stress relaxation data.

$$\sigma(\tau)/\sigma(0) = 1 - q_c(\tau)/N_{cr}(0) \approx \exp(-K\tau) \quad (3.34)$$

3. Determination of the Site of the Scission Reaction in Degrading Elastomers.

Comparison of equations 3.31. and 3.32. reveals that they are of the same form. This has serious implications, as it suggests, that unless the degradation mode is already known, it will be impossible to evaluate scission kinetics from chemical stress relaxation data. Several techniques have been developed in order to resolve this problem.

1. Technique Proposed by Tobolsky.

This method involves undertaking chemical stress relaxation studies under identical test conditions on elastomers of the same chemical structure but with a range of crosslink densities.

If degradation takes place by scission along the main chain then $q_m(\tau)$ will be independent of the initial crosslink density as shown in Fig 3/4. Thus three elastomers with chain densities of $N_{c_1}(0)$, $N_{c_2}(0)$, and $N_{c_3}(0)$, have the following respective equations for their chemical relaxation response:-

$$\sigma(\tau)/\sigma(0)_1 = \exp(-q_m(\tau)/N_{c_1}(0)) \quad (3.35)$$

$$\sigma(\tau)/\sigma(0)_2 = \exp(-q_m(\tau)/N_{c_2}(0)) \quad (3.36)$$

$$\sigma(\tau)/\sigma(0)_3 = \exp(-q_m(\tau)/N_{c_3}(0)) \quad (3.37)$$

This results in a variation in stress decay as:-

$$\sigma(\tau)/\sigma(0)_1 \neq \sigma(\tau)/\sigma(0)_2 \neq \sigma(\tau)/\sigma(0)_3 \quad (3.38)$$

In the case of degradation by scission of the crosslinkages the following expressions describe the stress decay of the three elastomers assuming that the networks have tetrafunctional crosslinks and the condition $N_{cr} = N_c / 2$ holds :-

$$\sigma(\tau)/\sigma(0)_1 = \exp(-q_{c_1}(\tau)/N_{c_1}(0)/2) \quad (3.39)$$

$$\sigma(\tau)/\sigma(0)_2 = \exp(-q_{c_2}(\tau)/N_{c_2}(0)/2) \quad (3.40)$$

$$\sigma(\tau)/\sigma(0)_3 = \exp(-q_{c_3}(\tau)/N_{c_3}(0)/2) \quad (3.41)$$

Under these conditions $q_c(\tau)$ is dependent upon the initial crosslink density of the elastomer as indicated in Fig 3.5. However Murakami and Ono⁽¹³⁰⁾ demonstrated that for scission of the crosslinks the following condition holds:-

$$q_{c_1}(\tau)/N_{c_1}(0)/2 = q_{c_2}(\tau)/N_{c_2}(0)/2 = q_{c_3}(\tau)/N_{c_3}(0)/2 \quad (3.42)$$

Thus the three elastomers will exhibit identical chemical relaxation responses ~~if degradation takes place by scission of the crosslinkages.~~

Empirical Technique Proposed by Osthoff et al.

An alternative method of scission site determination has been proposed by Osthoff et al⁽¹⁰³⁾. By analysing the shape of the chemical relaxation curve it is possible to discern if the scission reaction occurs at the crosslinks or randomly along the main chain.

Using an analogue model network of interconnecting springs the following relationship was derived for the chemical relaxation response of such a network undergoing degradation by a first order scission reaction occurring randomly along the main chain.

$$\sigma(\tau) = 2RT(X_0 - N_0)\rho(\exp(Kt) - 1 + \rho)^{-1} \cdot \phi(\lambda) \quad (3.43)$$

where:-

X_0 = number of moles of crosslinks/unit volume of elastomer.

N_0 = number of moles of polymer/unit volume before vulcanization.

ρ = the reciprocal of the degree of polymerisation of polymer chains between crosslinks.

K = rate constant for the chain scission process.

$\phi(\lambda)$ = a function of the extension of the sample which defines the shape of the stress-strain curve.

Equation 3.42. may be expanded to give the following expression:-

$$1/\sigma(\tau) = A(1 + Kt/\rho + (Kt)^2/\rho^2! + (Kt)^3/\rho^3! + \dots) \quad (3.44)$$

where A is a constant = $2RT(X_0 - N_0)\phi(\lambda)^{-1}$

As K is small we can neglect terms in equation 3.43. of $(Kt)^2$ and above which reduces the expression to:-

$$1/\sigma(\tau) = A(1 + Kt/\rho) \quad (3.45)$$

Multiplying through by the initial stress $\sigma(0)$ results in the expression:-

$$\sigma(0)/\sigma(\tau) = B(1 + Kt/\rho) \quad (3.46)$$

Where B is a constant of the value σ/A .

Equation 3.45 . may be expanded to give the final equation:—

$$\sigma(0)/\sigma(t) = B + K_s t \quad (3.47)$$

where K_s is a constant proportional to the rate constant of the random main chain scission reaction.

Hence it is apparent that the inverse stress ratio will vary in a linear manner, if degradation is taking place by a random main chain scission reaction.

3.5.4. Evaluation of Degradation Kinetics of Elastomers undergoing Simultaneous Scission and Crosslinking reactions.

Many elastomers undergo crosslinking and scission reactions simultaneously during degradation. In these circumstances it is possible to determine the rates of both the crosslinking and scission reactions by the use of intermittent stress relaxation data in conjunction with conventional, or continuous, stress relaxation data. It is assumed that the continuous stress relaxation response is not affected by the crosslinking reaction, as the network chains which are formed equilibrium at the constant strain employed during the stress relaxation test. Hence the equations previously derived for main chain scission and scission of the crosslinkages may still be successfully applied to systems in which appreciable amounts of crosslinking are occurring.

This assumption has been confirmed by a number of theoretical and experimental investigations (136-141). The elastomer may be envisaged as being comprised of two independent networks, the initial network, bearing

the stress, and a new stress free network comprising chains that have been crosslinked during stress relaxation. Consequently this model is known as the Tobolsky two-network hypothesis, or the double lattice theory.

The principle of intermittent stress relaxation testing is shown in Fig 3.6. The unloaded sample is rapidly loaded to a preset strain after a time interval t , the intermittent stress recorded, and the sample rapidly unloaded. This procedure is repeated over the whole time scale of the experiment. The time taken in loading, recording the stress, and unloading the sample is very small with respect to t , and it is therefore assumed that the number of crosslinks formed during this period may be neglected.

Consider the case of an elastomer degrading by simultaneous main chain scission and crosslinking reactions. Bearing in mind that the relationship between the initial network chain density and the initial crosslink density is given by:- (~~assuming that the crosslinkages in the network are tetrafunctional~~)

$$N_c(0) = 2N_{cr}(0) \quad (3.48)$$

The number of moles of additional crosslinks/unit volume in time t may be expressed as $\Delta N_{cr}(t)$ and the network chain density at this time may be given by the relationship:-

$$N_c(t) = 2N_{cr}(t) = 2N_{cr}(0) - q_m(t) + 2\Delta N_{cr}(t) \quad (3.49)$$

Employing equations 3.9. and 3.10 the intermittent stress measurement at time t can be represented by the following equation:-

$$\sigma_i(t) = (2N_{cr}(0) - q_m(t) + 2\Delta N_{cr}(t))RT(\lambda - \lambda^{-2}) \quad (3.50)$$

Similarly the stress measurement at the same time t in a continuous stress relaxation test may be given by the expression:-

$$\sigma_c(t) = (2N_{cr}(0) - q_m(t))RT(\lambda - \lambda^{-2}) \quad (3.51)$$

The continuous relaxation response may be subtracted from the intermittent relaxation response to give the relationship:-

$$\sigma_i(t)/\sigma_i(0) - \sigma_c(t)/\sigma_c(0) = 2\Delta N_{cr}(t)/N_c(0) = \Delta N_{cr}(t)/N_{cr}(0) \quad (3.52)$$

If the rate of crosslinking is approximately constant, equation 3.52 may be rewritten as:-

$$\sigma_i(t)/\sigma_i(0) - \sigma_c(t)/\sigma_c(0) = \Delta N_{cr}(t)/N_{cr}(0) = Kt/N_{cr}(0) \quad (3.53)$$

where K is a constant proportional to the rate of the crosslinking reaction.

Hence the fraction of crosslinkages formed in a particular time may be evaluated by subtraction of the intermittent relaxation response from the continuous relaxation response.

In the case of an elastomer degrading by simultaneous scission of the crosslinks and crosslinking reactions the network chain density may be given by the expression:-

$$N_c(t) = 2N_{cr}(t) = 2N_{cr}(0) - 2q_c(t) + 2\Delta N_{cr}(t) \quad (3.54)$$

Hence the intermittent stress at time t may be given by the equation:-

$$\sigma_i(\tau) = (2N_{cr}(0) - 2q_c(\tau) + 2\Delta N_{cr}(\tau))RT(\lambda - \lambda^{-2}) \quad (3.55)$$

Similarly the continuous stress value at this time can be represented by the expression:-

$$\sigma_c(\tau) = (2N_{cr}(0) - 2q_c(\tau))RT(\lambda - \lambda^{-2}) \quad (3.56)$$

As before the continuous relaxation response may be subtracted from the intermittent relaxation response to give the relationship:-

$$\sigma_i(\tau)/\sigma_i(0) - \sigma_c(\tau)/\sigma_c(0) = \Delta N_{cr}(\tau)/N_{cr}(0) \quad (3.57)$$

It can be seen that the above equation is identical to equation 3.53. indicating that the same procedure may be used for the evaluation of the crosslinking kinetics irrespective of whether the accompanying scission reaction takes place along the main chain or at the crosslinks.

3.6. Sol / Gel Fraction Measurements in Conjunction with Chemical Stress Relaxation Measurements.

Chemical stress relaxation data may be used in conjunction with sol fraction data to yield information on the scission reactions in degrading elastomers. Utilising the sol fraction equation proposed by Charlesby⁽¹²²⁾ in conjunction with equations relating the number and site of scissions in a network to the degree of swelling at equilibrium, Horix⁽¹⁴²⁾ proposed the following relationships between stress ratio from chemical relaxation studies, and sol fraction data for degradation by the following mechanisms:-

(i) Random scission along the main chain:-

$$\sigma(t)/\sigma(0) = ((1 - S(t)^{1/2})(1 - S(0)^{1/2}))^2 \quad (3.58)$$

(ii) Scission of crosslinkages:-

$$\sigma(t)/\sigma(0) = (S(0) + S(0)^{1/2})(1 - S(t)^{1/2}) / (1 - S(0)^{1/2})^2 (S(t) + S(t)^{1/2}) \quad (3.59)$$

id (iii) Selective scission near crosslink sites:-

$$\sigma(t)/\sigma(0) = ((1 - (2S(t))^{1/2}) / (1 - S(0)^{1/2}))^2 \quad (3.60)$$

Where $s(t)$ and $S(0)$ are the sol fractions at times t and 0 respectively

The method employed in identifying the site of the scission reaction is to simply plot the above three relationships as a function of time together with the respective chemical relaxation curve. The relationship which coincides with the relaxation curve identifies the site of the scission reaction. If the system under consideration exhibits no crosslinking during degradation, continuous stress relaxation is employed. If a small amount of crosslinking takes place during degradation then intermittent stress relaxation data is employed.

The advantage of this technique is that only one relaxation curve, in conjunction with the appropriate sol fraction data is required to determine the site of the scission reaction, unlike the method proposed by Tobolsky, ~~in Section 3.5.3.1.~~ which requires several relaxation curves.

The major disadvantage of this technique is that it is only applicable to elastomers which degrade by predominant scission reactions. It is invalid for elastomers which exhibit appreciable crosslinking during degradation.

4. Aspects of Irradiation Studies.

4.1. Basic Definition of Absorbed Dose and Units of Measurement.

In early investigations, the degree of interaction of radiation with polymers was expressed by a large variety of measurement units. The majority of these were not applied vigorously, making it difficult, almost impossible in some cases, to compare the findings of different workers. Only recently has there been a tendency to adopt only those units which correctly describe the process of radiation energy transfer to the irradiated substance.

The absorbed radiation energy may be defined as the difference between the total energy of all the particles and quanta, entering a given volume, and the total energy of all the particles and quanta leaving this volume, minus the energy equivalent of any increase in the rest mass in the volume studied as a result of nuclear reactions^(3g). The energy absorbed per unit mass of the irradiated substance is called the absorbed dose.

It must be emphasised that the energy transmitted by radiation to any substance is not necessarily the absorbed energy as part of the transmitted energy may leave the given volume in the form of secondary charged particles or electromagnetic radiation.

The unit of absorbed dose recommended by ICRU^(143,144) (International Commission on Radiological Units), and the one employed in our studies, is the rad, and is defined as:-

$$\begin{aligned} 1.0 \text{ rad} &= 100 \text{ ergs g}^{-1} \\ &= 6.25 \times 10^{13} \text{ eV g}^{-1} \\ &= 10^{-5} \text{ J g}^{-1} \end{aligned}$$

The new SI unit of absorbed dose is the Gray (Gy) and has the following definition:-

$$1.0 \text{ Gy} = 100 \text{ rads}$$

The unit that is generally used in the current literature is the Mrad, and there is, seemingly, a reluctance to introduce the Gray.

2. Radiation Sources.

Of the available radioactive isotopes, cobalt-60 is the most widely used as a consequence of its ease of preparation, fairly long half life, and penetrating power. It is produced by the activation of cobalt-59 in a high neutron flux, by the following mechanism:-



After neutron capture, the pure metallic cobalt in the form of small rods is hermetically sealed by double encapsulation in stainless steel. The ${}^{60}\text{Co}$ source emitting 0.31 MeV β -rays and two successive γ -photons of 1.17 and 1.33 MeV (mean energy of 1.25 MeV). The β -rays are absorbed in the ${}^{60}\text{Co}$ itself, or in the encapsulating material.

A second source, that is sometimes used, is ${}^{137}\text{Cs}$, which is obtained from the spent fuel rods of a nuclear reactor. On removal from the core the radioactivity decays in a very short period of time, and the rods are processed to obtain the fission products. After extensive separation the resultant ${}^{137}\text{Cs}$ is transformed to chloride or sulphate salt and encapsulated in the same type of container as for ${}^{60}\text{Co}$.

At one time it was thought that ${}^{137}\text{Cs}$ might replace ${}^{60}\text{Co}$, due to the large quantities of material that are available from nuclear reactor plants. However, the safety hazards associated with this source have prevented its widespread use in industrial and research applications.

4.3. Dosimetry.

There are many available methods that can be employed to experimentally determine the energy absorbed by a material exposed to ionising radiation. They can be divided into two groups; absolute, or relative methods, otherwise known as standard and routine methods, respectively.

The radiation field of a γ -source can be analysed using an absolute dosimeter, such as an ionisation chamber, or the Fricke dose meter. The latter is based on the radiation induced oxidation of ferrous ions, and is an irreversible reaction.

Once a radiation field has been determined by an absolute method, it is possible to calibrate other radiation indicators, which are more practicable. These include scintillation, photographic, and colourmetric dosimeters. A large number of solid substances, such as glasses, crystals, and certain plastics become discoloured, when exposed to ionising radiations. All these colour changes, when measured quantitatively, can be used for dosimetric purposes.

4.4. The Concept of the Radiation Yield.

As indicated in Section 2.2., the primary reactions which arise as a consequence of incident radiation can lead to a host of subsequent chemical, and physical changes in the structure of polymers. Many workers active in the field of radiation chemistry express these changes by the radiation yield G , which can be defined simply as the number of such changes that take place in a particular system during the absorption of 100 eV of radiation energy.

5. Experimental.

5.1. Materials.

5.1.1. Materials Selection.

The polymers chosen for study in the present investigation are from the two families of elastomers which possess outstanding thermal stability, the silicone elastomers, and the fluorinated hydrocarbon rubbers (145). It should be noted that these materials are not the most radiation resistant rubbers (109). An elastomer which possesses good thermal stability does not necessarily possess a high resistance to ionising radiations. Despite this fact these materials are used extensively in nuclear engineering applications where both thermal and radiative stability are required.

The silicone rubber selected for investigation was a simple polydimethylsiloxane elastomer (PDMS). This material is 'vinyl free' unlike commercial PDMS which has a small number of methylvinyl groups (0.1 mol%) incorporated in the main chain in order to achieve a more efficient cure . When cured with a diaryl peroxide PDMS forms a simple network structure by a well established curing mechanism making it an ideal material on which to conduct initial investigations. However, the exact curing mechanism of polydimethylvinylsiloxane (PDMS) is uncertain (146.) it may lead to the formation of several types of crosslinks and possibly the incorporation of peroxide residues in the crosslinkages, all of which will have a pronounced effect on the degradation of the elastomer. The PDMS network is virtually ideal with regard to the kinetic theory of rubber

elasticity, a feature which has led to its widespread use in the experimental verification of the theory⁽¹⁴⁷⁻¹⁵³⁾; Thus the basic chemorheological relationships (equations 3.17 - 3.57) can be applied successfully to this particular elastomer. The material contained no filler as this could influence degradation reactions.

In contrast, the fluorocarbon rubber studied was a low compression set formulation of a vinylidene fluoride-hexafluoropropylene copolymer marketed by Du Pont Ltd under the trade name Viton E60C.

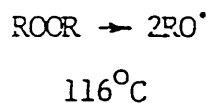
It is well known that the incorporation of styrene into the structure of PDMS by copolymerisation is a well established method for the production of silicone elastomers with enhanced radiation stability^(69,72,89-91). However recent findings by Astill⁽¹⁰⁰⁾ reported in section 2.6.1.1.3, suggest a far simpler and cheaper method of producing such materials. It appears that the irradiation of PDMS/PS blends containing 1 - 5wt% PS is a possible route for the synthesis of radiation resistant elastomers. Bearing in mind these findings it was decided that a range of these materials containing various percentages of PS would be produced and their degradation kinetics investigated and compared with those of PDMS elastomers.

5.1.2. Materials Preparation.

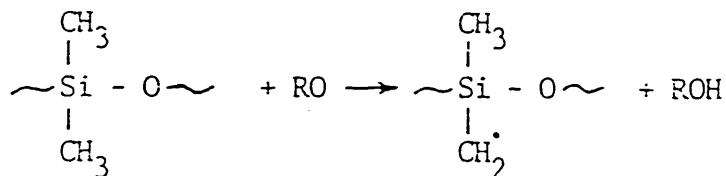
5.1.2.1. Preparation of Peroxide - Cured PDMS elastomer.

PDMS gum ($M_n = 84,000$) supplied by Dow Corning Ltd was cold milled with bis 2,4 - dichlorobenzoyl peroxide paste (50% 2,4 - DCBP in a low molecular weight silicone fluid) and press cured at 116°C and 400 p.s.i. in accordance with the manufacturers recommendations. The curing process which results in the formation of simple ethylene crosslinkages consists of the following stages :-

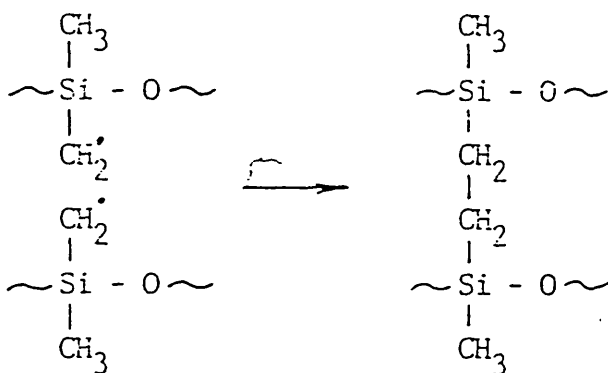
(1) Decomposition of the peroxide:-



(2) Hydrogen abstraction from a methyl side group:-



(3) Ethylene bridge formation by the combination of two radicals:-



Curing was followed by a stabilising post-cure treatment at 200°C in an air circulatory oven.

Samples for physical stress relaxation testing were taken from sheet approximately 1.5 mm in thickness. The material was milled with 2.0 wt% 2,4-DCBP paste and cured for 10 minutes prior to a post cure of 24 hrs.

Samples for chemical stress relaxation testing were produced as cylindrical slugs. These were cured for 20 mins followed by a 24 hr post cure. Material was manufactured with initial additions

of 1.0, 1.25, and 1.50 wt% 2,4-DCBP paste to give elastomers with a range of crosslink densities.

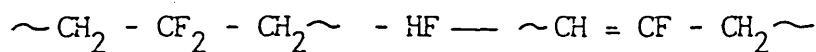
PDMS elastomers employed in cure / post cure investigations were prepared as sheet approximately 1.5 mm in thickness. Full details of peroxide additions and cure / post cure treatments are given in Table 6.4.3.1.

1.2.2. Preparation of Viton E60-C elastomer.

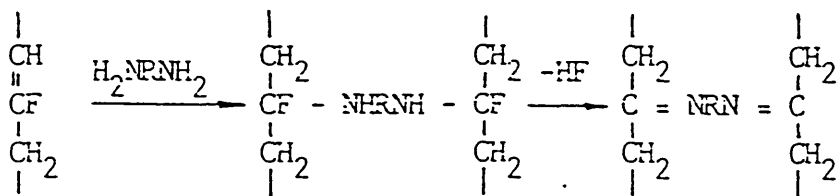
Viton E60C was supplied in the cured condition by DuPont Ltd. This is because processing is complex, and may be dangerous due to the evolution of toxic fumes such as hydrogen fluoride during curing. Material was supplied as sheet 2.0 mm in thickness for physical stress relaxation testing and as cylindrical slugs for chemical stress relaxation studies.

Curing is achieved by using a diamine derivative, in this case hexamethylene diamine carbamate, in conjunction with a metal oxide, usually MgO. The curing reaction is believed to consist of the following stages:-

(1) Dehydrofluorination takes place in the presence of the diamine derivative, which leads to the removal of fluorine from the hexafluoropropylene segment of the polymer:-



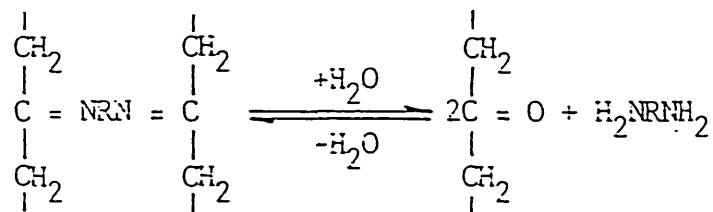
(2) Further diamine acts at the site of unsaturation to form amine crosslinkages:-



Throughout the reaction HF is removed from the system by magnesium oxide:-



Water resulting from the neutralisation of HF must be removed in order to stabilise the crosslinkage as the following equilibrium exists in the presence of water:-



This is achieved by incorporating a metal hydroxide in the blend and subjecting the elastomer to a stabilising post cure treatment.

Viton E60C was milled with Diak No 1. (hexamethylene diamine carbamate), 3 parts per hundred by weight of Maglite D (high activity magnesium oxide) and 6 parts per hundred by weight of calcium hydroxide. The material was press cured at 177°C for 15 minutes followed by a post cure treatment of 24 hrs in air at 232°C.

1.2.3. Preparation of PDMS Elastomer Containing Entrapped PS.

The required quantities of PDMS ($M_n = 253,000$) and PS ($M_n = 100,000$) to give resultant blends containing 1.0, 2.0, and 3.0wt% PS were dissolved in a common solvent (in this case tetrahydrofuran). After the polymers had been thoroughly mixed the solvent was removed by freeze drying and the blends then placed in cylindrical polyethylene moulds. Subsequent vulcanization took place by exposing the blends to a Co^{60} source where crosslinking of the PDMS occurred by the mechanisms described in section 2.6.1.1. Based on information from related studies on the irradiation of blends the samples were subjected to an absorbed dose rate of approximately 0.2 Mrad.hr to an integrated dose of 5.0 Mrad. Such a procedure ensures that the PDMS is crosslinked whilst leaving the PS unaffected⁽¹⁰⁾.

The resultant samples had dimensions which were identical to those employed in the stress relaxation studies on PDMS elastomer.

5.1.3. Materials Characterisation.

1.3.1. Characterisation of PDMS and VitonE60-C Elastomers.

The number average molecular weights (M_n) of the uncrosslinked polymers were determined by gel permeation chromatography at RAPRA using monodisperse polystyrene as a standard.

The crosslink densities (N_{CR}) of the vulcanized elastomers were determined by equilibrium stress-strain measurements. N_{CR} of cured slugs used in the chemical stress relaxation studies were determined under uniaxial compression using an Instron (model No 1112.) testing machine. The samples were lubricated with silicone fluid in order to prevent friction at the platen / sample interface, ensuring uniaxial compression conditions, and then deformed at a crosshead speed of 0.5 cm.min^{-1} . to $\lambda = 0.7$.

In order to assess sample homogeneity, specimens were taken at selected sites within a sample, as indicated in Table 6.1.2., and subjected to equilibrium swelling measurements. Measurements were carried out in accordance with BS 903 Part A16. Samples approximately 5.0 x 5.0 x 5.0 mm. were swollen in an appropriate solvent (toluene for PDMS and methylethylketone for Viton E60C). It was assumed that equilibrium conditions had been established (complete swelling) when the sample had attained constant weight. The change in volume method was used to determine N_{cr_s} .

N_{cr} of the cured sheet material used in the physical stress relaxation studies and preliminary cure / post cure trials on PDMS elastomer was determined under uniaxial tension. Samples were loaded at a crosshead speed of 0.5 cm.min⁻¹. to $\lambda = 1.5$.

1.3.2. Characterisation of PDMS elastomer Containing entrapped PS.

Unfortunately, the discrete PS phase present in these materials acted as a reinforcing filler and hence the crosslink density of the PDMS matrix could not be determined by the techniques employed in the previous section.

The morphology of the entrapped PS phase was revealed by a technique which utilises the different properties of the two polymers. Samples of material were fractured at - 95°C, a temperature intermediate between the glass transition temperatures of the PDMS (- 123°C) and the PS (100°C). At this temperature the PDMS had a leathery consistency and underwent tearing, whilst the PS phase was glassy and remained unfractured and embedded in the surface. Examination of the fracture surfaces was carried out using a Philips Joel 100b scanning electron microscope. Micrographs were taken of representative areas at a standard magnification of x 400 for the three elastomers (1.0, 2.0, and 3.0 wt% PS). The average particle size of the PS phase and its volume fraction were determined using an Optimax Quantimet instrument.

5.2. Experimental Procedure.

It is proposed that degradative reactions which take place when the above elastomers are subjected to heat and radiation are studied by the chemorheological techniques outlined in Section 3.5. However it will be appreciated that these techniques are only valid when they are applied to pure chemical stress relaxation data. The physical stress relaxation response must be evaluated to determine the role played by this process in the overall stress relaxation response. If this effect is significant then the stress relaxation data must be adjusted accordingly.

2.1. Physical Stress Relaxation Studies on PDMS and Viton E60-C elastomers.

The physical stress relaxation response of the elastomers was determined with a Rheovibron Model DDV-II-C Dynamic viscoelastometer. PDMS samples used in the investigations had dimensions of 1.5 x 4.0 x 17.0 mm. Viton E60C samples measured 2.0 x 4.0 x 17.0 mm.

Studies undertaken on PDMS elastomer were carried out over the temperature range -120 to -70°C using a low temperature cabinet. The samples were rapidly cooled by quenching in liquid nitrogen immediately before testing in order to prevent crystallization. Viton E60C elastomer was tested over the temperature range 20 to 200°C using the Rheo - 420 high temperature vessel. Temperature was monitored by a chromel - alumel thermocouple which was incorporated in the cabinet. The standard clamps were replaced by a set which were made according to the design proposed by Seferis^(15A) as shown in Fig 5.1. Samples were glued in the clamps by cyanoacrylate or epoxy adhesive in preference to using the securing screws, as this led to distortion of the samples in the clamps.

Storage shear modulus (G') and loss tangent ($\tan\delta$) values were measured over a range of temperatures and frequencies for both materials. Subsequently this data was treated in accordance with the time-temperature superposition principle to obtain storage shear modulus curves covering a more extended time range.

5.2.2. Thermal Degradation Studies.

5.2.2.1. Chemical Stress Relaxation Studies on PDMS and Viton E60-C Elastomers.

Studies were carried out on cylindrical samples measuring 27.0 x 30.0 mm diameter in the case of PDMS elastomer and 15.0 x 25.0 mm in diameter in the case of Viton E60C elastomer.

Both continuous and intermittent chemical stress relaxation studies were undertaken in air over the temperature range 25 - 300°C. Tests were performed under uniaxial compression conditions using an Instron (model No 1.1.1.2.) testing machine. Temperature control over the range 25 - 150°C was achieved using an Instron (model No 3.1.1.1.) environmental cabinet. Tests at the higher test temperatures of 200 and 300°C were carried out using a furnace and temperature control device (Honeywell model No C.L.40.). Water-cooled platens were used during the tests to prevent transfer of heat to the load cell. Once the cabinet / furnace had stabilised at the required test temperature, samples were placed on the platens and allowed to reach constant temperature throughout their section before testing commenced. Heating times were determined for the test temperatures employed by using the relevant thermal data for the elastomers.

The platen interfaces were lubricated with silicone fluid in order to prevent friction at the sample / platen interface during initial loading. Stress was monitored with an Instron load cell and the response recorded directly on the chart recorder.

Samples subjected to continuous stress relaxation studies were initially loaded at a crosshead speed of 0.5 cm.min^{-1} . to an extension ratio $\lambda = 0.85$. During the initial stages of the test, when stress relaxation is rapid, the stress was continuously monitored. At longer times, when the rate of stress decay had decreased, the stress was monitored on an intermittent basis. This was achieved by the use of an automatic chart control device incorporated in the drive unit. This enabled the chart to be activated after some preset time interval for a specific time. All tests were terminated after 10^6 secs.

Intermittent stress relaxation tests were carried out over the time range 0 to 10^6 secs. Samples were loaded at a crosshead speed of 0.5 cm.min^{-1} . and the stress recorded at a standard extension ratio of $\lambda = 0.85$. The sample was then rapidly unloaded. This procedure was repeated at regular time intervals (based on a logarithmic time scale) over the time range of the experiment.

2.2.2. Cure / Post Cure Trials on PDMS elastomer.

Material used in the cure / post cure investigations carried out on PDMS elastomer was in the form of sheet approximately 1.5mm. in thickness. Curing was carried out in a compression mould at a pressure of 2000 p.s.i. with a mould wall temperature of 116°C . Post curing was undertaken in an air circulatory oven at 200°C . Curing times ranged from 5 to 20 mins. and post cure times ranged from 2 to 24 hrs. Experimental details are given in Table 6.4.3.1

2.3. Combined Thermal / Radiative Degradation Studies.

3.1. Chemical Stress Relaxation Studies on PDMS and Viton E60-C Elastomers.

The continuous stress relaxation response of the above elastomers was monitored over the temperature range 40-200°C during γ -irradiation by a stress relaxation rig designed and manufactured at the polytechnic.

The assembled rig, which enables tests to be undertaken under conditions of uniaxial compression, is shown schematically in Fig 5.2. and in Plate 5.1. The whole assembly was enclosed between two circular flanges, which were supported by four pillars. The sample was loaded automatically by a pneumatic ram, which was driven by compressed air. When the lower ram was activated the lower platen was raised and held at constant displacement throughout the test by four spring-loaded pins located in the recess of the platen.

The pneumatic cell consisted of a single acting 25mm. stroke ram (Schrader Bellows Model No. 40 - 9010000). The ram was surrounded by an anodised aluminium housing, which contained the spring-loaded pins. This housing acted as a guide for the lower platen, ensuring that it was presented squarely to the sample. The lower platen was a composite which enabled its length to be altered in order to accommodate samples of various sizes.

The upper platen, which was connected to the load cell, was separated by a Kaolin wool strip in order to prevent heat transfer to the load cell. The load cell (AJB Associates Model No. 462.) consisted of a simple rectangular casting which contained a bridge network of four strain gauges, which were secured with epoxy resin.

The load cell was connected to a combined bridge supply, amplifier and balance unit (FE - 359 - TA. Fylde Instruments). The output from the unit was fed into a channel of a 5401 Honeywell chart recorder.

The sample was heated by a tube furnace, working from a 12V supply. Temperature control was achieved by using a chromel/alumel thermocouple, which was placed in the furnace adjacent to the sample, in conjunction with a Honeywell temperature control device (Model No. CL 40).

The output from the thermocouple was also fed to the Honeywell recorder so that both stress and temperature could be constantly monitored. The assembly can be enclosed in a glass cylinder, which is located on the silicone rubber seals which were set in the recesses of the top and bottom flanges. These seals were made from a room temperature vulcanising (RTV) elastomer known commercially as Silcaset. This feature provided the opportunity for undertaking tests under inert or any other specified environment.

Sample irradiation was carried out in the γ -cell at Berkeley laboratories and a schematic diagram of the facility is given in Fig 5.3. The source consisted of a cylindrical array of ^{60}Co pencils which were attached to an automatic loading/retracting mechanism. The protective surrounding walls were made of 1m thick concrete and were lead lined. The hydraulically activated door provided access into the cell.

The total absorbed dose depended on the proximity of the sample to the source, which effects the dose rate, and the length of time spent in the cell. Absorbed dose was measured using polymethylmethacrylate dosimeters.

All the tests were carried out at the maximum dose rate available from this facility (when the rig was as close as possible to the source). The maximum absorbed dose rate was found to be $1.05 \text{ Mrad.hr}^{-1}$

Before the commencement of a test the load cell was balanced and then calibrated with standard weights to ensure that it was still operational. A sample was then placed in the rig, which was outside the irradiation cell, and allowed to reach the desired test temperature. The rig was then introduced into the irradiation cell and the sample loaded immediately after the introduction of the source. Both temperature and stress were monitored throughout the duration of the stress relaxation test.

6. Results.

6.1. Characterisation of PDMS and Viton E60-C Elastomers.

Before investigations were undertaken the material was fully characterised using the techniques outlined in section 4. Equilibrium stress-strain measurements were employed in order to determine the overall crosslink density of the material comprising the samples. Equilibrium swelling measurements were used to determine the crosslink density of small volumes of material selected from specific sites within the samples in order to assess sample homogeneity.

The crosslink densities ($N_{cr_m}(0)$) of the material employed in the physical relaxation studies were $0.118 \times 10^{-6} \text{ mol.mm}^{-3}$ and $0.722 \times 10^{-6} \text{ mol.mm}^{-3}$ for PDMS and Viton E60C elastomers, respectively.

$N_{cr_m}(0)$ of the PDMS slugs employed in the chemical relaxation studies are presented in Table 6.1.1. The samples had average crosslink density values of $0.108 \times 10^{-6} \text{ mol.mm}^{-3}$, $0.118 \times 10^{-6} \text{ mol.mm}^{-3}$, and $0.129 \times 10^{-6} \text{ mol.mm}^{-3}$, corresponding to peroxide additions of 1.0, 1.25, and 1.50wt% 2,4-DCBP paste.

$N_{cr_s}(0)$ values of samples taken at specified sites within a test specimen in order to evaluate sample homogeneity are given in Table 6.1.2. for the three PDMS elastomers. The results indicate that all the samples have a slightly lower $N_{cr_s}(0)$ at the centre than at their edges.

$N_{cr_m}(0)$ of the Viton E60C slugs used in the chemical relaxation studies are reported in Table 6.1.3. The material had an average crosslink density of $0.722 \times 10^{-6} \text{ mol.mm}^{-3}$. Sample homogeneity studies (Table 6.1.4.) revealed that the samples had a constant crosslink density throughout their section.

In all the characterisation investigations it was observed that the crosslink densities obtained by equilibrium swelling measurements were correspondingly lower than those obtained by stress-strain measurements.

6.2. Characterisation of PDMS Elastomer Containing Entrapped PS.

The morphologies of the elastomers containing 1.0, 2.0, and 3.0 wt% PS additions are shown in Plates 6.2.1., 6.2.2., and 6.2.3. respectively. These are scanning electron micrographs of representative areas of fracture surfaces at a standard magnification of x 400.

From the SEM studies it became apparent that the materials consisted of two distinct phases; a predominantly PDMS phase and a distinct separate phase which had a spherical morphology. This phase was selectively removed from a fractured sample containing 1.0 wt% PS by immersion in toluene for 24 hrs. Evidence of this is provided in plate 6.2.4. where voids can clearly be seen at the sites once occupied by the phase.

Subsequent analysis of the extracted phase by IR analysis was not conclusive. It was established that the phase was predominantly PS but significant quantities of PDMS were also detected. It was unclear whether this had arisen from the PDMS matrix or the second phase.

6.3. Physical Stress Relaxation Studies on PDMS and Viton E60-C Elastomers.

Values of storage shear modulus (G') and loss tangent ($\tan \delta$) for PDMS elastomer ($N_{cr_m}(0) = 0.108 \times 10^{-6} \text{ mol. mm}^{-3}$) over a range of temperatures at test frequencies of 3.5, 10, and 35 Hz are presented in Fig 6.3.1. At all frequencies a pronounced decrease in both G' and $\tan \delta$ was observed in the region of -110°C indicating the proximity of

the glass transition ($T_g = -123^\circ\text{C}$ for linear PDMS). A small peak which may be attributed to some secondary transition was also present in all the curves in the region of -95°C to -100°C . The peak became more pronounced at higher frequencies. The master curve showing the variation in storage shear modulus with time for a reference temperature of -57°C is given in Fig 6.3.2. It can be seen that the storage shear modulus decreased with time finally reaching an approximately constant value of $3.75 \times 10^5 \text{ Nm}^{-2}$ in the region of 10^{-3} sec.

The corresponding master curve for Viton E60-C at a reference temperature of 100°C is presented in Fig 6.3.3. The storage shear modulus again decreased with time, as was the case with the previous elastomer, and attained an approximately constant value of $3.75 \times 10^6 \text{ Nm}^{-2}$ in the region of 10^{-1} sec. As the modulus curve for the Viton E60-C elastomer was more complete than that of the PDMS elastomer, the relevant WLF constants for the superposition of the storage shear modulus could be determined. This was achieved by constructing a curve of the shift factor required by each separate modulus-time curve at a particular temperature to attain superposition against the difference between the temperature at which the curve was recorded and the reference temperature. This relationship is presented in Fig 6.3.4. A curve of $(T - T_{\text{ref}}) / \log a_T$ vs $(T - T_{\text{ref}})$ was then constructed from this data (Fig 6.3.5.) and this enabled the constants to be determined from the following expressions:-

$$C_1 = -1/S$$

and $C_2 = -i/S$

where i is the intercept and S is the gradient of the curve.

Using the above approach the values of C_1 and C_2 were estimated as 3.67 and 221.0 K respectively.

6.4. Thermal Degradation Studies.

In accordance with Section 3.5.3 two kinds of stress relaxation tests were undertaken in the ensuing degradation studies; conventional stress relaxation testing, which yields data for the evaluation of scission kinetics, and intermittent stress relaxation testing, which enables cross-linking rates to be determined. In the case of PDMS elastomer the site of the scission reaction was investigated by using the technique proposed by Tobolsky, which involves undertaking conventional stress relaxation tests on elastomers of different initial crosslink densities under identical test conditions.

6.4.1 Chemical Stress Relaxation Studies on PDMS elastomer.

Continuous stress relaxation curves for elastomers of initial crosslink density $N_{cr} (0) = 0.108 \times 10^{-6} \text{ mol. mm}^{-3}$, $0.118 \times 10^{-6} \text{ mol. mm}^{-3}$, and $0.129 \times 10^{-6} \text{ mol. mm}^{-3}$ at a standard temperature of 150°C are presented in Fig 6.4.1.1. A variation in the stress relaxation response exhibited by the three elastomers is clearly evident. Furthermore the rate of stress decay appeared to increase with decreasing initial cross-link density.

Continuous stress relaxation curves for the elastomer ($N_{cr} (0) = 0.118 \times 10^{-6} \text{ mol. mm}^{-3}$) at temperatures over the range $25 - 200^{\circ}\text{C}$ are given in Fig 6.4.1.2. The rate of stress decay increased with increasing temperature.

The accompanying intermittent stress relaxation curves for this material over the temperature range $25 - 150^{\circ}\text{C}$ are shown in Fig 6.4.1.3. At the lower test temperatures (25 and 50°C) the intermittent curves are approximately linear. However, at the higher temperatures the curves

are nonlinear showing an increase in the intermittent stress ratio $\sigma_i(t) / \sigma_i(0)$ at longer times. The magnitude of this deviation appeared to increase as the temperature was increased.

The number of moles of main chain scissions / unit volume of elastomer taking place in time t , ($q_m(t)$) was estimated from the data of Fig 6.4.1.2. by application of the relationship proposed by Eyring (equation 3.31.). The results are given in Fig 6.4.1.4. All the curves exhibited the same shape. After an initial region in which the rate of increase of $q_m(t)$ decreased with time the curves became linear. Indicating a constant rate for the chain scission reaction. The gradient (K) of this region was taken as the rate constant of the chain scission reaction. It can be seen from the curves that the reaction rate constant increased with increasing temperature. In order to determine the activation energy of this reaction an Arrhenius plot of the data was constructed and is given in Fig 6.4.1.5. The curve was approximately linear and least squares regression analysis on the data to give the best fitting line yielded a value of $15 \pm 4 \text{ K mol}^{-1}$ for the reaction.

The chemical relaxation data of Fig 6.4.1.2. was treated by an alternative method proposed by Osthoff et al (section 3.5.3.2.) for determining the site of the scission reaction. The resultant curves of inverse stress ratio ($\sigma(0) / \sigma(t)$) vs t are presented in Fig 6.4.1.6. At all test temperatures the curves were linear. The gradient of the curve was taken as a constant which was proportional to the chain scission rate. An activation energy plot of $\ln K$ vs $1 / T$ for this data is given in Fig 6.4.1.7. The activation energy for the chain scission reaction using least squares regression was $19 \pm 2 \text{ KJ.mol}^{-1}$.

The kinetics of the crosslinking reaction were evaluated by subtracting values of the continuous stress ratio (Fig 6.4.1.2.) from corresponding values of the intermittent stress ratio (Fig 6.4.1.3.) to give the fraction of crosslinkages formed in time t , $\Delta N_{cr}(t) / N_{cr}(0)$. The results are presented in Fig 6.4.1.8. All the curves had the same characteristic shape. After an initial region in which the rate of increase of $\Delta N_{cr}(t) / N_{cr}(0)$ decreased with time the curves became linear. The gradient (K) of this region was taken as a constant proportional to the rate of the crosslinking reaction. The associated Arrhenius plot is given in Fig 6.4.1.9. The crosslinking reaction had an apparent activation energy of $16 \pm 3 \text{ KJ.mol}^{-1}$.

Continuous stress relaxation curves for the elastomer ($N_{cr_m}(0) = 0.129 \times 10^{-6} \text{ mol.mm}^{-3}$.) are presented in Fig 6.4.1.10. for the temperature range $25 - 150^\circ\text{C}$ and the associated intermittent curves are given in Fig 6.4.1.11. The rate of the continuous stress relaxation response increased with increasing temperature but occurred at a slower rate in comparison to the previous elastomer ($N_{cr_m}(0) = 0.118 \times 10^{-6} \text{ mol.mm}^{-3}$.). Comparison of the intermittent curves for both elastomers revealed that the curves had the same shape but that the upturn in the intermittent stress ratio observed at longer times was more pronounced at all temperatures for the elastomer with the higher initial crosslink density. The data was treated in the manner previously described to give chain scission and crosslinking rates. The resultant $q_m(t)$ vs t curves and the associated Arrhenius plot are given in Fig 6.4.1.12. and Fig 6.4.1.13. The resultant $N_{cr}(t) / N_{cr}(0)$ vs t curves and the resultant Arrhenius curve are presented in Fig 6.4.1.14. and Fig 6.4.1.15. Comparison with the curves obtained from the previous elastomer revealed that they had the

ame characteristic shape. Subsequent treatment of the data revealed that
ission reaction associated with this material had an apparent activation
nergy of $12 \pm 3 \text{ KJ.mol}^{-1}$, whilst the crosslinking reaction was found to
ve an apparent activation energy of $36 \pm \text{KJ.mol}^{-1}$.

For reasons presented in the discussion it was deduced that the
bserved crosslinking response in PDMS elastomer is due to the subsequent
eformation of cleaved chains. Furthermore, the increase in the intermittent
tress ratio observed in these materials indicated that during degradation
ot only were chains cleaved during the stress relaxation test being
eformed but also chains that had been cleaved prior to the commencement
of the test. In order to separate the rates of these chain reformation
processes the following procedure was adopted:-

The kinetics of the chain reformation reaction associated with
the reformation of chains cleaved during the stress relaxation test were
evaluated by subtracting the continuous stress ratio from a value of 1.0.
The resultant curves for the elastomer ($N_{\text{cr}_m}(0) = 0.118 \times 10^{-6} \text{ mol.mm}^{-3}$.)
are presented in Fig 6.4.1.16. It can be seen that the curves have a
similar shape to the curves indicating the crosslinking rates of the
previous elastomers. Again the gradients of the linear regions of the
curves were taken as constants proportional to the rates of the cross-
link formation reactions. The associated arrhenius curve for this data
is given in Fig 6.4.1.17. Constructing the best fitting curve to these
data points yielded an apparent activation energy of $12 \pm 2 \text{ KJ.mol}^{-1}$.
for the reaction.

The kinetics of the reaction involving the reformation of chains cut
prior to the commencement of the stress relaxation test were determined
by subtracting a value of 1.0 from the intermittent stress ratio. The
relevant data is presented in Fig 6.4.1.18. and again it can be seen
that the curves still possess the same characteristic shape.

The approximately linear regions of these curves were used to evaluate the rate constant for the reaction in a manner described previously and were used to construct the arrhenius plot given in Fig 6.4.1.19. The best fitting curve gave an apparent activation energy of $21 \pm 5 \text{ KJ.mol}^{-1}$ for the reaction.

The continuous and intermittent data for elastomer ($N_{\text{cr}_m}(0) = 0.129 \times 10^{-6} \text{ mol.mm}^{-3}$.) was treated in a manner identical to that described for the case of the previous elastomer in order to resolve the kinetics of the two chain reformation reactions.

Using the data in Fig 6.4.1.10. and the associated data in Fig 6.4.1.11. resulting $1.0 - \sigma_c(t) / \sigma_c(0)$ vs t , and $\sigma_i(t) / \sigma_i(0) - 1.0$ vs t curves were constructed. Examination of these curves presented in Fig 6.4.1.20. and Fig 6.4.1.22. respectively, indicates that again they have the same characteristic shape. As in the previous case the approximately linear regions of the curves were used to evaluate the rate constants for the two reactions at the various test temperatures. These are given in Fig 6.4.1.21. and 6.4.1.23. From these curves it was estimated that the activation energy of the reaction associated with the reformation of chains cleaved during the test had an apparent value of $15 \pm 3 \text{ KJ.mol}^{-1}$ whilst the activation energy of the reaction associated with the reformation of chains cut prior to the onset of the test had a apparent value of $35 \pm 9 \text{ KJ.mol}^{-1}$.

For convenience the activation energies of the various reactions that have resulted from the thermal degradation studies on PDMS elastomer are summarised in Table 6.4.1.1.

Chemical Stress Relaxation Studies on Viton E60-C Elastomer.

Continuous stress relaxation curves for Viton E60C elastomer over the temperature range 25 - 300°C are presented in Fig 6.4.2.1. The associated intermittent stress relaxation curves are given in Fig 6.4.2.2. At all test temperatures below 300°C the intermittent curves were approximately linear having a stress ratio value in the region of 1.0 at all times. However, at 300°C a pronounced increase in the stress ratio was observed as the test progressed.

It was deduced that this particular elastomer was undergoing thermal degradation by random scission of the network crosslinkages (see Section 7.4.2.). In accordance with the relevant theory (Section .5.) the number of crosslink scissions per unit volume $q_c(t)$ was estimated by application of equation 3.34. to the data in Fig 6.4.2.1. It was observed that the resultant scission curves presented in Fig 6.4.2.3. all showed the usual characteristic shape and consisted of two zones; an initial region after the onset of the test where the rate of the scission reaction increased with time, and then a region in which the scission rate was approximately constant with respect to time. The gradients of the curves in the linear regions were taken to be proportional to the rate constant of the scission reaction. The resultant activation energy plot constructed from this data is presented in Fig 6.4.2.4. The best fitting curve to this data yielded an apparent activation energy of $21 \pm 5 \text{ KJ.mol}^{-1}$ for the assumed crosslink scission reaction.

The fraction of crosslinks formed with time were evaluated using the same method previously employed for PDMS elastomer and are given in Fig 6.4.2.5. Again characteristic curves were obtained. The temperature dependence of the rate constant associated with crosslink formation which is presented in Fig 6.4.2.6. gave an apparent activation energy of $12 \pm 2 \text{ KJ.mol}^{-1}$ for the process.

e / Post Cure Investigations on PDMS Elastomer.

N_{cr_m} values of material with initial peroxide paste additions 1.0, 1.25, 1.5, 2.0 and 3.0 wt% 2,4-DCBP subjected to cure times ranging from 5 to 20 mins, and post cure times ranging from 2 to 4 hrs are presented in Figs 6.4.3.1., 6.4.3.2., 6.4.3.3., 6.4.3.4., 6.4.3.5., and also in Table 6.4.3.1. A statistical analysis of these results is presented in Table 6.4.3.2. Several general trends are apparent from an examination of the results. For all the formulations considered the crosslink density attained within the first five minutes of curing remained virtually unchanged with further curing time. However, post curing operation resulted in a significant reduction in N_{cr_m} of the elastomers. Furthermore the magnitude of this reduction was most significant in those materials with the highest peroxide paste additions.

Combined Thermal / Radiative Degradation Studies.

Chemical Stress Relaxation Studies on PDMS Elastomer.

The continuous stress relaxation curves for the elastomer ($N_{cr_m}(0) = 0.118 \times 10^{-6} \text{ mol. cm}^{-3}$) subjected to a standard irradiation dose of 1.05 Mrad.hr in air are presented in Fig 6.5.1.1. for temperatures ranging from 40 - 200°C. The data was treated in an identical manner to the thermal data reported previously to yield relevant kinetic data. As it is believed that the scission reaction induced by irradiation in this material occurs randomly along the main chain (see discussion Section 7.5.1.) the data could be treated in the manner previously described in order to evaluate the total number of chain scissions induced by temperature and by exposure to γ -irradiation.

The resultant $q_m(t)$ vs t curves evaluated from the data of Fig 6.5.1.1.

are given in Fig 6.5.1.2. It can be seen that the combined scission rates estimated at all the test temperatures become approximately constant after an initial region in which the chain scission rate appears to increase with time. The gradients of the curves in the regions where they are approximately linear were assumed to be constants proportional to the combined thermal/radiative scission rates. The Arrhenius plot constructed from this data was clearly not linear (Fig 6.5.1.3.) hence an activation energy for the combined process could not be established. However it is apparent that the combined effects of temperature and gamma irradiation have a synergistic effect on the rate of degradation.

Chemical Stress Relaxation Studies on Viton E60-C Elastomer.

The stress relaxation curve of Viton E60-C elastomer subjected to constant irradiation dose of $1.05 \text{ Mrad.hr}^{-1}$ is presented in Fig 6.5.2.1. Reference to the pertinent literature indicated that the material would be thermally stable at this temperature but undergo radiative degradation via a random main chain scission reaction. Therefore the data was treated accordingly by application of equation 3.31 to give the number of main chain scissions incurred per unit volume as a function of time. These results are presented in Fig 6.5.2.2. After an initial region in which the scission rate increased with time it assumed an approximately constant value. The gradient of this region was assumed to be a constant proportional to the chain scission reaction and had an apparent value of $0.7 \times 10^{-12} \text{ mol.mm}^{-3} \cdot \text{s}^{-1}$.

cussion.

Material Characterisation of PDMS and Viton E60-C Elastomers.

A comparison of the two methods available for the characterisation of elastomer network structures reported in Section 4. led to the following conclusions:-

From a theoretical standpoint equilibrium swelling measurements are to be preferred to equilibrium stress-strain measurements as they yield a more accurate value of the crosslink density (N_{cr}). This is because chain entanglements are not measured by this technique. During stress-strain measurements these act as pseudo-crosslinks contributing to the load bearing properties of the network, that is the recorded value of the shear modulus G , and therefore lead to an overestimation of the crosslink density.

If the experimental procedures involved in N_{cr} determination are compared, equilibrium stress-strain measurements are advantageous as they are less time consuming. Several days are required to carry out a swelling test during which time the solvent is fully absorbed by the elastomer and equilibrium swelling conditions are established. In contrast equilibrium stress-strain measurements consist of either a simple tensile or compression test under conditions of uniaxial stress.

Equilibrium swelling measurements must be undertaken on samples of relatively small cross-section (the relevant standard quotes a maximum sample volume of 1000mm^3) in order to obtain reliable data. Only under such conditions can equilibrium swelling be attained within

a realistic period of time. This fact implies that the technique cannot be employed successfully for the characterisation of the cylindrical stress relaxation samples as their section is far too large.

iv) The resultant errors incurred in the evaluation of crosslink density by both techniques were evaluated and it was established that equilibrium stress-strain measurement was inherently the most accurate method. These errors were evaluated from equations 3.13 and 3.11 for equilibrium swelling and stress-strain techniques, respectively. The relative error in crosslink density determination by stress-strain measurement was estimated at $\Delta N_{cr_m} / N_{cr_m} = 0.04$ while the relative error associated with swelling measurement was estimated at $\Delta N_{cr_s} / N_{cr_s} = 0.16$.

This large error encountered with the swelling method arises from two major sources. The first is the error in the sample weight which arises from the small sample sizes which have to be used with this technique. The second is the error in the swollen sample weight. In order to evaluate the volume fraction of polymer in the swollen gel (section 3.16), a sample of polymer containing absorbed solvent must be weighed. During the weighing operation solvent was continually evaporating from the sample surface resulting in a continuous change in the sample weight. This made it extremely difficult to obtain an accurate weight. The effect was significantly reduced by weighing the sample in an enclosed vessel. However a significant relative error in the swollen sample weight was still encountered ($W_{sp}/W_{sp} = 0.06$).

In view of the above considerations it was decided to adopt stress-strain measurements for the characterisation of test samples as

the technique appeared to be the quickest and inherently the most accurate.

If one considers the determination of crosslink density by stress-strain measurement it will become apparent that the N_{cr} value obtained by this method is an average value for the whole sample, and as such the technique will not detect any fluctuations in crosslink density which may be present. In order to assess sample homogeneity it was decided to carry out equilibrium swelling measurements on samples taken from specific sites within a test specimen.

The relevant homogeneity studies on PDMS stress relaxation samples revealed that there was a significant reduction in the crosslink densities of the samples at the sites located near the surfaces (see table 6.1.2.). It is believed that this inhomogeneity has arisen as a consequence of the post cure operation, and the effect is discussed further in Section 7.4. Because of the fluctuations which are present within the samples it may be thought that they are unsuitable for chemical stress relaxation, as it is probable that regions of different N_{cr} will degrade at different rates. However this is not the case if it is remembered that the stress relaxation technique yields data on the net changes that are encountered in the sample it will become apparent that studies undertaken using samples of comparable net N_{cr} although N_{cr} may fluctuate throughout the sample section, will yield comparable kinetic data to studies undertaken on homogeneous samples with the same crosslink density.

The net N_{cr} values of the PDMS samples used in the stress relaxation programme, and the statistical analysis of the data, presented in table 6.1.1. show several features. Apart from the increase in N_{cr} of

bles with higher additions of peroxide curing agent, which would
obviously be expected, the net N_{cr} of the samples showed a significant
variation from the mean. The reasons for this variation of net N_{cr}
in the sample population are two-fold. Firstly, there is an error
which arises from the determination of the crosslink density from
the stress-strain technique itself (this has been mentioned previously),
secondly, there are errors which arise from variations in material
preparation conditions. Such errors may be due to variations in cure,
post cure temperature, or to the uneven distribution of the curing
agent due to insufficient milling. There is also the possibility of
entrainment of dust particles in the material during the milling
operation, and these could act as a reinforcing filler which could lead
to variations in the estimated N_{cr} value.

Obviously, the error arising from these effects cannot be predicted
therefore the overall error in the sample population arising from
errors in both N_{cr} determination, and material preparation procedure
cannot be calculated. However, a rough idea of the magnitude of this
estimated error can be gained from an examination of the sample
population.

If one assumes that the sample populations are normal and that 99.95%
of samples fall within $\pm 3\sigma$ of the mean, then the following relationship
is used in order to express the largest value in the relative error
in net crosslink density of the samples which would be encountered:-

$$\Delta N_{cr} / N_{cr} = 3\sigma / N_{cr} \quad (7.1)$$

Using the above relationship the maximum relative errors which may be

encountered in the PDMS elastomers used in the stress relaxation test programme were found to have the following values:-

$$\Delta N_{cr}/N_{cr} = 0.05 \quad \text{for 1.00wt\% peroxide paste}$$

$$\Delta N_{cr}/N_{cr} = 0.05 \quad \text{for 1.25wt\% peroxide paste}$$

$$\Delta N_{cr}/N_{cr} = 0.07 \quad \text{for 1.50wt\% peroxide paste}$$

These values show an interesting feature. It is apparent that the overall relative error which may be encountered increases with increasing peroxide paste additions. Assuming that the errors incurred in N_{cr} determination for each group of elastomers is comparable (this is a reasonable assumption as an identical procedure was used for N_{cr} determination of all the materials) it can be concluded that the errors incurred as a consequence of variations in material preparation conditions are greater for the higher peroxide paste formulation. The reasons for this effect have not been established but one possible explanation is the increasing difficulty which was encountered in evenly distributing the curing agent throughout the material in the 1.5wt% peroxide paste formulation. This effect would be expected to increase the variation in net N_{cr} between samples of the same batch.

In contrast, the net crosslink densities of the Viton E60-C elastomers employed in the stress relaxation studies were more consistent. Applying the above analysis to the sample population presented in Table 6.2.3. gave a value of 0.006 for the predicted value of the overall relative error in the net crosslink density of the samples. Reference to the data of Table 6.1.4. indicates that the levels of inhomogeneity within the samples are relatively low and that there is little variation in N_{cr} throughout their section. These phenomena have been attributed to the superior control of process variables during the manufacture of this material (Section 5.1.2.2.).

2. Material Characterisation of PDMS Elastomer Containing Entrapped PS.

As mentioned in Section 5.1.3.2., due to the two phase nature of these materials the crosslink density of the PDMS network which was formed by exposure to γ -irradiation could not be determined by the conventional techniques. Consequently studies were confined to the examination of low-temperature fracture surfaces by scanning electron microscopy.

The results of these investigations were far from conclusive, however they provided circumstantial evidence which corroborated some of the findings of Rupprecht and Astill reported in Section 2.6.1.4. As expected from the low miscibility of the two components considerable phase separation was in evidence, as can be seen in the micrographs presented in Plates 6.2.1. to 6.2.3. Two distinct phases are present and it is apparent from the observed fracture characteristics that the discrete phase has a far higher modulus than the phase comprising the matrix. In the light of the above evidence it is reasonable to assume that the matrix and discrete phases are predominantly crosslinked PDMS and predominantly PS respectively.

Further evidence of incompatibility is provided by the morphology of the discrete phase. It can clearly be seen that the phase is spherical in shape. This is a classical feature of incompatible systems as this particular morphology results in the minimum interfacial area (area of contact) between the two phases. Also, the smooth surfaces of the discrete phase is a clear indication of the incoherence of the phase interface. From these findings it is apparent that if any degree of mixing has taken place between the two components, it must be extremely limited.

Unfortunately, this problem could not be resolved by the available electron optics techniques, as quantitative analysis of the constituent phases by electron probe microanalysis was not possible. Therefore the

ited solubility of PS in the PDMS network which has been proposed by
till⁽¹⁰⁰⁾ in order to explain the observed enhancement in the radiation
bility of such materials could not be verified.

The discrete, predominantly PS phase was successfully extracted from
fracture surface of an elastomer containing 1.0wt% PS by immersion
the sample in toluene (as demonstrated in Plate 6.2.4.). Subsequently,
lysis of the residue by infra-red spectroscopy indicated that it
predominantly PS, but a significant quantity of PDMS was also detected.
ever the origin of this PDMS was not certain, as it could have arisen
in the discrete phase or the matrix phase⁽¹⁰⁰⁾ and therefore these
other attempts at detecting possible miscibility were inconclusive.

An attempt was made to determine the particle size distribution and
volume fraction of the discrete phase in the three elastomers which
were prepared. However, no standardised technique was developed for the
manufacture of the material, and consequently there was no control over
rate of freeze drying, which has a significant influence on the size
of the PS rich phase, and its distribution. It is apparent from the
micrographs that the preparation technique has not been developed to
the level required for the production of regular size spheres that are
homogeneously distributed throughout the material. Consequently an
analysis of the distribution and size of the PS rich phase was inappropriate.

ical Stress Relaxation Studies.

The importance of evaluating the physical stress relaxation responses of elastomers has already been emphasised in Section 5.2. It was realised that an indication of the kinetics of the physical stress relaxation processes operative in these materials could be gained by establishing the time dependence of the relative storage moduli. Preliminary investigations indicated that this could not be achieved from conventional stress relaxation measurements, as the relaxation of the modulus was extremely rapid, even at the lowest test temperature in the Instron Model No 3.1.1.1.) environmental cabinet. As testing at lower temperatures, where the relaxation response would be retarded, was impracticable, it was obvious that another technique covering a lower time scale range was required. Consequently, dynamic tests on the Rheovibron seemed appropriate.

It is essential that materials are single phase, or rheologically stable if the superposition method referred to in Section 5.2.1. is to be applied. The range of temperature in which modulus data could be utilised for the construction of a master curve was established for each material from dynamic mechanical analysis (DMA) studies. These investigations revealed that Viton E60-C elastomer remained single phase over the temperature range of interest. However, this was not the case with PDMS elastomer, as can be seen by reference to Fig 6.3.1. Apart from the significant increase in both $\tan \delta$ and G' associated with the glass transition around -100°C a small peak is also apparent in the region of -95 to -100°C . Studies by Lee⁽¹⁵⁵⁾ on a wide range of polysiloxanes subjected to a variety of heating and cooling rates indicated that this peak may be associated with the onset of cold crystallisation. It therefore seemed prudent not to utilise data below this temperature.

An examination of the storage modulus vs time master curves, presented in Figs 6.3.2. and 6.3.3. for PDMS elastomer ($N_{CRm}(0) = 0.108 \times 10^{-6} \text{mol. mm}^{-3}$.) and Viton E60-C elastomers, respectively, suggests that the moduli in these materials is relaxing by physical relaxation processes.

Furthermore, the attainment of a constant, time independent modulus in each case suggests that these processes were eventually suppressed by the pinning action of the network, which restricts further chain movement.

Once the time dependent physical relaxation processes have been terminated, the network is said to be at equilibrium. Under such conditions it is apparent, by reference to Section 3.3. that this modulus may be estimated from equation 3.10. The theoretical values calculated in this manner were found to be $3.88 \times 10^5 \text{Nm}^{-2}$, and $2.24 \times 10^6 \text{Nm}^{-2}$, for the PDMS and Viton E60-C elastomers, respectively. It can be seen from the above figures that these values are in close agreement with the experimentally determined values.

Due to the limited data which was available for modulus superposition on the studies on PDMS elastomer, the relevant WLF constants could not be estimated with any degree of confidence. However, the data from studies on Viton E-60C elastomer were more comprehensive, and this enabled the values of the constants C_1 and C_2 to be determined. However, an examination of Fig 6.3.5. indicates that a reasonably accurate prediction of the physical relaxation response of this material, utilising the WLF relationship with the above constants, can only be made within the temperature range 50 - 150°C.

It will be noticed that dynamic studies on the other PDMS elastomers ($N_{CRm}(0) = 0.118 \times 10^{-6} \text{mol. mm}^{-3}$. and $N_{CRm}(0) = 0.129 \times 10^{-6} \text{mol. mm}^{-3}$.) have not been reported. Unfortunately, due to equipment failure, the storage modulus master curves for these materials could not be established. Despite

this, we can make some reasonable assumptions about the rates of the relaxation processes in these materials. As they possess higher crosslink densities it is apparent that the relaxation processes which take place in these materials will be retarded due to the increased restrictions imposed on chain motion. However, as a consequence of the higher crosslink density, the equilibrium, time independent modulus, which will be attained will be higher. As a consequence of these effects it seems reasonable to assume that the relaxation processes, operative in these materials will be completed in comparable times.

The implications of the above findings are clear. It is apparent that the physical relaxation processes which take place in these elastomers at the temperatures employed in the studies reported in Section 5.2.1.1. will be extremely rapid, and be completed during the time taken in loading of the samples prior to the commencement of the tests. It is therefore believed that the stress relaxation responses reported in sections 6.4.1. and 6.4.2., and 6.5.1. and 6.5.2. are due, entirely, to changes in the network structure arising from degradation reactions.

Thermal Degradation Studies.

PDMS Elastomer.

Initial investigations on PDMS elastomer were confined to conventional chemical stress relaxation studies, and armed with the knowledge that the material was degrading by random scission of the main chain (Section 2.6.1.3.) the data was treated accordingly, as described in Section 4.5.5.1. in order to determine appropriate scission rates, which were subsequently employed to evaluate the activation energy of the process. The relatively low value of the resultant activation energy, together with evidence of acidic residual decomposition products suggested that degradation was taking place by the hydrolysis mechanism (Section 2.6.2.3.) A similar effect has been recorded in the case of a benzoyl peroxide elastomer, and the predominance of the hydrolytic mechanism in the degradation of PDMS elastomers has been substantiated since the time of our investigations⁽¹⁰⁴⁾.

It became apparent, after the conclusion of the intermittent test programme, that the kinetics associated with thermal degradation, were more complex than had been expected. Intermittent stress relaxation curves clearly indicate that the crosslink densities of the elastomers were increasing as degradation proceeded. These results appeared to be in direct contradiction to the established mechanisms. The pertinent literature indicates that degradation in these materials is confined to chain scission and subsequent chain reformation mechanisms, i.e. there is no independent crosslinking reaction taking place. The only possible explanation which could be put forward, to account for these effects, was that changes in the network structure of the materials had taken place prior to their utilisation in chemical stress

laxation studies. The validity of this hypothesis was substantiated by
sequent cure / post cure trials on PDMS elastomers.

Peroxide cured elastomers are notoriously unstable when in the cured state.
This is attributed to the presence of acidic peroxide decomposition products,
which catalyse the hydrolytic scission reaction⁽¹⁰³⁾. Consequently, these
materials are usually subjected to a post cure treatment in order to volatilize
these products and hence improve resistance to thermal degradation. In accordance
with this standard practice, our materials were subjected to a post cure
treatment before they were employed in subsequent investigations.

It is evident from an examination of the results presented in Figs 6.4.3.1
6.4.3.5., and Tables 6.4.2.1. and 6.4.3.2., that the stabilising post cure
treatment has been unsuccessful as the elastomers appear to have degraded by
predominant hydrolytic scission as a consequence of this treatment. It is
apparent that this reaction will predominate in materials containing high
concentrations of acidic catalyst, and water. These favourable conditions
are believed to have arisen from the following factors:-

- (i) possible pick up of H₂O during milling and / or subsequent storage
- (ii) the retention of the acidic catalyst in the elastomer throughout the
post cure operation.

Unfortunately, effect (i) has not been substantiated in these investigations.
However, there is circumstantial evidence in support of effect (ii). The acidic
decomposition product associated with the curing agent employed in our
materials is 2,4-Dichlorobenzoic acid (2,4-DCBA) and it is known that this
compound is relatively non-volatile in comparison with the decomposition
products of other curing agents⁽¹⁵²⁾. It is this particular property
which suggested that 2,4-dichlorobenzoyl peroxide would be the ideal curing

gent for our chemical stress relaxation samples, as the phenomena of blooming, due to the evolution of gaseous decomposition products in materials of large section is avoided. Unfortunately, it was subsequently realised that this effect had resulted in the failure of the post cure treatment, to effectively remove the acidic catalyst from the material.

Further evidence of catalyst retention was provided by 'blooming'. Over a period of time (approx 3 months) significant quantities of a white powdery deposit was detected on the surfaces of the stress relaxation samples. Subsequent analysis of the powder by IR indicated that it was 2,4-DCBA.

We can therefore picture the material in the post cured condition as having a partially degraded network containing a significant fraction of cleaved chains. It would be expected, if the above propositions are valid, that greater N_{cr} reductions would be experienced in formulations containing higher initial peroxide additions, as a consequence of having higher associated concentrations of acidic catalyst. An examination of Figs 6.4.3.1. to 6.4.3.5. indicates that these underlying trends are evident, with the highest peroxide paste formulation (3.0wt%) apparently resulting in a reduction of approximately 40% in the number of network chains which are incorporated in the network.

It is now apparent that the observed intermittent stress relaxation responses reported in Figs 6.4.1.3. and 6.4.1.11. are due to the reformation of chains cleaved during the stress relaxation test and also chains cleaved during the attempted post cure treatment. Furthermore the greater increase in intermittent stress ratio observed in the higher wt% peroxide paste elastomer is obviously a direct consequence of the greater number of cleaved chains that are available in this material for reformation.

the findings of the cure / post cure trials, and the chemical stress relaxation studies, appear to be contradictory, as elastomers which degrade predominantly by chain scission during the post cure operation, are subsequently reforming, under apparently similar conditions, during stress relaxation testing, by predominant chain reformation. These significant differences can be explained when it is realised that the catalyst levels in the materials immediately prior to stress relaxation testing are considerably lower than were during the post cure treatment. The extensive 'blooming' that has already been reported provide clear evidence of the migration of catalyst from the material during the interim storage period. It seems plausible to assume that this reduction in catalyst level has resulted in a drastic reduction in the rate of chain scission.

Consequently, at this stage the material will contain relatively low concentrations of catalyst, but still contain the appreciable amounts of water that were present after the post cure operation. It is apparent that if such a material were tested at elevated temperatures, then appreciable amounts of water would be removed from the system during testing, with the result that subsequently reformed chains would reform by condensation.

Although it is appreciated that under these conditions, chains cleaved during the post cure operation, may possibly combine with chains cut during the stress relaxation test, it is possible to represent the overall chain reformation response, operative in these materials, by a model consisting of the following crosslink formation responses:-

The reformation of chains cut during the stress relaxation test. The rate of this reaction would be governed by the rate at which the chains are cut, and would therefore possess an identical activation energy)

(ii) The reformation of chains cut prior to the stress relaxation test.

(the activation energy of this process is associated with the removal of water from the material)

Accordingly, the overall chain reformation response may be represented by the following relationships:-

$$\Delta N_{cr} / N_{cr} = \Delta N_{cr(i)} / N_{cr} + \Delta N_{cr(ii)} / N_{cr} \quad (7.2)$$

where:-

$\Delta N_{cr} / N_{cr}$ = total chain reformation response

$\Delta N_{cr(i)} / N_{cr}$ = response associated with reformation of chains cut during stress relaxation

and $\Delta N_{cr(ii)} / N_{cr}$ = response associated with reformation of chains cut during post cure

It can be seen from Fig 7.4.1.1. that the kinetics of these components may be evaluated from the following relationships:-

$$\Delta N_{cr(i)} / N_{cr} = \sigma_i(t) / \sigma_i(0)_{(i)} - \sigma_c(t) / \sigma_c(0) \quad (7.3)$$

$$\text{and } \Delta N_{cr(ii)} / N_{cr} = \sigma_i(t) / \sigma_i(0) - \sigma_i(t) / \sigma_i(0)_{(i)} \quad (7.4)$$

where:-

$\sigma_i(t) / \sigma_i(0)_{(i)}$ = intermittent stress ratio associated with reformation of chains during stress relaxation

$\sigma_i(t) / \sigma_i(0)$ = overall intermittent stress ratio

and $\sigma_c(t) / \sigma_c(0)$ = conventional stress ratio

Under conditions where chain cleavage and reformation rates are balanced, as is the case in the reported literature, then the intermittent stress ratio

will have a value of 1.0 at all times, and the above relationships will reduce to:-

$$\Delta N_{cr(i)} / N_{cr} = 1.0 - \sigma_c(t) / \sigma_c(0) \quad (7.5)$$

$$\text{and } \Delta N_{cr(ii)} / N_{cr} = \sigma_i(t) / \sigma_i(0) - 1.0 \quad (7.6)$$

It can be seen from Figs 6.4.1.16 to 6.4.1.23. that the above approach, when applied to the intermittent and continuous stress relaxation data of the elastomers that, as expected, the corrected crosslink formation values predicting the response in the absence of reformation of chains cut during the post cure operation were comparable with the scission data.

It can be seen from an examination of Figs 6.4.1.16. to 6.4.1.23. that the kinetic data of the PDMS elastomers has successfully been resolved into its constituent components. As expected, the activation energy values for the reaction associated with the reformation of chains cleaved during the stress relaxation test were comparable with the estimated activation energy for the random chain scission processes.

However, the estimated activation energy for the reaction associated with the reformation of chains cleaved during the post cure operation, differed considerably for the two PDMS elastomer formulations (cf Figs 6.4.1.19. and 6.4.1.23.). This highlights an unfavourable aspect of the technique, in that any errors are compounded during treatment of the data, making the quantitative estimation of activation energies by the above method highly subjective.

It was decided to subject our materials to the methods outlined in section 4.5.5.3. for the evaluation of the site of the scission reaction. As this is well established as a random main chain scission reaction it was believed that this procedure would assess the applicability of these techniques to our materials.

The data presented in Fig 6.4.1.6. suggests that the Osthoff method can be employed for the determination of the scission site in these materials, despite its highly empirical nature. Furthermore, subsequent treatment of data obtained at various temperatures enabled an activation energy to be determined, which was comparable with the value obtained in the traditional manner by application of equation 3.31. . (cf Figs 6.4.1.7. and 6.4.1.5. for PDMS elastomer ($N_{CR_m}(0) = 0.118 \times 10^{-6} \text{ mol. mm}^{-3}$.)

Whilst attempting to evaluate the site of the scission reaction by the technique proposed by Tobolsky, a discovery was made, which has far reaching implications, as it challenges the validity of utilising equation 3.31. for the quantitative evaluation of scission kinetics in our elastomers.

As stated in Section 3.5.3.1, for conditions of random main chain scission in a series of elastomers, with identical chemical, and physical structures, the following characteristics are to be expected:-

(i) A variation in chemical stress relaxation response, with the rate of relaxation being inversely proportional to the initial crosslink density of the elastomer.

ii) Equal rates of random scission exhibited by the elastomers

Reference to the chemical stress relaxation curves for three elastomers of varying N_{CR} presented in Fig 6.4.1.1. suggest that characteristic (i) is observed, despite the distinct possibility that the curve associated with PDMS elastomer ($N_{CR_m}(0) = 0.108 \times 10^{-4} \text{ mol. mm}^{-3}$.) may be erroneous. However, upon subsequent evaluation of the associated chain scission kinetics, it became clear that characteristic (ii) was not present, as a distinct variation in the calculated rates of scission for the elastomers was apparent.

is effect can most clearly be seen from a comparison of the scission rates presented in Figs 6.4.1.4. and 6.4.1.12. which distinctly show that the calculated scission rates for PDMS elastomer ($N_{cr_m}(0) = 0.129 \times 10^{-6} \text{ mol. mm}^{-3}$.) are lower at all temperatures, than the corresponding rates for PDMS elastomer ($N_{cr_m}(0) = 0.118 \times 10^{-6} \text{ mol. mm}^{-3}$.)

The reasons for these observed variations will become apparent from consideration of the physical structures of the elastomers. As mentioned previously, in the post cured state, the elastomer network structure is partially degraded, resulting in the presence of a significant number of non-load bearing chains in the material. Now it will be appreciated by reference to Section 4.5.5.1. that the theory of irreversible scission does not take into account the possibility of multiple chain cleavage, i.e. the subsequent cleavage of non-load bearing chains created during stress relaxation. However, it is apparent that cleavages of non-load bearing chains which are present before the commencement of the test will not be accounted for. Hence it is obvious that equation 3.31. when applied to our PDMS elastomers will result in an underestimation of the chain scission rate. Furthermore, the magnitude of this underestimation will obviously be greater in higher N_{cr} elastomers as a consequence of them containing higher concentrations of acidic peroxide decomposition products, and hence having a greater percentage of cleaved network chains.

Bearing in mind the above, it may be thought that the data in Figs 6.4.1.4. and 6.4.1.12. cannot be used for the calculation of the activation energy of the main chain scission reaction. However this assumption may be untrue. If the scission reaction is random, then the ratio of detected scissions to total scissions will be independent of time at a particular temperature. Consequently, the actual and apparent scission curves will have the same

characteristic shape, and the same gradient in the steady state region where $q_m(t)$ is time independent, indicating that the approximate data can be employed for the determination of the activation energy of the scission reaction.

2. Viton E60-C Elastomer.

The findings of the thermal degradation studies on Viton E60-C elastomer, were both unexpected and disappointing. Although intermittent data presented in Fig 6.4.2.2. indicated that no appreciable changes in N_{CR} are experienced until temperatures are in excess of 200°C, it was apparent from continuous data (Fig 6.4.2.1.) that appreciable structural reorganization is taking place at far lower temperatures. Reference to the pertinent literature in Section 2.6.2.3. suggests that only one possible mechanism can be proposed in order to explain the observed scission kinetics; and this is a reversion reaction associated with hydrolytic scission of the amine crosslinkages. The occurrence of such a reaction is a clear indication that the material has not received a suitable post cure treatment, in order to remove water which is generated by the neutralisation of HF generated during the curing reaction by the base (MgO). Accordingly, the continuous data was treated by the method presented in Section 4.5.5.2. in order to evaluate the associated activation energy for the mechanism. Little comment can be made about this value, except that it is relatively low, a characteristic which appears to be common in hydrolytic scission mechanisms⁽⁶⁷⁾.

It is apparent that the predominant crosslink formation response observed at temperatures in excess of 200°C is associated with the possible ring formation mechanisms, which have been proposed for these materials⁽¹¹⁸⁾. Unfortunately, their exact nature has yet to be resolved, but it is apparent

t these cyclic structures effectively act as crosslinkages, and it may be
ght that the kinetics of this mechanism can be evaluated from the
tinuous and intermittent data. However, such an approach was not deemed
be suitable, as there was a distinct possibility that another crosslink
ation reaction could be taking place.

It has been reported that the formation of cyclic structures depicted
reaction 2.33. does not take place at temperatures lower than approximately
°C, but an examination of the associated intermittent curves clearly
ests that crosslink formation is taking place at a rate comparable to
sslink scission, under these conditions. The only plausible mechanism
t can be proposed for this effect is a condensation reaction, which is
eversal of the hydrolytic crosslink scission mechanism, previously
cussed. The rate of this reaction would be expected to increase with
reasing temperature, due to the increase in the rate of removal of residual
ter from the material. Hence, the condensation mechanism would be expected
make a significant contribution to the observed crosslink formation
sponse observed at 300°C.

Consequently, it can be appreciated that the kinetics of these crosslink
formation reactions which are believed to be operative during thermal
gradation cannot be evaluated from the available data, as the contribution
de by each to the overall crosslinking response cannot be established.

Combined Thermal / Radiative Studies.

The failure of the stress relaxation rig described in Section 5.2.3.1.
er a total absorbed dose of approximately 4.54×10^9 rad . severely
tricted the original test programme. Consequently stress relaxation
ts were carried out at a single dose rate of 1.05×10^3 rad.hr⁻¹, the

highest available from the γ -irradiation facility employed. Studies on PDMS elastomer ($N_{cr_m}(0) = 0.118 \times 10^{-6} \text{ mol. mm}^{-3}$.) were performed over the temperature range 40 - 200°C, however, there was no opportunity of repeating the tests in order to substantiate the results. Only a single test was performed on Viton E60C elastomer at 40°C.

It is apparent that the conclusions which can be drawn from this data, especially in the case of Viton E60C elastomer, will be limited.

PDMS Elastomer.

The scission mechanism operative in PDMS elastomers upon exposure to γ -irradiation, is well established, and believed to occur by a random main chain scission process, as depicted in Section 2.6.1.1.. It will be evident that as both the predicted thermal and radiative scission reactions are random main chain scission reactions, then we are justified in treating the continuous stress relaxation data of Fig 6.5.1.1. by application of equation 3.31 in order to yield the total number of scissions which are taking place in the material under these conditions (Section 6.5.1.). The same arguments, which have been expounded in Section 7.4.1. are also appropriate under these conditions, and that as a consequence of the peculiar physical structure of the elastomer, it must be expected that the overall scission rates, given in Fig 6.5.1.2., are apparent and not true values. However, in spite of this fact it has been demonstrated that the data may still be employed for the evaluation of the temperature dependence of the combined thermal / radiative scission kinetics.

Comparison of the estimated overall scission rates with those obtained from thermal degradation studies (Fig 6.5.1.3.) clearly indicate that the combined influences of temperature and γ -irradiation have had a synergistic

effect on the combined main chain scission rates. The reasons for this effect, which has never before been reported in PDMS elastomers, is uncertain. It is possible that the effect could be caused by a temperature enhancement of the radiation induced scission reaction, or by an enhancement of the thermal scission reaction, or by a combination of both. However, it is difficult to conceive of a mechanism for the enhancement of the thermal scission rate by γ -irradiation, as the thermal mechanism is ionic in nature, whilst the radiation induced reaction is a radical mechanism.

Temperature enhancement of the radiation induced scission reaction has been observed in some hydrocarbon elastomers⁽¹⁵⁶⁻¹⁶⁰⁾ and these effects have been attributed to oxidative scission processes (Section 2.4.), but no such mechanisms are believed to be operative during the radiative degradation of polysiloxanes (Section 2.6.1.1.).

It may be that the observed phenomena have arisen as a consequence of the post cure operation, which has resulted in the unusual physical structure of these elastomers, or perhaps are connected in some way with the low levels of acidic peroxide decomposition products, which are believed to be present in these materials.

Viton E60-C Elastomer.

A comparison of Figs 6.5.2.1. and 6.4.2.1. indicates that the observed stress relaxation response during exposure to γ -radiation is due entirely to radiation induced scission processes. As reported in Section 2.6.2.1. the possible scission mechanisms operative in these materials have received little attention but it is believed to be a random main chain scission process. Subsequently equation 3.31. was applied to the data of Fig 6.5.2.1. in order to evaluate the relevant scission kinetics.

The kinetic data obtained for this material must be treated with caution, as there is a distinct possibility that autocatalytic oxidation processes will be operative. Although, such reactions will probably have a negligible influence on the measured scission rates, as significant concentrations of oxygen will be restricted to the immediate vicinity of the sample surfaces at the test temperature employed in our studies. (65,66)

cluding Remarks.

The objectives of the investigation, i.e. to evaluate the kinetics of the radiation reactions operative in PDMS and Viton E60-C elastomers when subjected to γ -irradiation at various temperatures, were only partly fulfilled. Upon reflection this was attributed to the following major factors:-

Experimental procedure:-

A number of stress relaxation studies that were undertaken on elastomers subjected to γ -irradiation were restricted because of the complexity of the test procedure, and also because of the fact that tests had to be carried out sequentially, and not concurrently, as we only had the single rig, and a single irradiation facility at our disposal.

Complex thermal degradation mechanisms:-

Both PDMS and Viton E60-C elastomers degraded by unexpectedly complex thermal degradation mechanisms, and these had to be resolved before the results of combined thermal / radiative studies could be evaluated. In hindsight, it was realised that these complications had arisen as a result of the particular materials preparation treatments used.

In the case of PDMS elastomers, significant reductions in the crosslink densities of the materials were experienced during the post cure operation. These effects have been attributed to the presence of acidic decomposition products which have arisen from the curing agent, and are believed to have resulted in the predominance of hydrolytic main chain cleavage under these conditions.

Consequently, although thermal degradation of these materials appeared to take place by hydrolytic cleavage of the main chain and subsequent chain termination by condensation of the silanol chain end groups, abnormally high

s of chain reformation were recorded. It is believed that this effect is to the reformation of chains cut during the stress relaxation tests, and to the reformation of chains cleaved during the post cure operation. Accordingly, a model was developed in order to rationalize this observed crosslink formation response. It was concluded that the rate of the crosslink formation reaction occurring during stress relaxation was governed by the rate of chain scission, whilst the rate of reformation of chains cleaved during the post cure treatment appeared to be governed by the rate at which residual water was removed from the material during the stress relaxation treatment.

It became apparent that the PDMS networks contained an appreciable number of cleaved chains after the post cure treatment and it was therefore concluded that the standard chemorheological relationships could not be utilised to determine the true number of main chain scissions taking place in our materials during thermal degradation. However, it was reasoned that the chemical stress relaxation data could still be employed for the determination of the activation energies of the thermal degradation reactions.

Thermal degradation studies on Viton E60-C elastomers revealed that although a net change in the crosslink densities of these materials were observed at temperatures below 200°C, appreciable scission and crosslink formation reactions were taking place. It was believed that scission under these conditions occurred by hydrolytic cleavage of the crosslinkages, and was an indication that the material had received an inadequate post cure treatment in order to remove the by-product generated from the curing process.

It is believed that the predominant crosslink formation reaction operative in these materials at these relatively low temperatures is a condensation

action, which is a reversal of the hydrolytic scission reaction. The constant crosslink densities which were observed under these conditions were attributed to comparable rates of hydrolytic scission and condensation reactions.

At higher temperatures ($>200^{\circ}\text{C}$) a significant increase in the crosslink density of the elastomer was observed. This has been attributed to the existence of a concurrent crosslink formation reaction, involving the formation of ring structures.

The data obtained from combined thermal / radiative studies on Viton E60-C elastomer was limited, and consequently little comment can be made, except that the observed chemical stress relaxation response at 40°C during γ -irradiation is attributed solely to a radiation induced scission reaction. It is believed that the mechanism is a random main chain scission reaction.

The results of simultaneous degradation studies on PDMS elastomer were quite substantial, and it was apparent from the observed chemical stress relaxation responses that the combination of temperature and radiation had a synergistic effect on the overall rates of the scission reactions which are operative during degradation. However, at the present time, no plausible mechanisms can be put forward in order to account for this phenomenon.

The processing route has successfully been established for the production of a potential radiation resistant elastomer, which is believed to consist of an entrapped, predominantly PS phase, in a radiation cured PDMS network. However, at the present time the method of manufacture is still relatively crude, and has not been developed to the stage where consistent material can be manufactured.

commendations for Further Work.

It is apparent that further investigations will need to be carried out in the following areas if the objectives of the project are to be fulfilled:-

Studies on PDMS elastomer.

Repeat stress relaxation tests should be carried out on peroxide cured elastomers during γ -irradiation at various temperatures, in order to substantiate the synergistic effect of temperature and radiation on the induced scissions, observed in our materials. If the phenomenon does exist, then comparable studies on radiation cured elastomers may prove useful in identifying the mechanisms that are responsible for this effect, as their networks will be whole (not partially degraded) and the materials will be free of acidic composition products.

Study on E60-C Elastomer.

There seems little point in pursuing combined thermal / radiative studies on the present material, as the complex thermal degradation kinetics will make the rationalization of data from these studies extremely difficult. Accordingly, tests should be carried out on material that has received a sufficient post cure treatment. It is envisaged that a test programme comprising a considerable number of tests will be required if the predominant mechanisms which are operative under these conditions are to be established. This is because the elastomer is prone to oxidative degradation, and hence the ensuing degradation kinetics will be dependent on dose rate, temperature, oxygen concentration of the surrounding atmosphere, and sample geometry.

All of these effects must be considered if data is to be interpreted correctly.

Elastomer Containing Entrapped PS.

ere is a distinct possibility that at temperatures below the glass transition of PS the thermal and combined thermal / radiative degradation kinetics of these materials can be evaluated from stress relaxation experiments, as under these conditions, the predominantly PS phase will act as an inert filler. Consequently, the relevant chemorheological equations will be applicable to the materials in this condition. However, it seems likely that the materials will be amenable to this technique at higher temperatures, where the stress-strain properties of the materials will no longer be predicted by rubber elasticity theory.

General Considerations.

Although our investigations have established that the stress relaxation rig used for the evaluation of scission kinetics operative in elastomers under irradiation, it may also be used for the determination of associated crosslinking reaction kinetics, under these conditions. This is achieved by a simple modification to the rig, involving the removal of the locating pins and replacement of the single acting ram by a double acting ram, in order to facilitate intermittent testing. The rig may also be enclosed in a glass container so that tests can be carried out under a variety of environments. It is believed that the versatility of the rig makes it a potentially valuable piece of equipment for the study of the simultaneous degradation of elastomers, especially in conditions approximating to the nuclear environment.

References.

- Campbell.F.J.,Radiat.Phys.Chem. 18,1-2,p109(1981).
- Grassie.N. & Scott.C. "Polymer Degradation and Stabilisation."
Cambridge University Press (1985). (a) chapt 7,p208. (b) chapt 2,p43.
(c) chapt 2,p39. (d) chapt 4,p92. (e) chapt 5,p122.
- Makhlis.F.A. "Radiation Physics and Chemistry of Polymers."
Keter Publishing House,Jerusalem (1975). (a) chapt 3,p128.
(b) chapt 5,p226. (c) chapt 3,p146. (d) chapt 3,p133. (e) chapt 3,p159.
(f) chapt 3,p160. (g) chapt 3,p120.
- Magee.J.L. & Burton.M.,J.Amer.Chem.Soc. 73,p523(1961).
- Libby.W.F.,J.Chem.Phys. 35,p1714(1961).
- Charlesby.A. "Irradiation of Polymers." Advances in Chemistry Series
No.66. Washington (1966).
- Charlesby.A. "Atomic Radiation and Polymers." Pergamon Press (1960).
- Lawton.E.J.,Beuche.A.,& Balwit.J.S.,Nature.172,p76 (1953).
- Miller.A.A.,Lawton.E.J.,& Balwit.J.S.,J.Polym.Sci. 14,p503(1954).
- Wall.L.A.,J.Polym.Sci. 17,p141(1955).
- Sisman.O. & Bopp.C.D.,ONR.Symp.Rep.ACR-2,Dec(1954).
- Wundrich.K.,Kolloid und Polymere Zeitschrift. 226,p116(1968).
- Wheland.G.W. "Resonance in Organic Chemistry.",pp75-152. New York (1955)
- Geymer.D.O.,Makromolek.Chem. 100,p186(1967).
- Alexander.P. & Toms.D.J.,Radiat.Res. 9,p509(1958).
- Turner.D.T.,J.Polym.Sci. 27,p503(1958).
- Charlesby.A. & Garret P.G.,Proc.Roy.Soc. A273,p117(1963).
- Kuri.Z. et al.,J.Chem.Phys. 32,p371(1960).
- Garret.P.G. & Ormerod.H.G. Int.J.Rad.Biol. 6,p281(1963).
- Charlesby.A. et al.,Nature. p194(1962).
- Charlesby.A. & Copp.R.M. Proc.Roy.Soc. A291,p129(1966).
- Lawton E.J. et al.,J.Polym.Sci. 32,p257(1958).

- Sobue.H. & Tasima.I., Nature. 188,p315(1960).
- Ormerod.H.G., Phil.Mag. 12,p118(1965).
- Kawai.T. et al., Phil.Mag. 12,p657(1965).
- Kitamaru.R. & Mandelkern.L., J.Amer.Chem.Soc. 86,p3529(1964)
- Kitamaru,L. et al., J.Polym.Sci. B2,p311(1964).
- Kawai.T. & Keller.A., Phil.Mag. 12,p673(1965).
- Kawai.T. & Keller.A., Phil.Mag. 14,p687(1965).
- Salovey.R. et al., J.App.Phys. 35,p3216(1964).
- Charlesby.A. & Davison.W.H., Chem.Inds.Lond. p232(1957).
- Zeppenfield.G. & Wuckel.L. "Radiation Chemistry." "Proceedings of (1962) Tihany Symposium. Ed. Jobo.J., Budapest, Akad.Kiado (1964).
- Chapiro.A. in "Encyclopedia of Polymer Science and Technology." Chapt 11,702(1969).
- Alexander.P. et al., Proc.Roy.Soc. A232,p31(1955).
- Florin.R.E. et al., J.Polym.Sci. A1,p1521(1963).
- Fischer.H. et al., J.Polym.Sci. 56,p33(1962).
- Tutia.M. & Yamamoto.K., Jap.J.App.Phys. 7,p440(1968).
- Grassie.N. in "Encyclopedia of Polymer Science and Technology." Vol 4,p651(1969).
- Wall.L.A. et al., J.Amer.Chem.Soc. 76,p3430(1954).
- Wall.L.A. & Straus.S., J.Polym.Sci. 44,p313(1960).
- Madorsky.S.L., J.polym.Sci. 9,p133(1952).
- Madorsky.S.L., J.Polym.Sci. 11,p491(1953).
- Straus.S. & Madorsky.S.L., J.Res.Natl.Bur.Std. 50,p165(1953).
- Straus.S. & Madorsky.S.L., J.Res.Natl.Bur.Std. 40,p417(1948).
- Straus.S. et al., J.Res.Natl.Bur.Std. 42,p499(1949).
- Straus.S. et al., J.Polym.Sci. 4,p639(1949).
- Straus.S. et al., J.Res.Natl.Bur.Std. 51,p327(1953).

9. Madorsky.S.L. & Straus.S.,J.Res.Natl.Bur.Std. 55,p223(1955).
0. Wall.L.A. & Florin.R.E.,J.Res.Natl.Bur.Std. 60,p451(1958).
1. Straus.S. & Madorsky.S.L.,J.Res.Natl.Bur.Std. 61,p77(1958).
2. Madorsky.S.L.,J.Res.Natl.Bur.Std. 62,p219(1959).
3. Madorsky.S.L. & Straus.S.,J.polym.Sci. 36,p183(1959).
4. Madorsky.S.L. & Straus.S.,J.Res.Natl.Bur.Std. 63A,p261(1959).
5. Wall.L.A.,& Straus.S.,J.Polym.Sci. 44,p313(1960).
6. Simha.R. & Wall.L.A.,J.Polym.Sci. 5,p615(1950).
7. Simha.R. & Wall.L.A.,J.Phys.Chem. 56,p707(1952).
8. Simha.R. & Wall.L.A.,J.Polym.Sci. 6,p39(1951).
9. Simha.R.,Trans.N.Y.Acad.Sci. 14,p151(1952).
0. Grassie.N.,Europ.Polym.J. 14,p875 (1978).
1. Tessler.M.M.,J.Polym.Sci. A1,p2521 (1966).
2. Grassie.N. in"Encyclopedia of polymer Science" Vol 4,p703 (1969).
3. Bolland.J.L.,Quart.Rev. 3,p1 (1949).
4. Bateman.L.,Quart.Rev.8,p147 (1954).
5. Dole.M. et al.,J.Amer.Chem.Soc. 76,p4307 (1954).
6. Charlesby.A.,Proc.Roy.Soc.Lond. A215,p187(1952).
7. Schnabel.W."Polymer Degradation-Principles & Applications" Chapt 7,
Sect 2. Hanser Int.Macmillan Pub Co (1981).
8. Charlesby.A.,Proc.Roy.Soc.Lond. A230,p120(1955).
9. Warrick.E.L.,Ind.Eng.Chem. 47,p2388(1955).
0. St Pierre.L.E. et al.,J.Polym.Sci. 36,p105 (1959).
1. Dewhurst.H.A.,J.Phys.Chem. 69,p1063(1960).
2. Zack.J.F. at al.,J.Chem.Eng.Data. 6,p279 (1961).
3. Kilb.R.N.,J.Phys.Chem. 63,p1838 (1959).
4. Langley.N.R.,J.Polym.Sci.Polym.Phys.Edn. 12,p1023(1974).
5. Squire.D.R. & Turner.D.T.,Macromol. 5,p401 (1972).

76. Delides.C.G. & Shepherd.I.W.,Rad.Phys.Chem. 10,p379(1977).
77. Tanny.G.B. et al.,J.Phys.Chem. 75,p2430 (1971).
78. Epstein.L.M. et al.,Rubber Age. 82,5,p825 (1958).
79. Falender.J.R. & Yeh.G.S.Y.,Amer.Chem.Soc.Div.Polym.Chem.Polym. Prep. 19,2,p743 (1978).
80. Delides.C.G. & Shepherd.I.W.,Polymer. 18,p1191 (1977).
81. Pryzbla.R.L.,Rubb.chem.Technol.
82. Miller.A.A.,J.Amer.Chem.Soc. 82,p3519 (1960).
83. Fischer.D.J. Rubb.Age. 88,p816 (1961).
84. Jenkins.R.K.,J.Polym.Sci.A-1,4,p2161 (1966).
85. Jenkins.R.k.,J.Polym.Sci.A-1,4,p771 (1966).
86. Tanny.G.B. et al.,J.Polym.Sci.Polym.Lett. 9,p863 (1971).
87. Miller.A.A.,J.Amer.Chem.Soc. 83,31 (1961).
88. Miller.A.A.,I & EC.Prod.Res & Dev. 3,No 3,p252 (1964).
89. Charlesby.A.A. et al.,Proc.Roy.Soc. A230,p136 (1955).
90. Koike.M. & Danno.A.,J.Phys.Sci.Jap. 15,(8),p1501 (1960).
91. Delides.C.G.,Rad.Phys.Chem. 16,p345 (1980).
92. Hildebrand.J.H. & Scott.R.L. "The Solubility of Non-Electrolytes". Reinhold.New York (1950).
93. Beuche.A.M.,J.Polym.Sci. 15,p97 (1955).
94. Hauser.R.L. et al.,Ind.Eng.Chem. 48,p1202 (1956).
95. Price.F.P.,Martin.S.G., & Bianchi.J.P.,J.Polym.Sci. 22,p49 (1956).
96. Dewhurst.H.A. et al.,J.Polym.Sci. 36,p105 (1959).
97. Boyer.R.F. & Spencer.R.S.,J.Polym.Sci. 3,p97 (1948).
98. Manson.J.A. & Sperling.L.H. "Polymer Blends" Vol I. Academic Press.New york (1978).

Galin.M. & Rupprecht.M.C.,Macromol. 12, (3) p506 (1979).

Astill.D.T. PhD Thesis.Sheffield City Polytechnic (1985).

Astill.D.T. "Materials for Microlithography" ACS.Symp.Series. 24,No 266.

Thomas.D.K. Polymer. 7,p99 (1966).

Osthoff.R.C.,Bueche.A.M. & Grubb.W.T.,J.Amer.Chem.Soc. 76, p4659 (1954).

Vondracek.P. et al.,J.App.Polym.Sci. 27,No 11,p4517 (1982).

Dole.M. "Radiation Chemistry of Macromolecules" Academic Press (1973).

Bohm.G.G.A. et al.,Rubber.Chem.Technol. 55,3,p575 (1982).

Dixon.S.,Rexford.D.R. & Rugg.J.S.,Ind.Eng.Chem. 49,p1687 (1957).

Jackson.W.W. & Hale.D.,Rubber Age. 77,p865 (1955).

Harrington.R.,Rubber Age. 82,p461 (1957).

Florin.R.E. & Wall.L.A.,J.Res.Nat.Bur.Std. 65A,p375 (1961).

Rugg.J.S.,Du Pont.Dept.Div.Prod.Rep.No 3.April (1957).

Rugg.J.S. & Stevenson.A.C.,Rubber Age. 82,p102 (1957).

Smith.J.F. & Perkins.G.T.,Rubber.Plant.Age. 59(1961).

Kryukova.A.B. et al.,Rubber.Chem.Technol. 47,p212 (1974).

Smith.J.F.,Proc.Int.Conf.Washington DC. 575 (1959).

Smith.J.F. et al.,J.App.Polym.Sci. 5,p460 (1969).

Kennedy.J.P. & Tornqvist.E.G.M."Polymer Chemistry of Synthetic Elastomers"Part 1.chapt 4E.Interscience (1968).

Smith.J.F.,Rubber.World. 142,No 3,p102 (1960).

Smith.J.F. & Perkins.G.T.,J.App.Polym.Sci,5,p460 (1961).

Charlesby.A.A. "Radiation Research" p265 Amsterdam.N.Holland Pub.Co (1967).

Dole.M. in"Crystalline Olefin Polymers" Vol 1,Chapt 16,N.Y. (1965).

Charlesby.A.A. & Pinner.S.H.,Proc.Roy.Soc. A 249,p367 (1959).

Guth.E. & James.H.M., J.Chem.Phys. 11,p455 (1945).

Wall.F.T., J.Chem.Phys. 10,p485 (1942).

Flory.P.J. & Rehner.J., J.Chem.Phys. 11,p512 (1943).

Flory.P.J., Chem.Rev. 35,p51 (1944).

Flory.P.J., J.Chem.Phys. 11,p521 (1943).

Flory.P.J., J.Chem.Phys. 11,p12 (1943).

Flory.P.J., J.Chem.Phys. 18,p108 (1950).

Murakami.K. & Ono.K. "Chemorheology of Polymers" Polymer Science Library.1.Elsevier (1979).

Flory.P.J., J.Amer.Chem.Soc. 58,p1877 (1936).

Beuche.A.M., J.Chem.Phys. 21,p614 (1953).

Berry.J.P. & Watson.W.F., J.Polym.Sci. 18,p201 (1955).

Yu.H., Polym.Lett. 2,p631 (1964).

Tobolsky.A.V., Metz.D.J. & Mesrobian.R.B., J.Amer.Chem.Soc. 72,p1942 (1950).

Flory.P.J., Trans.Farad.Soc. 56,p722 (1960).

Scanlan.J., Trans.Farad.Soc. 57,p839 (1961).

Thomas.D.K., Polym. 7,p125 (1966).

Barry.J., Watson.W.F. & Scanlan.J., Trans.Farad.Soc. 52,p1137 (1956).

Murakami.K. et al., J.Soc.Matls.Sci.Jap. 15,p312 (1966).

Murakami.K. et al., Bull.Chem.Res.Inst.Non-Aqueous Solns. Jap. 19,p243 (1969).

Horix.M.M., J.Polym.Sci. 19,p445 (1956).

International Commission on Radiological Units.Nat.Bur.Stds. Handbook. 47 (1950).

International Commission on Radiological Units.Copenhagen. Denmark. 7th International Congress of Radiology.July (1953).

45. Morton.M. in "Rubber Technology" 2nd Edn. Van Nostrand. Revinhold (1973).
46. Kennedy.J.P. & Tornqvist.E.G.M."Polymer Chemistry of Synthetic Elastomers" Part 2.chapt 8B.Interscience (1969).
47. Llorente.M.A.,Andrady.A.L. & Mark.J.E.,J.Polym.Sci.Polym.Phys. Edn. 18,p2263 (1980).
48. Meyers.K.O.,By.M.L. & Merril.E.W.,Macromolecules. 13,p1045 (1980).
49. Ciferri.A.,J.Polym.Sci. 45,p528 (1960).
50. Mark.J.E. & Flory.P.J.,J.Amer.Chem.Soc. 86,p138 (1964).
51. Sperling.L.H. & Tobolsky.A.V. Macromol.Chem. 1,p799 (1966).
2. Barrie.J.A. & Standen.J.,Polymer. 8,p97 (1967).
3. Price.C. & Padget.J.C.,Polymer. 10,p573 (1969).
4. Seferis.J.C. & Wedgewood.A.R. Polymer. 22,p966 (1981).
5. Lee.C.L.,et al.,Amer.Chem.Soc.Div.Polym.Chem.Polym.Preprints. 10,(2),p1311 (1969).
6. Ito.M. et al.,Rad.Phys.Chem. 17,p203 (1981).
7. Ito.M. et al.,Rep.Prog.Polym.Phys.Jap. 22,p541 (1979).
8. Ito.M. et al.,Rep.Prog.Polym.Phys.Jap. 21,p247 (1978).
9. Yoshida.T.,Florin.R.E. & Wall.L.A.,J.Polym.Sci. A3,p1685 (1965).
- . Evans.D. et al.,J.Polym.Sci. A27,p725 (1969).

Electrical Equipment

Power cable	Valve actuator motors
Control cable	Solenoid valves
Instrumentation cable	Pneumatic activators
Pump drive motors	Level switches
Fan drive motors	Differential pressure switches
Limit switches	Electrical enclosures
Relays	Electrical penetrations
Transmitters	Capacitors
Terminal blocks	Transformers
Connectors	

Mechanical Equipment Components

Gaskets	Seals
O-rings	Motor mounts
Spacers	Flexible tubes
Sheaths	Protective coatings

le.1.1. The range of components to be found in a typical nuclear reactor⁽¹⁾.

predominant crosslinking	predominant scission
<p>polyethylene. polymethylene. polypropylene. polystyrene. polyvinyl acetate. polyisoprene. polybutadiene. neoprene. nylon. polysiloxanes. polyacrylic esters. polyacrylic acid. polyacrylamide. polyvinylalkyl ethers. polyvinylmethyl ketones. polyesters. polyperfluoropropylene- -vinylidene fluoride.</p>	<p>polyisobutylene polytetrafluoroethylene. polychlorotrifluoroethylene. polyvinylchloride. polymethylmethacrylate. cellulose. butyl rubber. polymethacrylic acid. poly methacrylamide. polyvinylidene chloride. poly-α-methylstyrene.</p>

Table 2.1. Behaviour of polymers subjected to γ -irradiation in the absence of oxygen^(8,9).

<u>STRUCTURE.</u>	<u>OCCURRENCE.</u>
$\sim\text{CH}-\underset{\text{C}_6\text{H}_5}{\text{C}}\sim$	repeat unit - polystyrene.
$\sim\text{CH}-\underset{\text{C}_6\text{H}_4}{\text{N}}\sim$	repeat unit aniline formaldehyde.
$\sim\text{CH}=\text{CH}\sim$	present in many elastomers.
$\sim\text{CH}_2-\text{CH}_2\sim$	repeat unit polyethylene.
$\sim\underset{\text{O}}{\text{C}}-\underset{\text{H}}{\text{N}}\sim$	present in nylon.
$\sim\text{Si}(\text{CH}_3)_2-\text{O}\sim$	repeat unit polydimethylsiloxane. present in silicone rubber.
$\sim\text{C}_6\text{H}_4-\text{CH}\sim$	repeat unit phenol formaldehyde.
$\sim\text{CH}-\text{O}\sim$	repeat unit polyallyldiglycol carbonate.
$\sim\text{CH}_2-\text{S}\sim$	present in thiokols.
$\sim\text{C}_6\text{H}_4-\underset{\text{O}}{\text{C}}\sim$	present in Dacron.
$\sim\text{CH}_2-\underset{\text{Cl}}{\text{CH}}\sim$	repeat unit polyvinylchloride.
$\sim\text{C}_6\text{H}_3(\text{OH})(\text{CH}_2)-\text{O}\sim$	repeat unit cellulose.
$\sim\text{CF}_2-\text{CF}_2\sim$	repeat unit polytetrafluoroethylene.
$\sim\text{C}_i-\text{C}_{R_1R_2}\sim$	$R_1=R_2=\text{CH}_3$ butyl rubber. $R_1=\text{CH}_3, R_2=\text{phenyl, poly-}\alpha\text{-methylstyrene.}$

The effect of chemical structure on radiative stability⁽¹¹⁾.

compound	resonance energy (KJ.mol ⁻¹)	compound	resonance energy (KJ.mol ⁻¹)
1,3-butadiene	12.56	perylene	527.31
benzene	150.66	furan	66.12
toluene	149.40	thiophene	120.11
m-xylene	145.64	carbazole	309.69
diphenylmethane	280.40	pyridene	96.26
styrene	159.45	quinoline	197.95
trans-stilbene	321.83	phenol	150.66
diphenyl	279.14	aniline	159.03
fluorine	317.64	methylaniline	163.22
naphthalene	255.29	dimethylaniline	146.48
anthracene	349.45	α -naphthylamine	267.84
phenanthrene	382.10	β -naphthylamine	267.84
naphthacene	460.35	diphenylamine	326.43
benz- α -anthracene	467.05	benzophenone	301.32
3,4-benzphenanthrene	458.68	benzoquinone	16.74
chryzene	487.55	benzoic acid	196.70
triphenylene	492.57	urea	125.55
tetracene	460.35	azulene	138.11
pyrene	456.17		

Table 2.3. Resonance energies of specific compounds⁽¹³⁾.

compound	intrinsic viscosity	gel fraction (wt%)	amount of additive governed by its solubility.
iodene	0.55	0	-
methylmercaptan	0.55	0	11
isobutylene	0.62	0	-
isopropyl alcohol	0.62	0	2.6
3-methylpentane	0.66	0	12
isopropylamine	0.70	0	-
methylamine	0.73	0	4.7
2-butanone	0.76	0	-
acetone	1.18	0	10.4
neopentane	-	34	13.4
tert-butylamine	-	36	5.0
n-pentane	-	36	-
tert-butyl alcohol	-	63	2.3
ammonia	-	74	1.3

Table 2.4. Influence of various compounds on the degree of radiation induced crosslinking in polyethylene⁽¹⁴⁾.

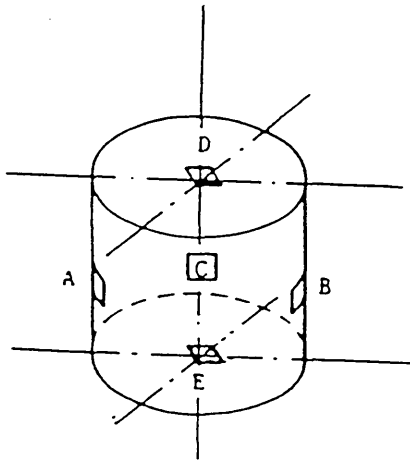
* the samples received an absorbed dose of 40 Mrad, and irradiation was carried out under vacuum.

main chain linkage under attack	products of hydrolysis	polymer type(s)
$\begin{array}{c} & & \\ -C & -C- & O-C- \\ & & \\ & O & \end{array}$	$\begin{array}{c} \\ -C-OH \\ \end{array} + HO-\begin{array}{c} \\ C- \\ \end{array}$	polyester
carboxylic acid ester		
$\begin{array}{c} & O^{(-)} \\ & \\ -O-P-O-C- \\ & \\ & O \end{array}$	$\begin{array}{c} & O^{(-)} \\ & \\ -O-P-OH \\ & \\ & O \end{array} + HO-\begin{array}{c} \\ C- \\ \end{array}$	nucleic acids (DNA, etc)
phosphoric acid ester		
$\begin{array}{c} & & \\ -C & -O- & C- \\ & & \end{array}$	$\begin{array}{c} \\ -C-OH \\ \end{array} + HO-\begin{array}{c} \\ C- \\ \end{array}$	polyether, and polysaccharides (cellulose, amylose, etc)
ether, glycoside		
$\begin{array}{c} & & \\ -C & -C- & N-C- \\ & & \\ & O & H \end{array}$	$\begin{array}{c} \\ -C-C-OH \\ \\ & O \end{array} + H_2N-\begin{array}{c} \\ C- \\ \end{array}$	polyamides, proteins, polypeptides
amide (peptide)		
$\begin{array}{c} & & \\ -C & -O-C- & N-C- \\ & & \\ & O & H \end{array}$	$\begin{array}{c} \\ -C-OH \\ \end{array} + CO_2 + H_2N-\begin{array}{c} \\ C- \\ \end{array}$	polyurethanes
urethanes		
$\begin{array}{c} & & \\ -Si & -O- & Si- \\ & & \end{array}$	$\begin{array}{c} \\ -Si-OH \\ \end{array} + HO-\begin{array}{c} \\ Si- \\ \end{array}$	polysiloxanes
siloxanes		

Table 2.5. Some common polymer structures that are susceptible to hydrolysis, and their respective degradation mechanisms⁽⁶⁷⁾.

SAMPLE IDENTITY	$N_{CR_m}(0) \times 10^6 / \text{mol} \cdot \text{mm}^{-3}$.		
	1.00 wt% 2,4-DCBP PASTE.	1.25 wt% 2,4-DCBP PASTE.	1.50 wt% 2,4-DCBP PASTE.
1	0.112	0.121	0.132
2	0.110	0.115	0.129
3	0.109	0.118	0.125
4	0.103	0.119	0.128
5	0.107	0.121	0.127
6	0.109	0.115	0.130
7	0.105	0.118	0.133
8	0.108	0.118	0.131
9	0.110	0.117	0.129
10	0.108	0.119	0.127
11	0.105	0.117	0.127
12	0.107	0.122	0.131
13	0.109	0.126	0.133
14	0.110	0.120	0.129
15	0.107	0.116	0.125
$\bar{N}_{CR_m}(0)$	0.108	0.118	0.129
$\sigma N_{CR_m}(0)$	0.002	0.002	0.003

Table 6.1.1. Material characterisation of the PDMS elastomers employed in the stress relaxation studies.



- KEY:-
- A = centre of sample edge
 - B = centre of sample edge (opposite)
 - C = centre of sample
 - D = centre of top face (relative to mould)
 - E = centre of bottom face (relative to mould)

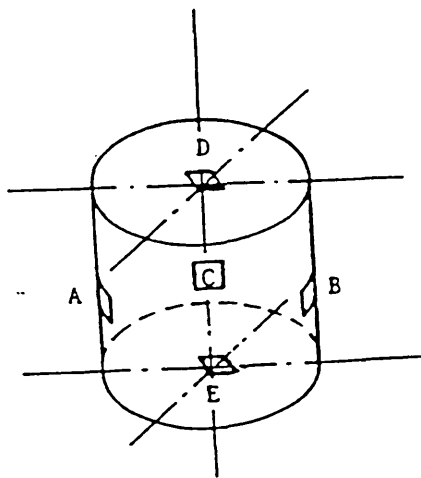
Sample locations for assessment of sample homogeneity

SAMPLE LOCATION	$N_{CRS} \times 10^6 / \text{mol} \cdot \text{mm}^{-3}$		
	1.00 wt% 2,4-DCBP PASTE	1.25 wt% 2,4-DCBP PASTE	1.50 wt% 2,4-DCBP PASTE
A	0.091	0.100	0.113
B	0.092	0.100	0.112
C	0.088	0.097	0.110
D	0.090	0.100	0.112
E	0.093	0.102	0.116
$\bar{N}_{CRS}(0)$	0.091	0.100	0.113
$\sigma N_{CRS}(0)$	0.002	0.002	0.002

6.1.2. Assessment of sample homogeneity of polydimethylsiloxane elastomers employed in the chemical stress relaxation studies.

SAMPLE IDENTITY	$N_{cr_m}(0) \times 10^6 / \text{mol} \cdot \text{mm}^{-3}$
1	0.722
2	0.721
3	0.720
4	0.719
5	0.726
6	0.721
7	0.727
8	0.722
9	0.719
10	0.718
$\bar{N}_{cr_m}(0)$	0.722
$\sigma N_{cr_m}(0)$	0.003

Table 6.1.3. Material characterisation of Viton E60-C Elastomers employed in the chemical stress relaxation studies.



KEY:-
 A = centre of sample edge
 B = centre of sample edge (opposite)
 C = centre of sample
 D = centre of top face (relative to mould)
 E = centre of bottom face (relative to mould)

Sample locations for assessment of sample homogeneity

SAMPLE LOCATION	$N_{crs} \times 10^6 / \text{mol} \cdot \text{mm}^{-3}$
A	0.710
B	0.711
C	0.707
D	0.712
E	0.712
$N_{crs} (0)$	0.710
$\sigma_{N_{crs}}$	0.001

Table 6.1.4. Assessment of sample homogeneity of Viton E60C elastomer employed in the chemical stress relaxation studies.

Degradation Reaction	Activation Energy E_a (KJ.mol ⁻¹)
<u>Polydimethylsiloxane elastomer</u>	
(N _{cr_m} (0) = 0.118 x 10 ⁻⁶ mol.mm ⁻³ .)	
random chain scission (interchange)	15 ± 4
random chain scission (interchange) (method proposed by Osthoff et al)	19 ± 2
crosslinking (overall)	16 ± 3
crosslinking (reformation of chains cleaved during stress relaxation)	12 ± 2
crosslinking (reformation of chains cleaved prior to stress relaxation)	21 ± 5
<u>Polydimethylsiloxane elastomer</u>	
(N _{cr_m} (0) = 0.129 x 10 ⁻⁶ mol.mm ⁻³ .)	
random chain scission (interchange)	12 ± 3
crosslinking (overall)	36 ± 6
crosslinking (reformation of chains cleaved during stress relaxation)	15 ± 3
crosslinking (reformation of chains cleaved prior to stress relaxation)	35 ± 9

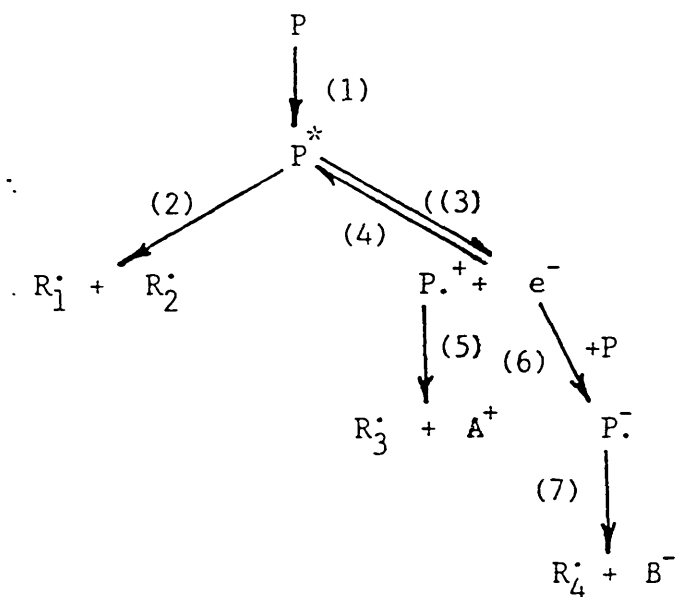
Table 6.4.1.1. Activation energies from the thermal degradation studies undertaken on polydimethylsiloxane elastomer.

Treatment		crosslink density $N_{cr} \times 10^6 / \text{mol} \cdot \text{mm}^{-3}$									
POST CURE TIME (hrs)	CURE TIME (mins)	1.00wt%		1.25wt%		1.50wt%		2.00wt%		3.00wt%	
		2,4-DCBP PASTE		2,4-DCBP PASTE		2,4-DCBP PASTE		2,4-DCBP PASTE		2,4-DCBP PASTE	
0	5	0.259	0.278	0.259	0.278	0.350	0.318	0.341	0.318	0.341	0.318
0	10	0.261	0.233	0.261	0.233	0.252	0.282	0.364	0.282	0.364	0.282
0	15	0.250	0.234	0.250	0.234	0.256	0.324	0.348	0.324	0.348	0.324
0	20	0.258	0.225	0.258	0.225	0.233	0.300	0.345	0.300	0.345	0.300
2	5	0.140	0.156	0.140	0.156	0.208	0.225	0.230	0.225	0.230	0.225
2	10	0.122	0.144	0.122	0.144	0.200	0.227	0.223	0.227	0.223	0.227
2	15	0.120	0.130	0.120	0.130	0.203	0.200	0.202	0.200	0.202	0.200
2	20	0.118	0.148	0.118	0.148	0.195	0.208	0.210	0.208	0.210	0.208
3	5	0.095	0.158	0.095	0.158	0.209	0.202	0.221	0.202	0.221	0.202
3	10	0.087	0.130	0.087	0.130	0.204	0.234	0.232	0.234	0.232	0.234
3	15	0.081	0.133	0.081	0.133	0.207	0.210	0.187	0.210	0.187	0.210
3	20	0.090	0.148	0.090	0.148	0.210	0.195	0.216	0.195	0.216	0.195
6	5	0.130	0.160	0.130	0.160	0.221	0.190	0.174	0.190	0.174	0.190
6	10	0.110	0.137	0.110	0.137	0.201	0.200	0.190	0.200	0.190	0.200
6	15	0.121	0.110	0.121	0.110	0.205	0.167	0.148	0.167	0.148	0.167
6	20	0.110	0.118	0.110	0.118	0.210	0.170	0.166	0.170	0.166	0.170
24	5	0.070	0.087	0.070	0.087	0.190	0.121	0.112	0.121	0.112	0.121
24	10	0.064	0.080	0.064	0.080	0.174	0.108	0.122	0.108	0.122	0.108
24	15	0.070	0.059	0.070	0.059	0.186	0.102	0.090	0.102	0.090	0.102
24	20	0.068	0.070	0.068	0.070	0.168	0.103	0.101	0.103	0.101	0.103

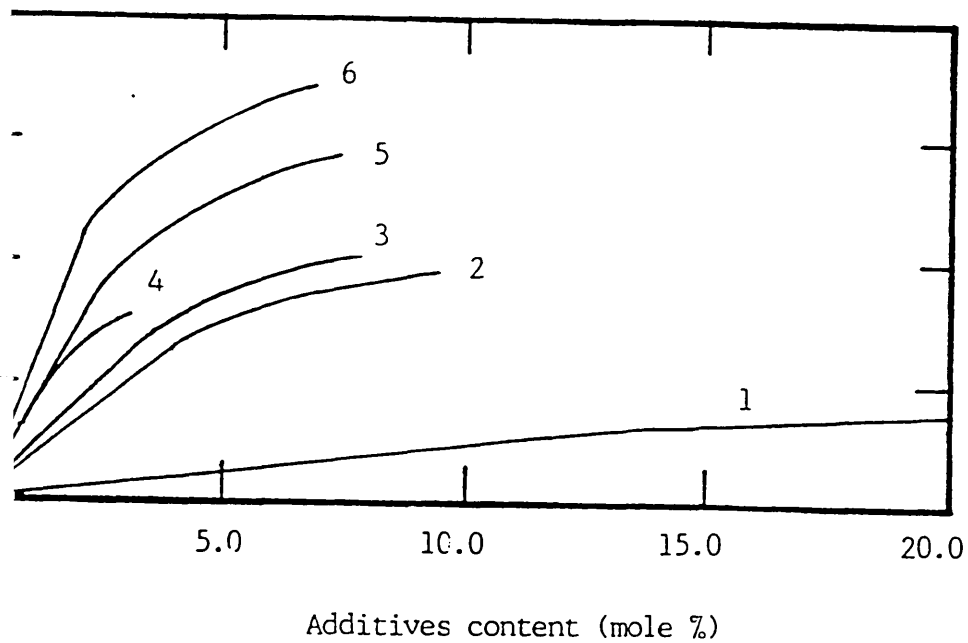
Table 6.4.3.1. Cure / post cure trials on PDMS elastomers.

POST CURE TIME (hrs)	MEAN & STD. DEV	1.00wt% 2,4-DCBP PASTE	1.25wt% 2,4-DCBP PASTE	1.50wt% 2,4-DCBP PASTE	2.00wt% 2,4-DCBP PASTE	3.00wt% 2,4-DCBP PASTE
0	$\bar{N}_{cr_m} (0)$ $\sigma N_{cr_m} (0)$	0.257 0.005	0.243 0.024	0.273 0.053	0.306 0.019	0.350 0.010
2	$\bar{N}_{cr_m} (0)$ $\sigma N_{cr_m} (0)$	0.125 0.010	0.145 0.011	0.202 0.005	0.215 0.013	0.216 0.013
3	$\bar{N}_{cr_m} (0)$ $\sigma N_{cr_m} (0)$	0.088 0.006	0.142 0.013	0.208 0.003	0.210 0.017	0.214 0.019
6	$\bar{N}_{cr_m} (0)$ $\sigma N_{cr_m} (0)$	0.118 0.010	0.131 0.022	0.209 0.009	0.182 0.016	0.170 0.018
24	$\bar{N}_{cr_m} (0)$ $\sigma N_{cr_m} (0)$	0.068 0.003	0.074 0.012	0.180 0.010	0.109 0.009	0.106 0.014

Table 6.4.3.2. Statistical analysis of the data presented in Table 6.4.3.1.



1. Possible primary reactions induced by γ -radiation in polymers^(2a).
 (numbers refer to reactions in text)

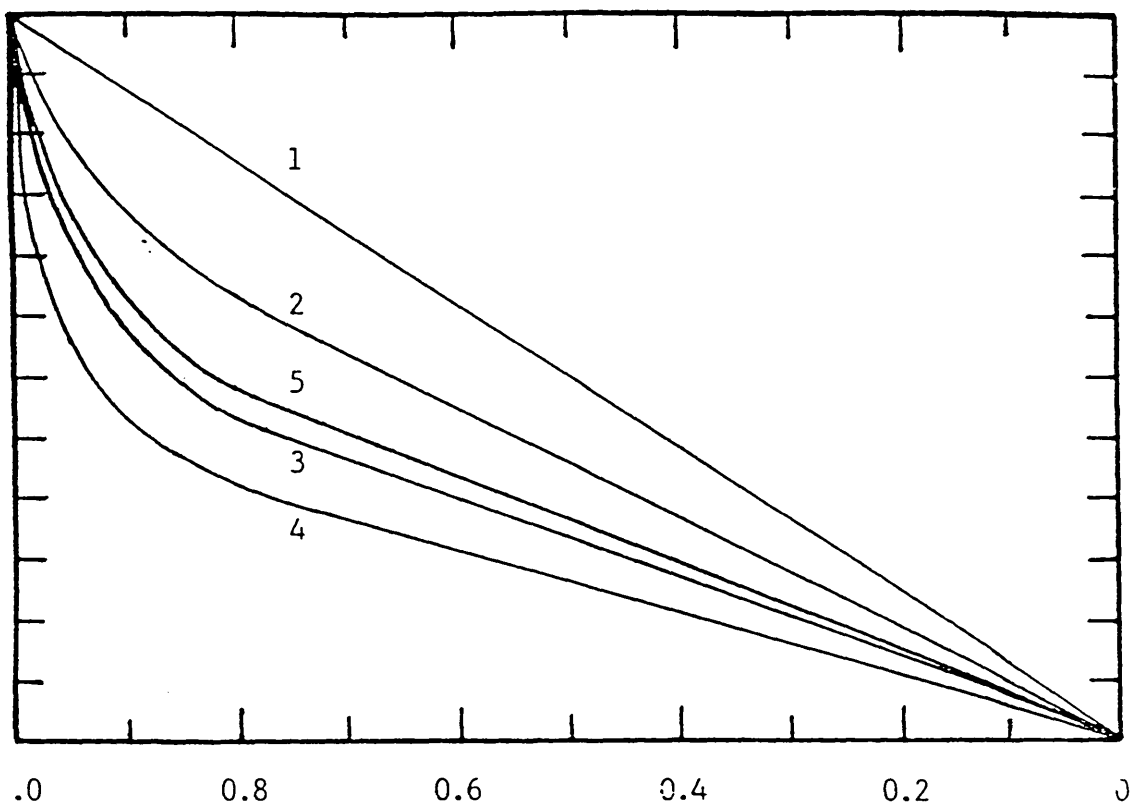


radiative degradation of polymethylmethacrylate as a function of the content of various aromatic additives.

Key:-

- 1 - benzene
- 2 - naphthalene
- 3 - phenanthrene
- 4 - anthracene
- 5 - pyrene
- 6 - benz-(α)-anthracene

and G are the degradation yields without and with the protective
 and respectively.



Polyethylene content (electron fractions)

Radiation yields of hydrogen from mixtures of polyethylene with aromatic compounds, and from polyethylene to which styrene has been grafted.

- Key:-
- 1 - calculated under conditions where the additivity rule applies.
 - 2 - polyethylene and polystyrene mixture
 - 3 - mixtures of polyethylene with naphthalene and anthracene
 - 4 - mixture of polyethylene with phenanthracene
 - 5 - polyethylene with grafted styrene

Electron fractions were calculated by application of the following relationships:-

$$f_1 = \frac{a_1 n_1}{a_1 n_1 + a_2 n_2} \quad \text{and} \quad f_2 = \frac{a_2 n_2}{a_1 n_1 + a_2 n_2}$$

where a_1 and a_2 , are the number of moles per unit volume of material, n_1 and n_2 , are numbers of electrons per mole, and f_1 and f_2 , the electron fractions, of components 1 and 2 respectively.

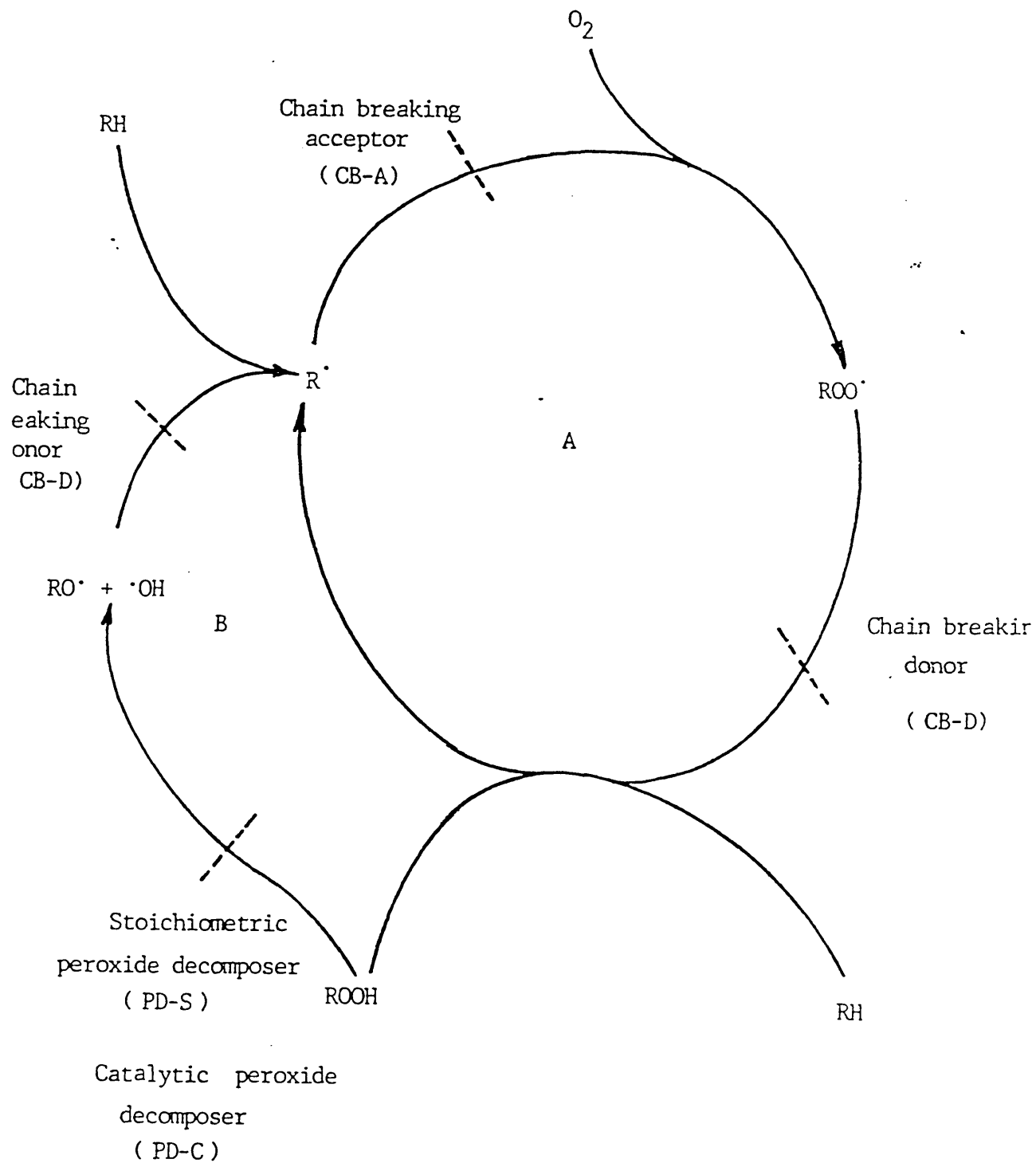


Fig 2.4. Autoxidation mechanism of hydrocarbon polymers, and possible anti-oxidant action.

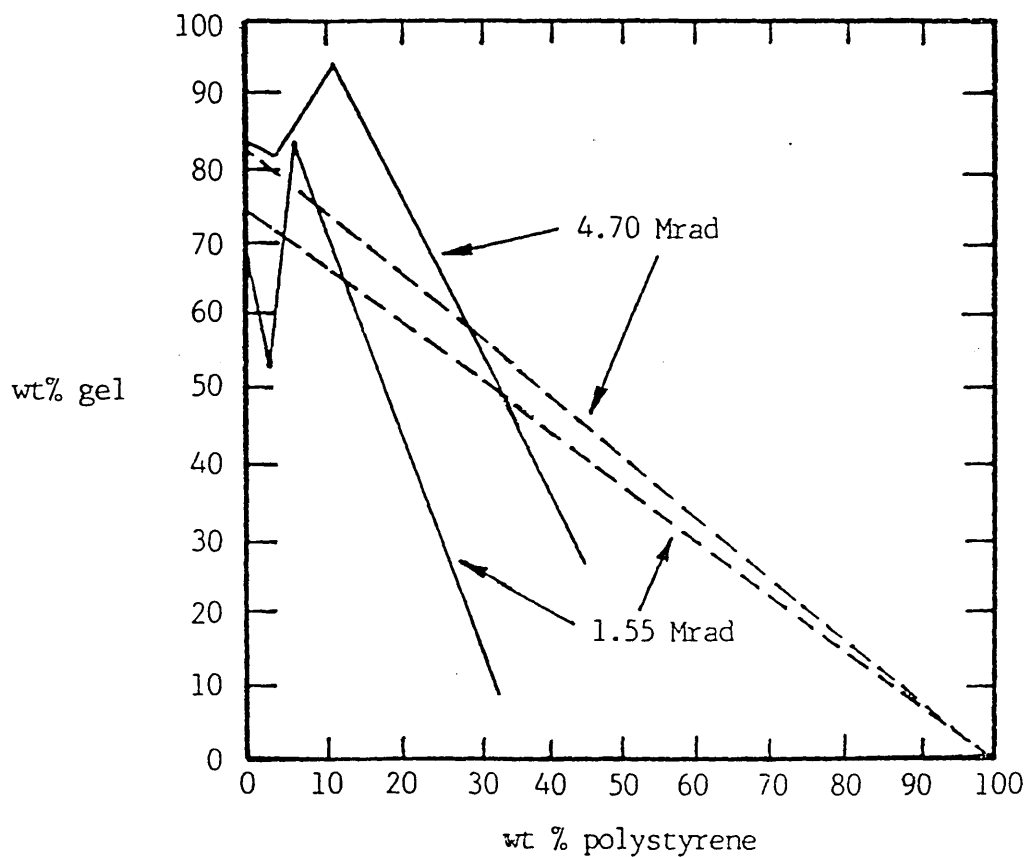
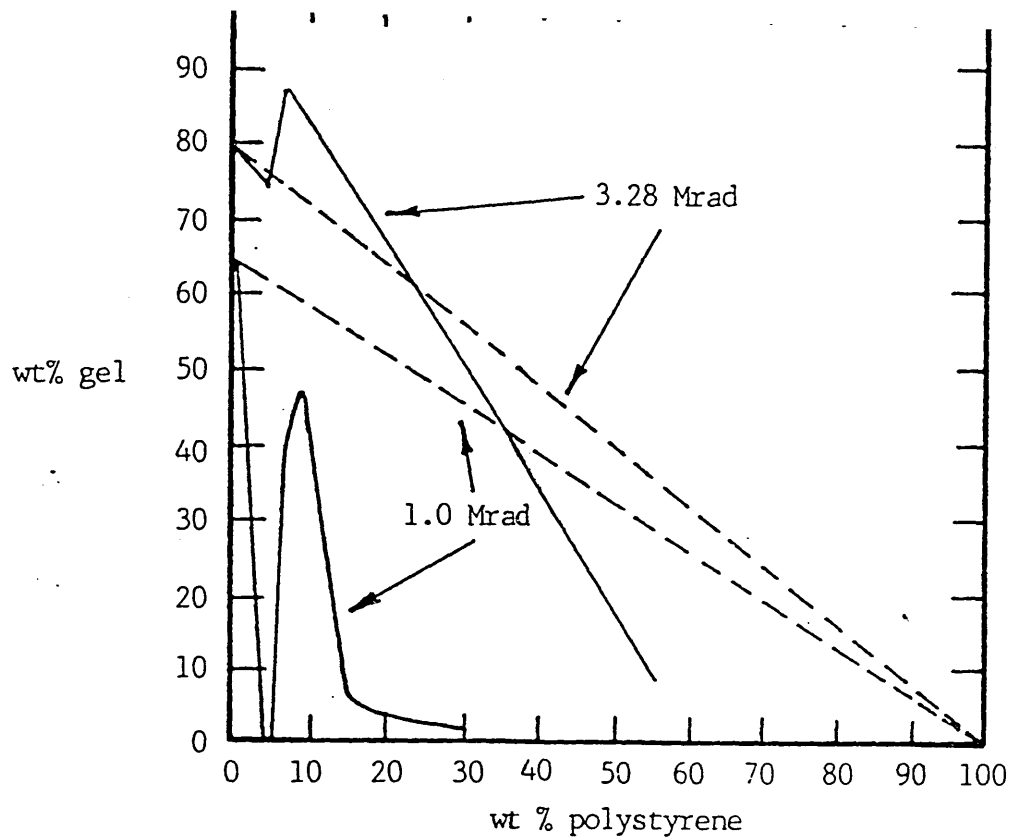


Fig 2.5. Irradiation studies of polystyrene-polydimethylsiloxane blends. (continuous lines are experimental data, and dotted lines are the estimated gel contents using the additivity rule).

* Dose rates ranged from 0.2-1.5 Mrad.hr⁻¹, depending upon the integrat. dose required.

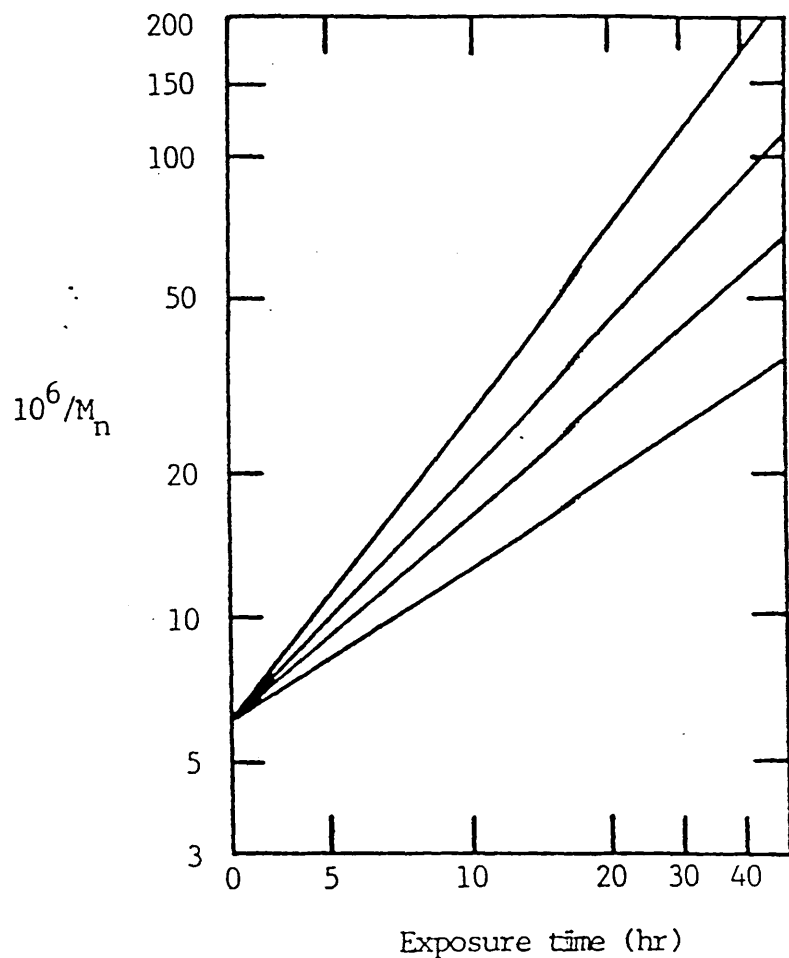


Fig 3.1. Variation in the number average molecular weight of polyisobutylene, irradiated under vacuum at various temperatures⁽¹²⁰⁾.

key:-
 1 - -196°C
 2 - -78°C
 3 - +35°C
 4 - +80°C

* a dose rate of 0.8 Mrad.hr⁻¹ was employed in the investigations.

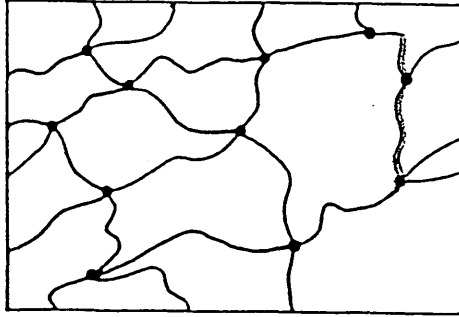


Fig 3.2a. Schematic representation of ideal elastomer network structure.

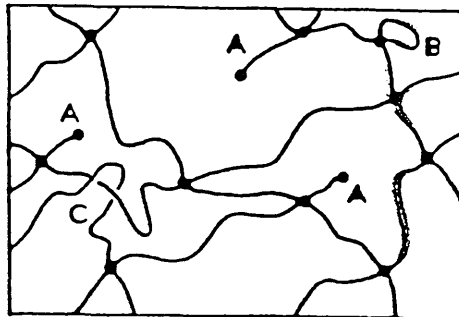


Fig 3.2b. Schematic representation of real elastomer network structure, showing:-

A - free chain ends.

B - loops.

and C - entanglements.

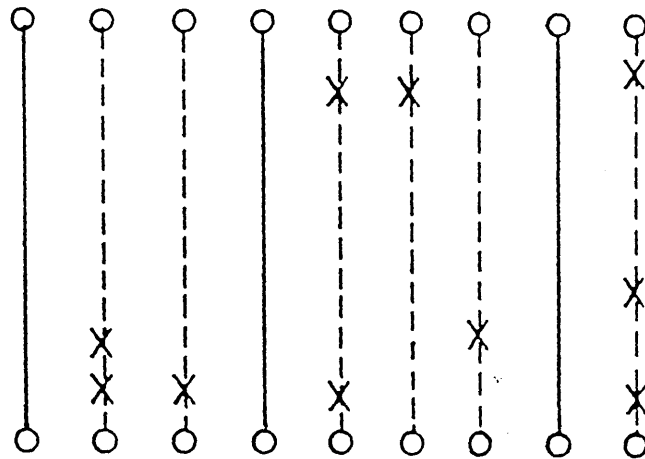


Fig 3.3. Schematic representation of a unit volume of elastomer network.

solid lines represent load-bearing chains,
dotted lines represent non-load-bearing chains.

Once a chain has undergone a scission it is rendered elastically ineffective.

Therefore in the above example:-

number of scissions of load-bearing chains = 6

total number of chain scissions $q_m(t) = 10$

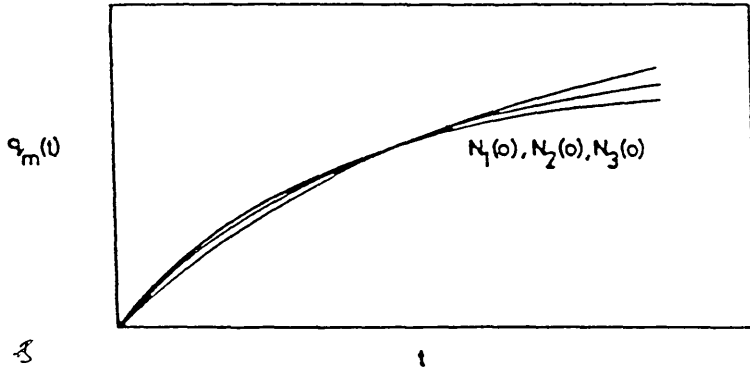


Fig 3.4a. $q_m(t)$ vs t for elastomers having different initial crosslink densities undergoing degradation by main-chain scission.

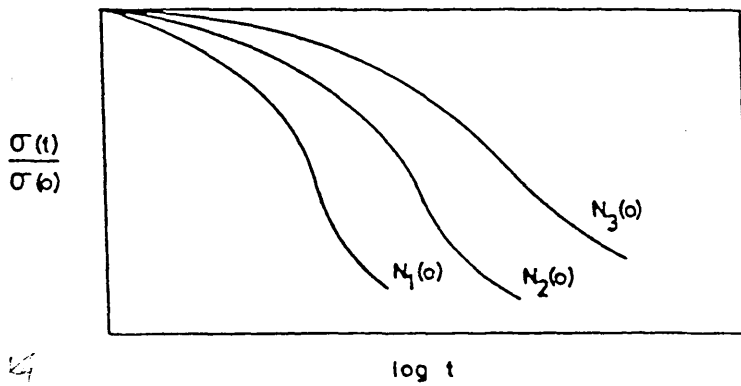


Fig 3.4b. $\sigma(t) / \sigma(0)$ vs $\log t$ for elastomers having different initial crosslink densities undergoing degradation by main-chain scission.

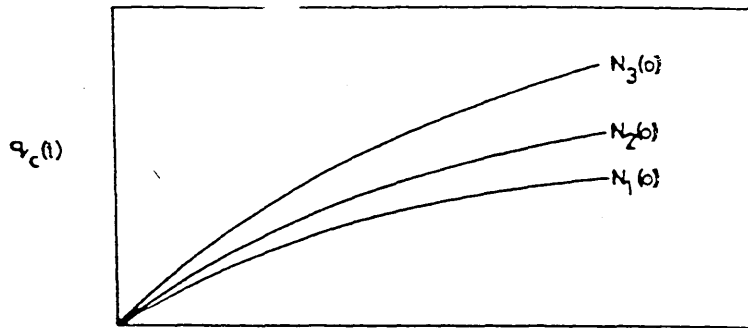


Fig 3.5a. $q_c(t)$ vs t for elastomers having different initial crosslink densities undergoing degradation by scission of the crosslinkages.

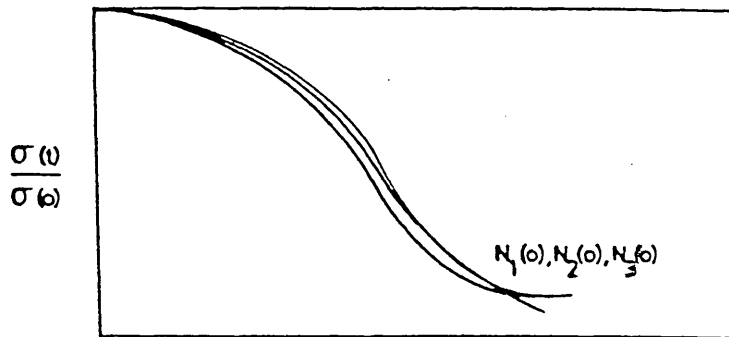


Fig 3.5b. $\sigma(t) / \sigma(0)$ vs $\log t$ for elastomers having different initial crosslink densities undergoing degradation by scission of the crosslinkages.

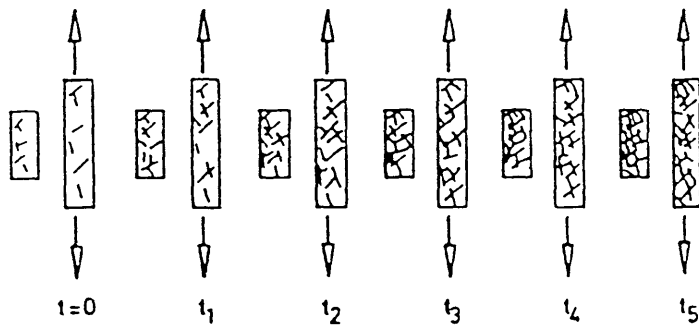
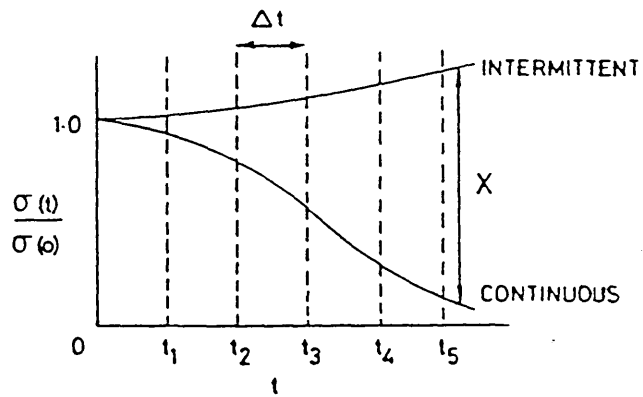


Fig3.6. The principle of intermittent stress relaxation.

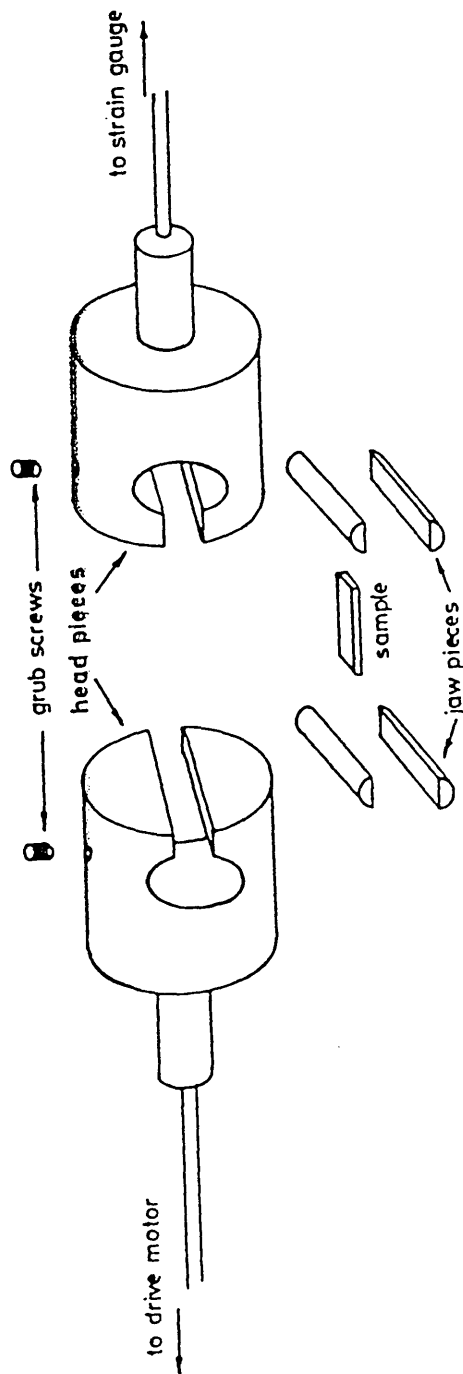


Fig 5.1. Schematic of the modified clamp design proposed by Seferis⁽¹⁵⁴⁾ employed in the physical stress relaxation studies.

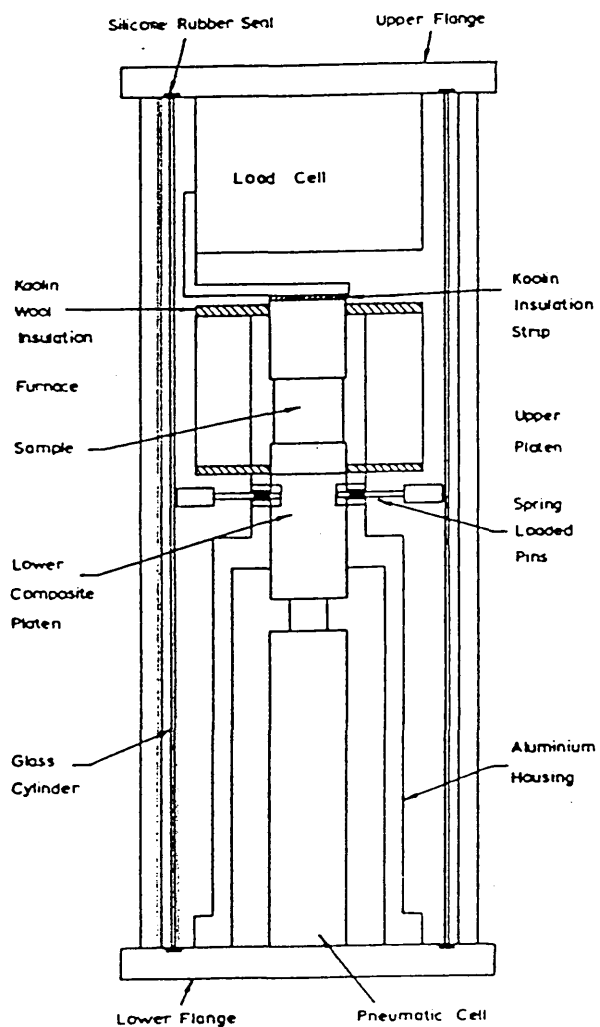


Fig 5.2. Schematic of the stress relaxation rig employed in the thermal/radiative degradation studies.

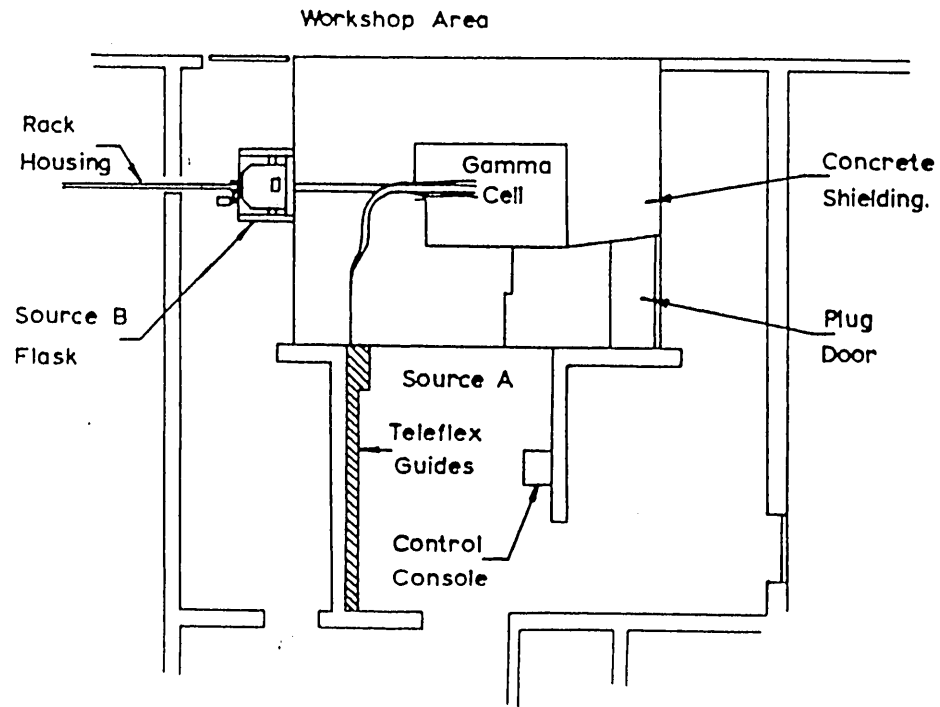


Fig 5.3. Layout of the irradiation facility employed in the radiative/thermal degradation studies.

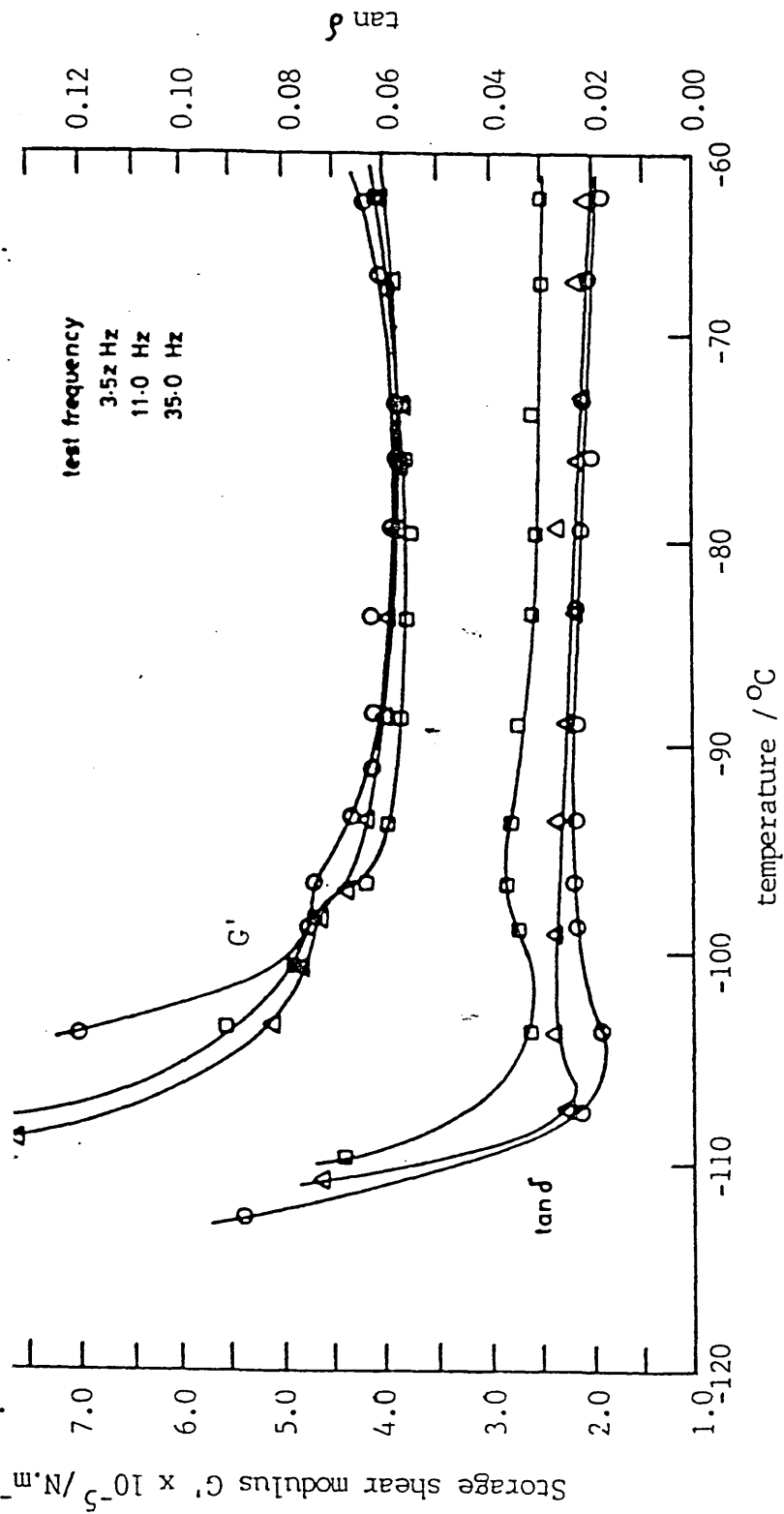


Fig 6.3.1. DMA studies on PDMS elastomer ($N_{cr_m}(0) = 0.108 \times 10^{-6} \text{ mol.mm}^{-3}$.)

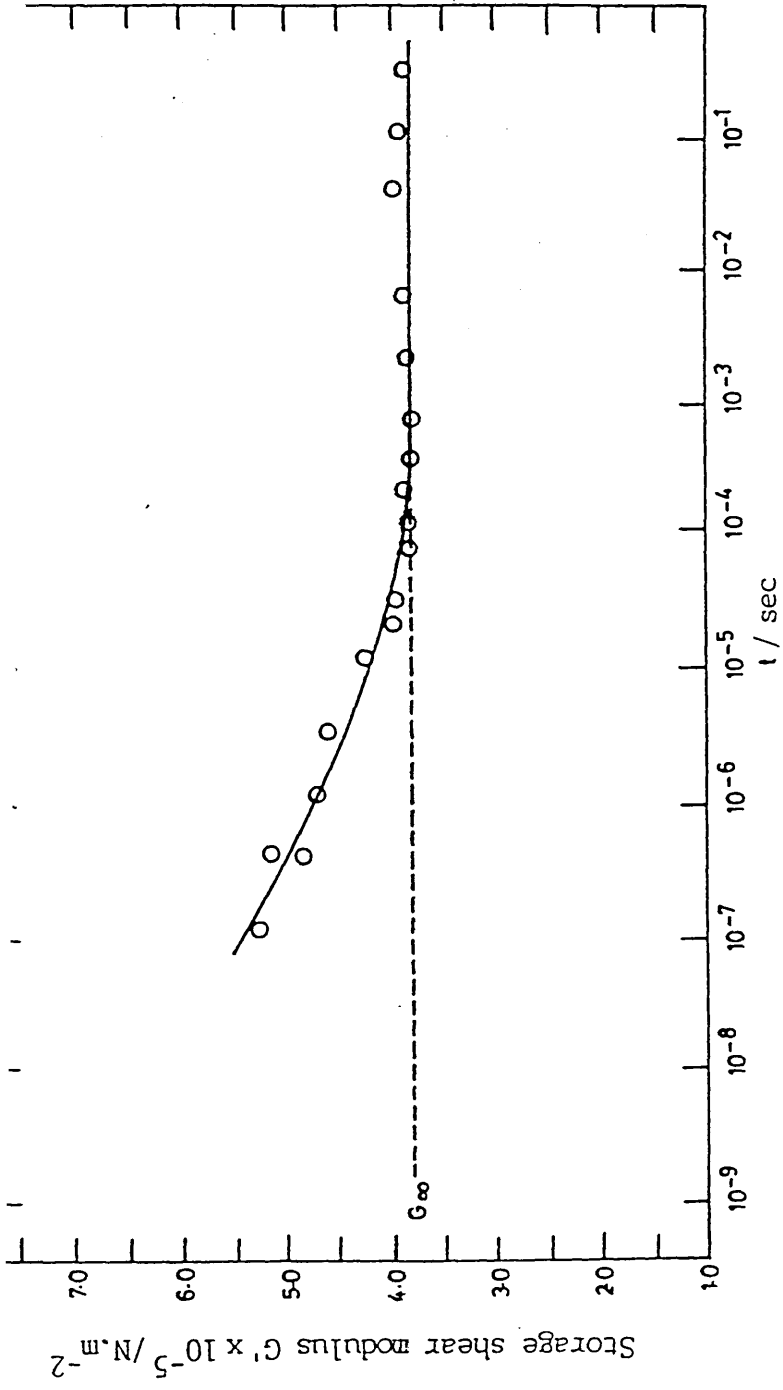


Fig 6.3.2. Variation in storage shear modulus of PDMS elastomer with time at -57°C . ($N_{Cr,m}(0) = 0.108 \times 10^{-6} \text{ mol.lmm}^{-2}$)

* master curve prepared by the application of the time-temperature superposition principle to dynamic data.

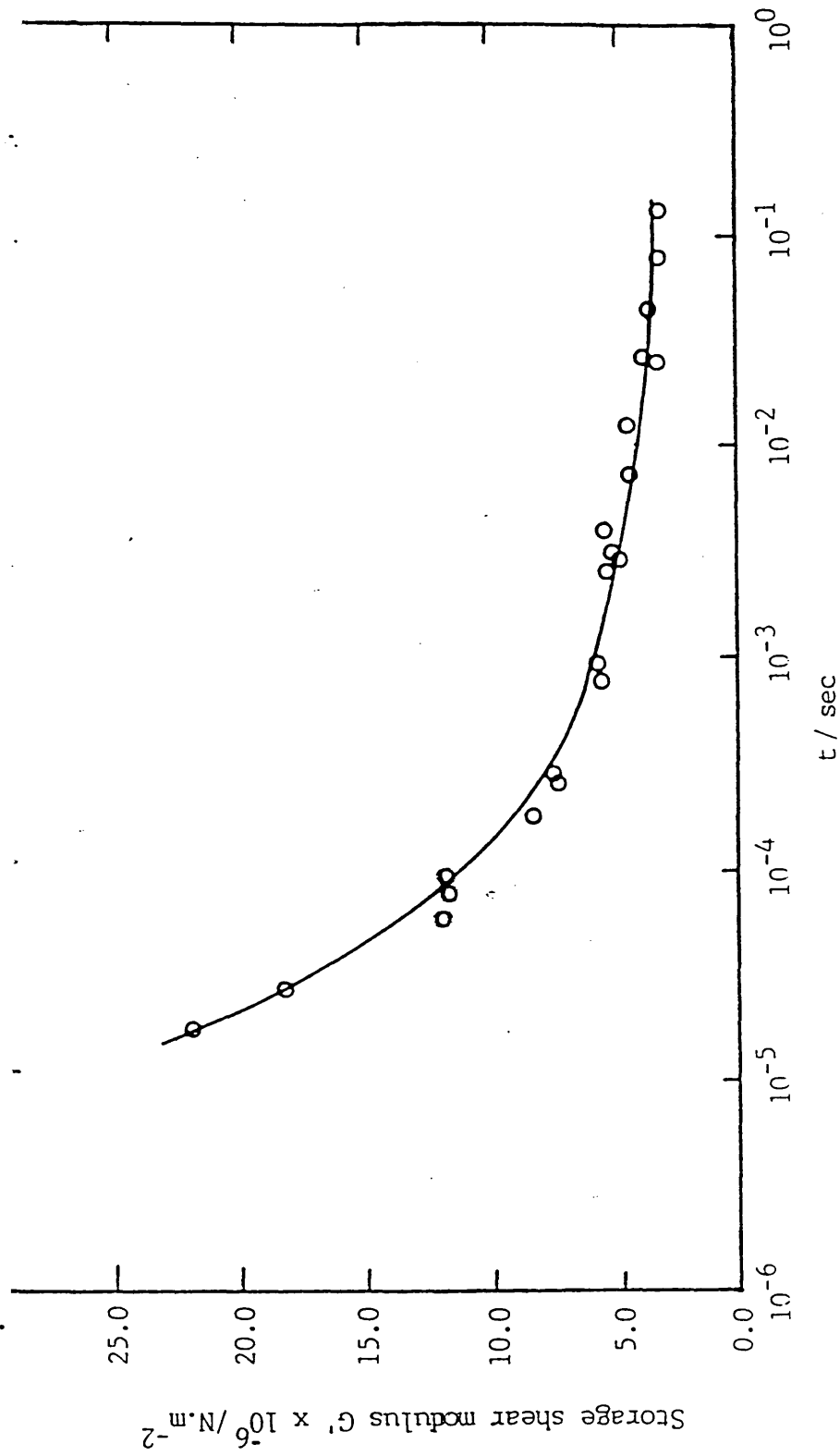


Fig 6.3.3. Variation in storage shear modulus of Viton E60-C elastomer with time at 100°C
 ($N_{cr_m}(0) = 0.722 \times 10^{-6} \text{ mol}\cdot\text{mm}^{-3}$)

* master curve prepared by the application of the time-temperature superposition principle to dynamic data.

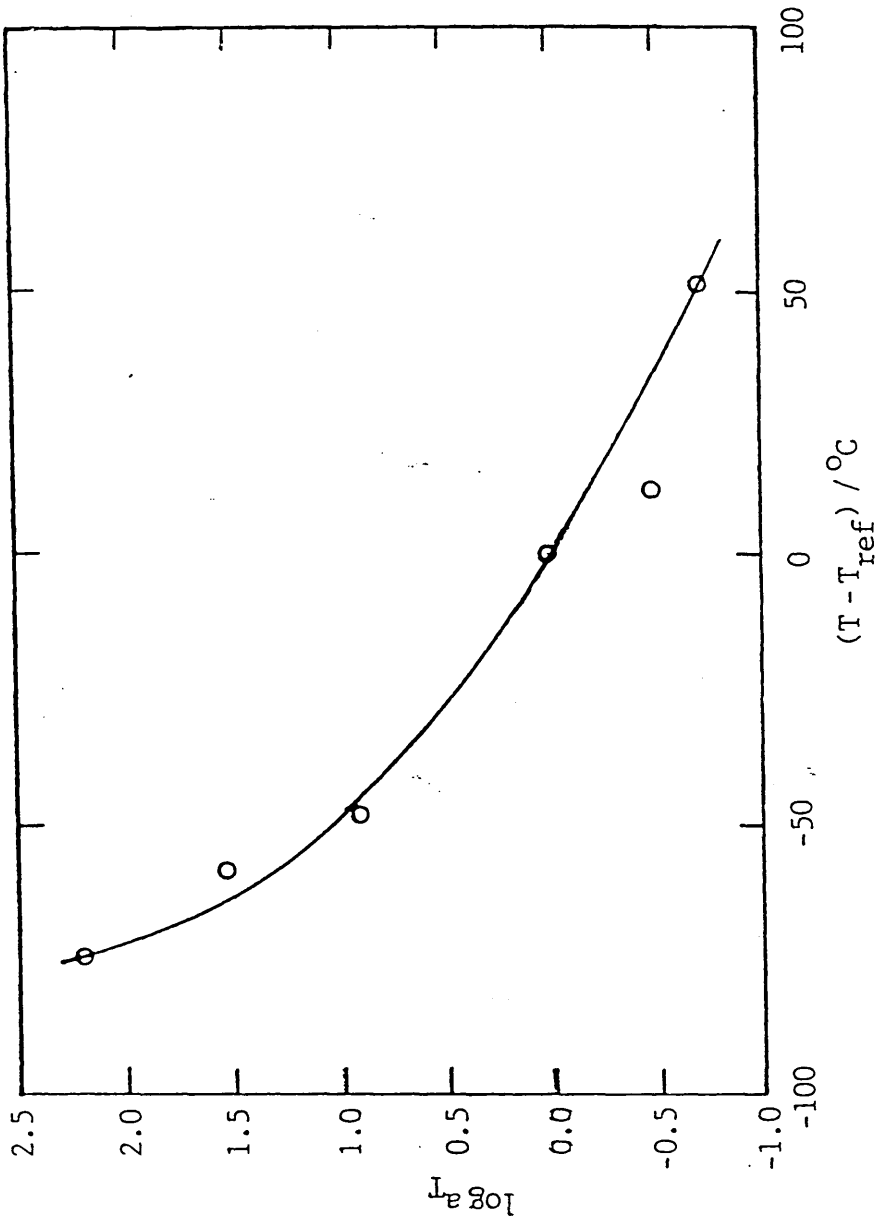


Fig 6.3.4. Variation of shift factor with $(T - T_{ref})$ encountered during the construction of the master curve (Fig 6.3.3.)

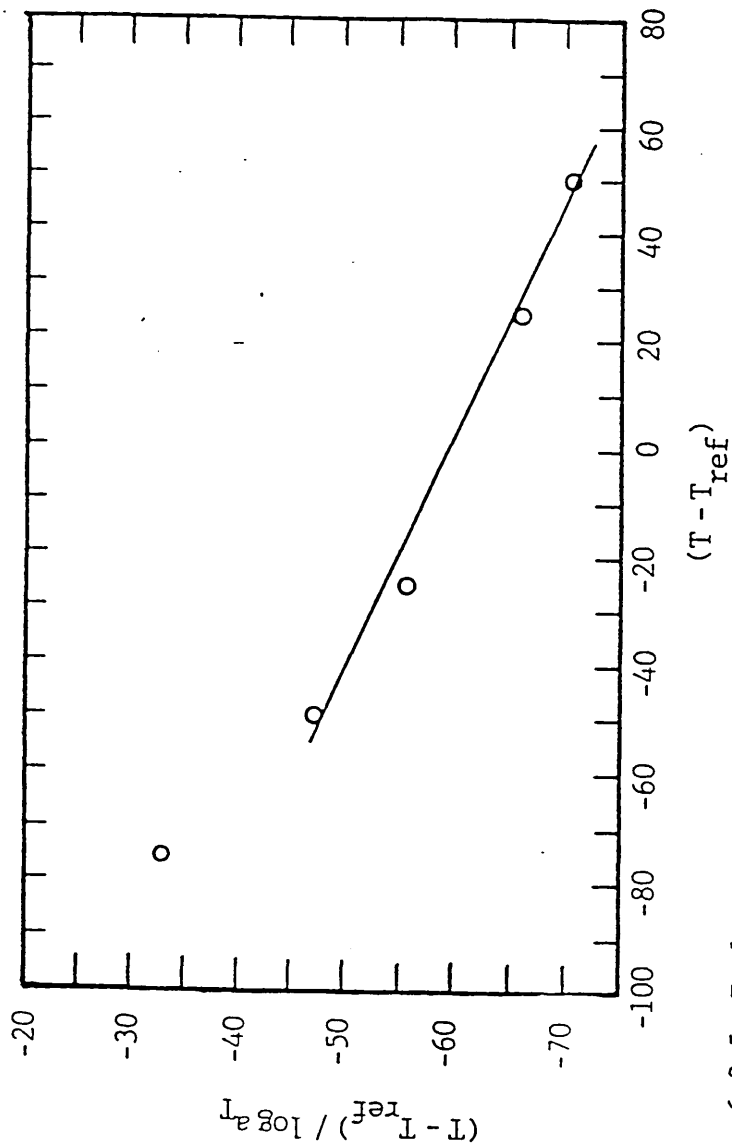


Fig 6.3.5. Evaluation of the WLF constants for the superposition of the storage shear modulus from the data of Fig 6.3.4.

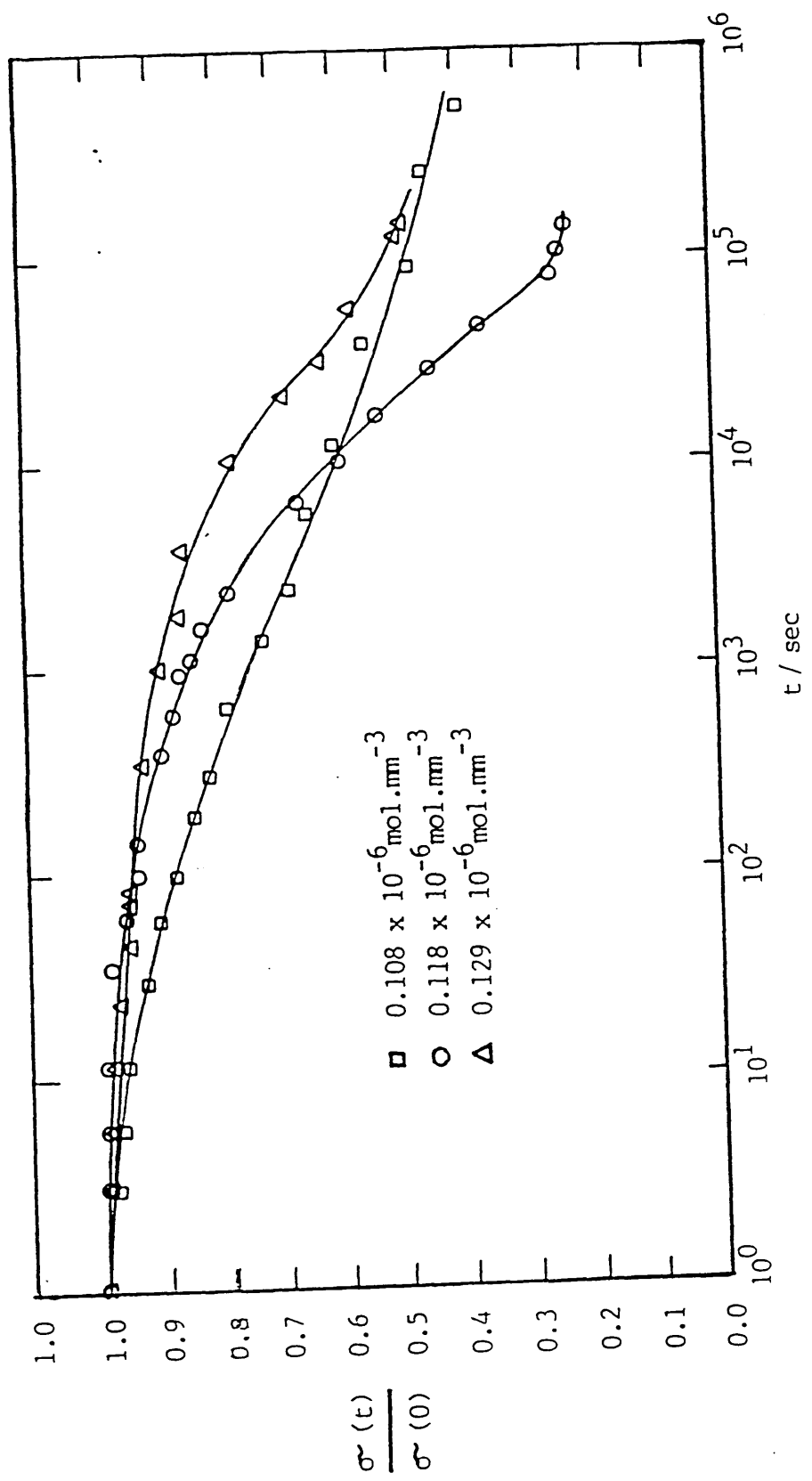


Fig 6.4.1.1. Stress relaxation of PDMS elastomers with various initial crosslink densities at 150°C.

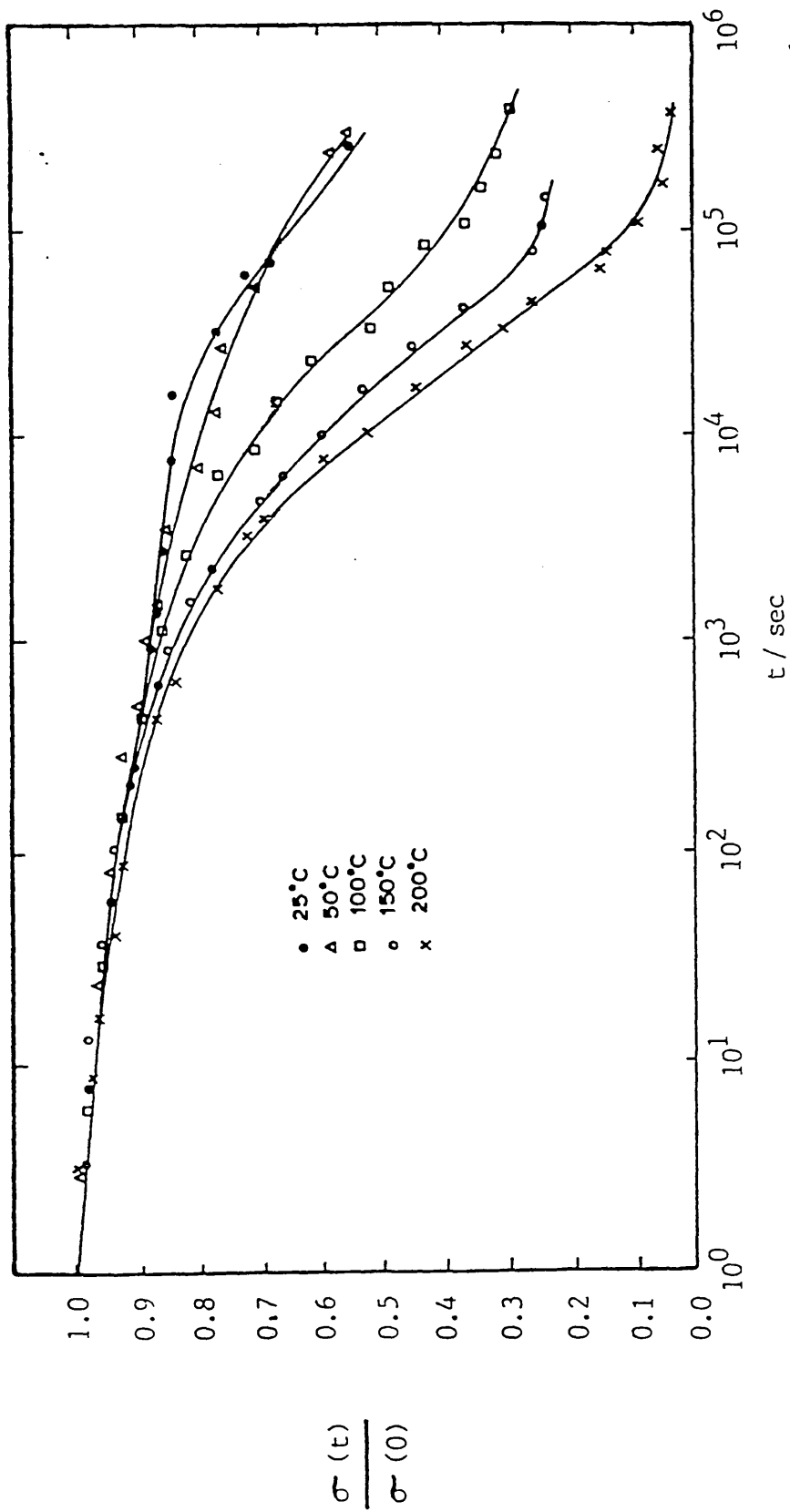


FIG 6.4.1.2, STRESS relaxation of PDMS elastomer at various temperatures. ($N_{cr}(0) = 0.118 \times 10^{-6} \text{ mol. mm}^{-3}$.)

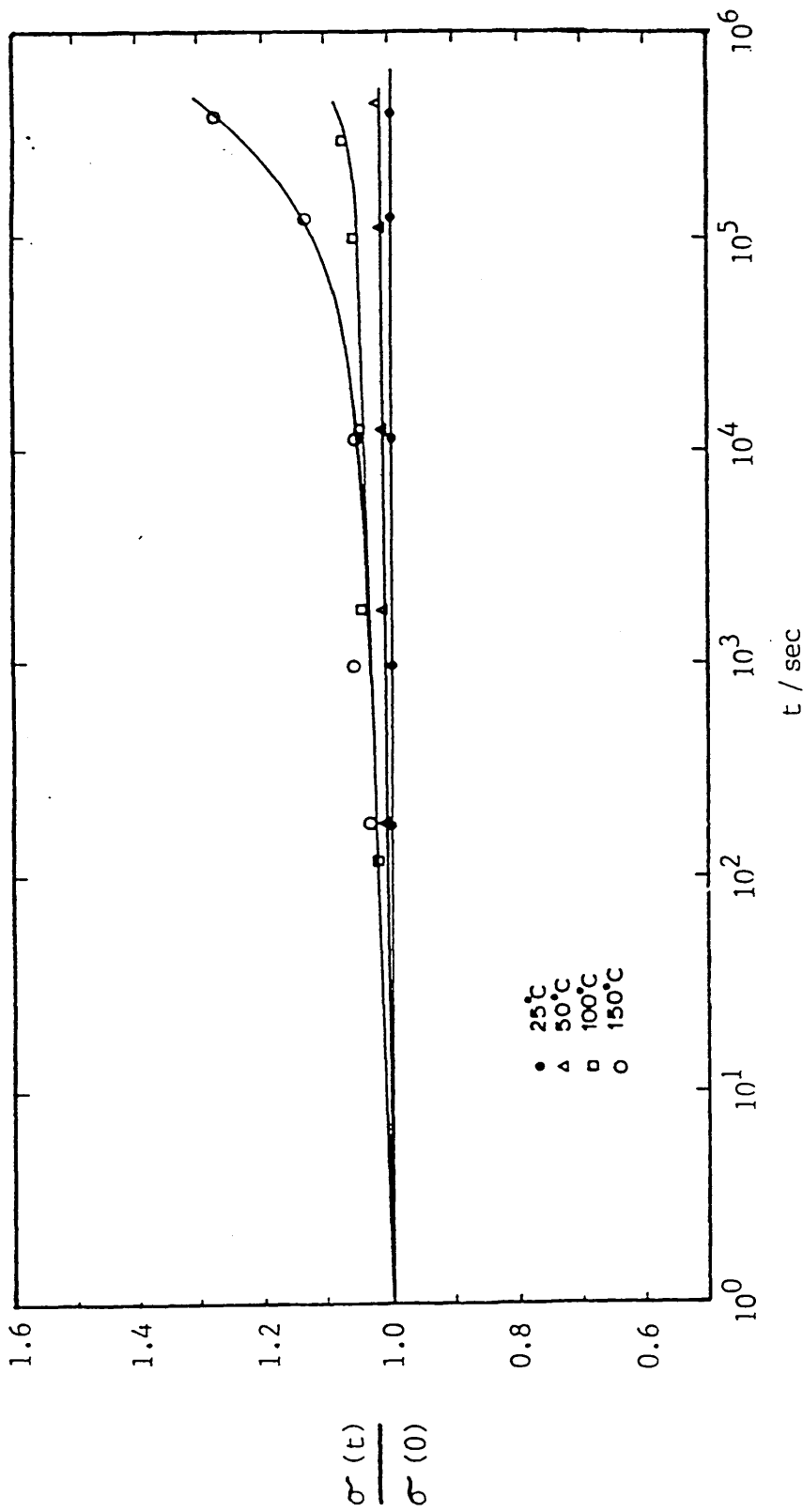


Fig 6.4.1.3. Intermittent stress relaxation of PDMS elastomer at various temperatures. ($N_{cr}(0) = 0.118 \times 10^{-6} \text{ mol} \cdot \text{nm}^{-3}$.)

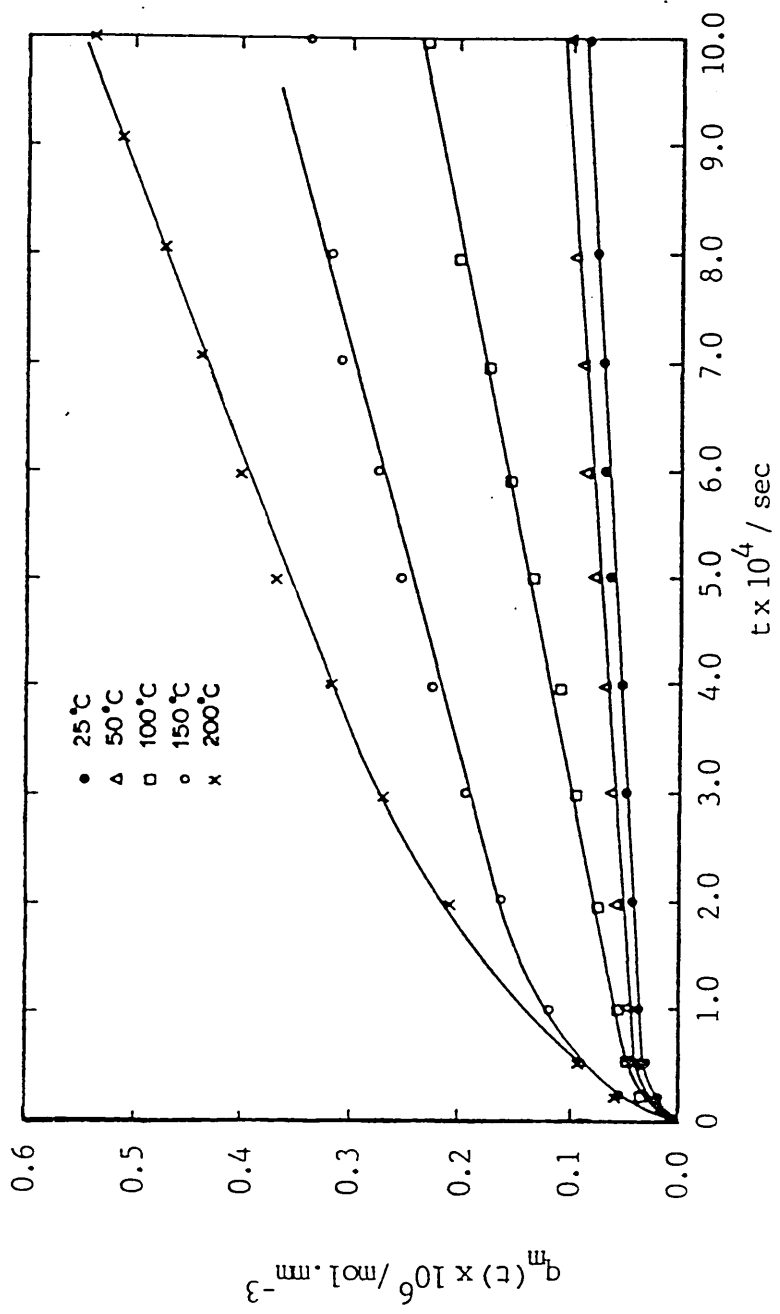
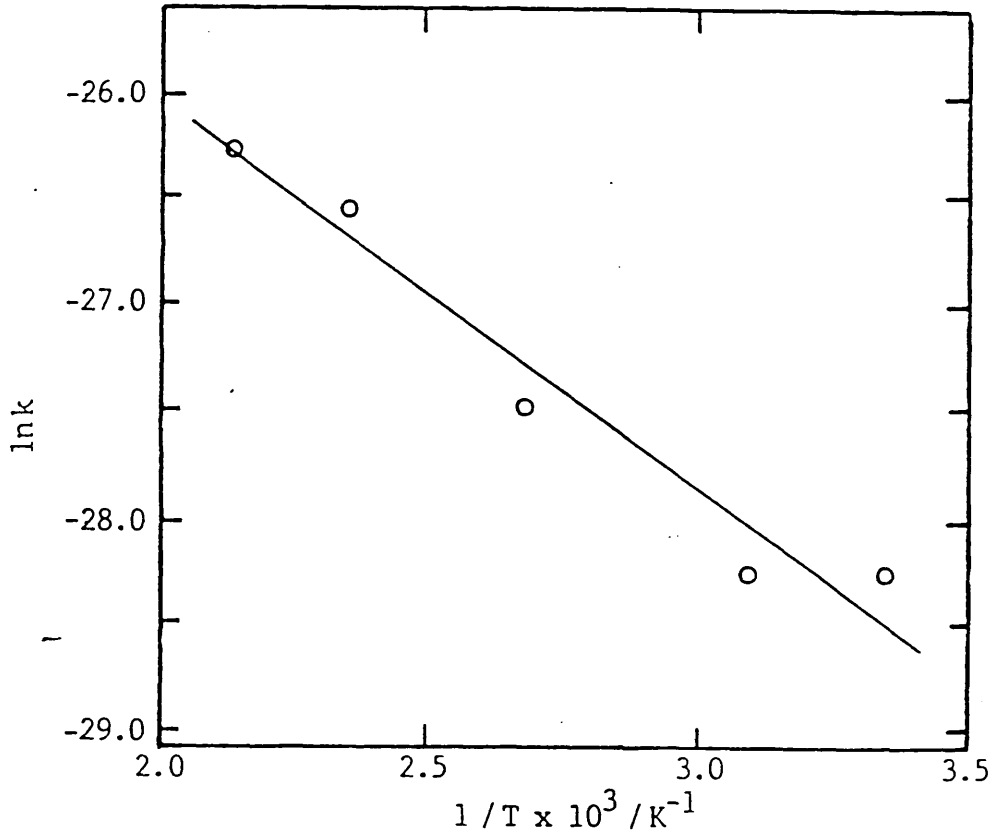


Fig 6.4.1.4. Variation in the number of main chain scissions per unit volume with time occurring inPDMS elastomer at various temperatures. ($N_{Cr}(0) = 0.118 \times 10^{-6} \text{ mol. mm}^{-3}$.)



6.4.1.5.. Arrhenius plot for the determination of the activation energy of the main chain scission reaction occurring in PDMS elastomer. ($N_{cr_m}(0) = 0.118 \times 10^{-6} \text{ mol. mm}^{-3}$.)

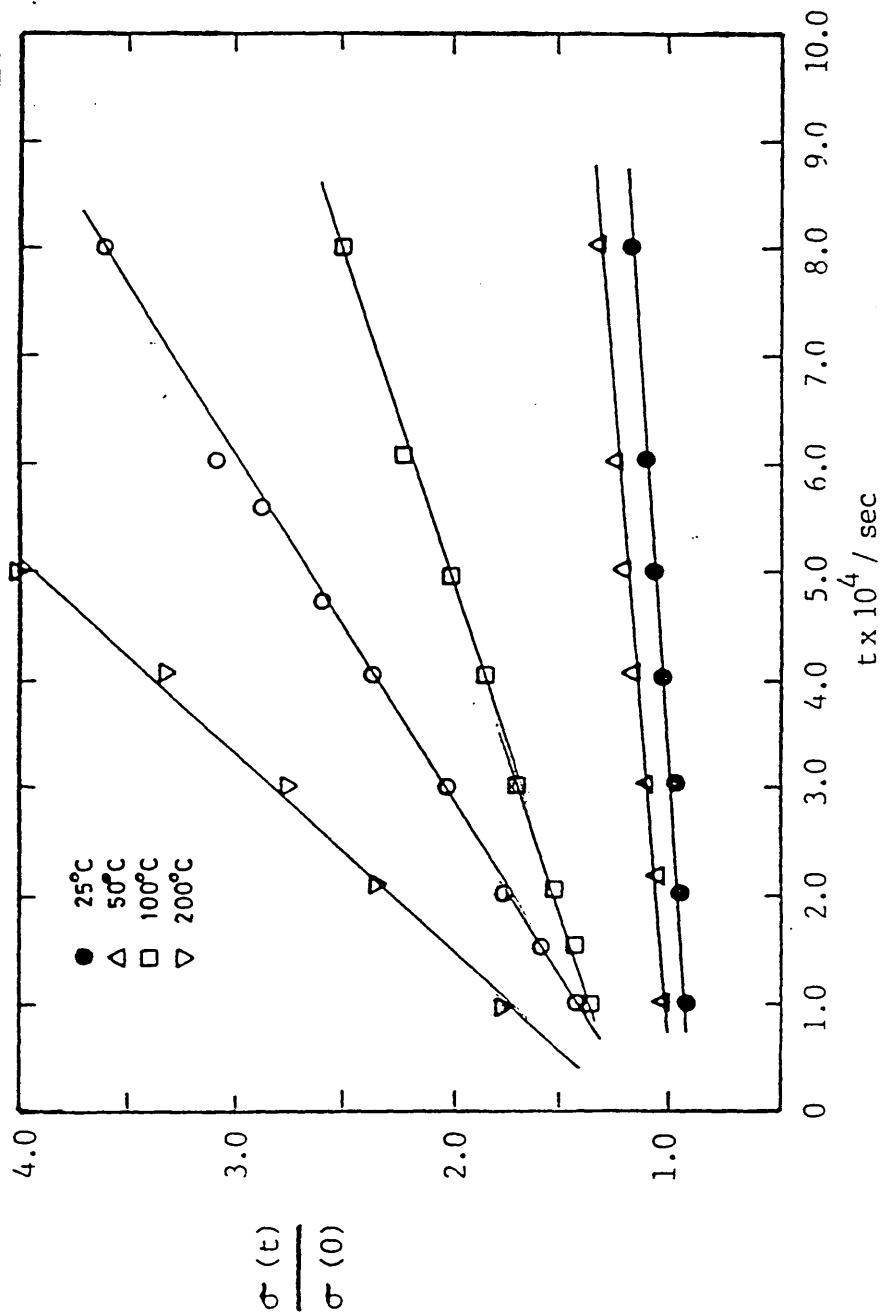
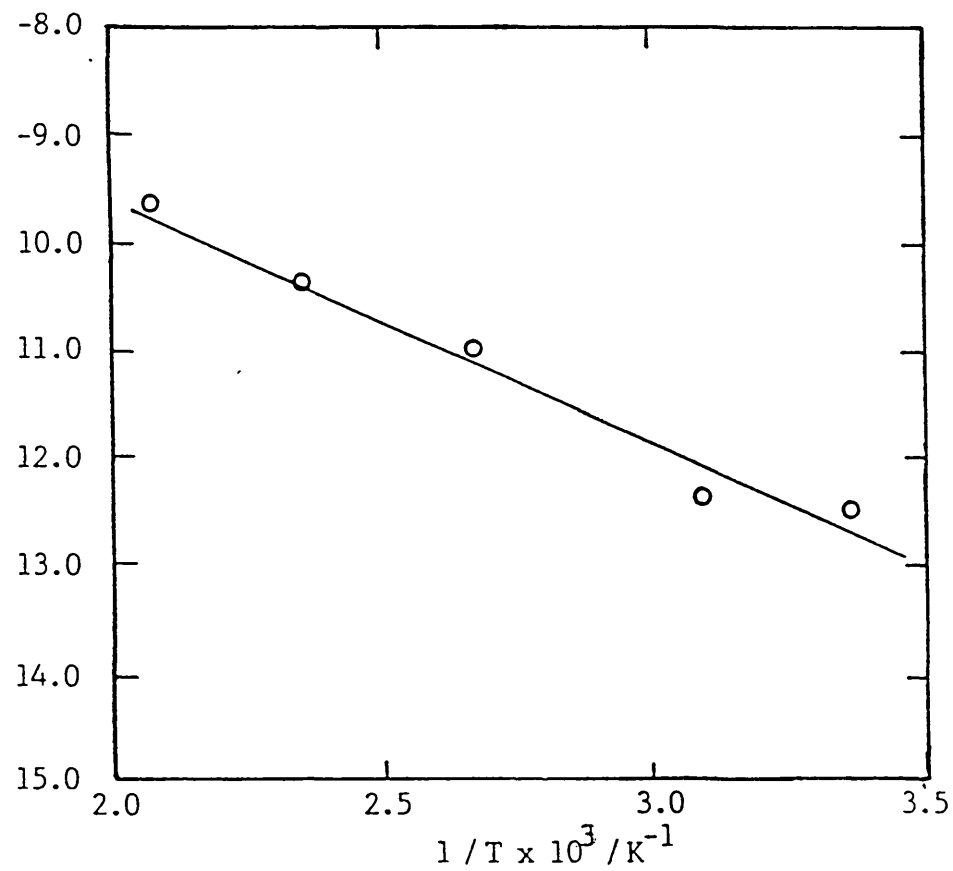


Fig 6.4.1.6. Variation of the inverse stress ratio with time during the stress relaxation of PDMS elastomer at various temperatures. ($N_{cr}(0) = 0.118 \times 10^{-6} \text{ mol} \cdot \text{nm}^{-3}$.)

* data treated by the method proposed by Osthoff et al (1C3)



1.7. Arrhenius plot for the determination of the activation energy of the main chain scission reaction in PDMS elastomer.

$$(N_{cr_m}(0) = 0.118 \times 10^{-6} \text{ mol} \cdot \text{mm}^{-3}.)$$

* data treated by the method proposed by Osthoff et al⁽¹⁰³⁾

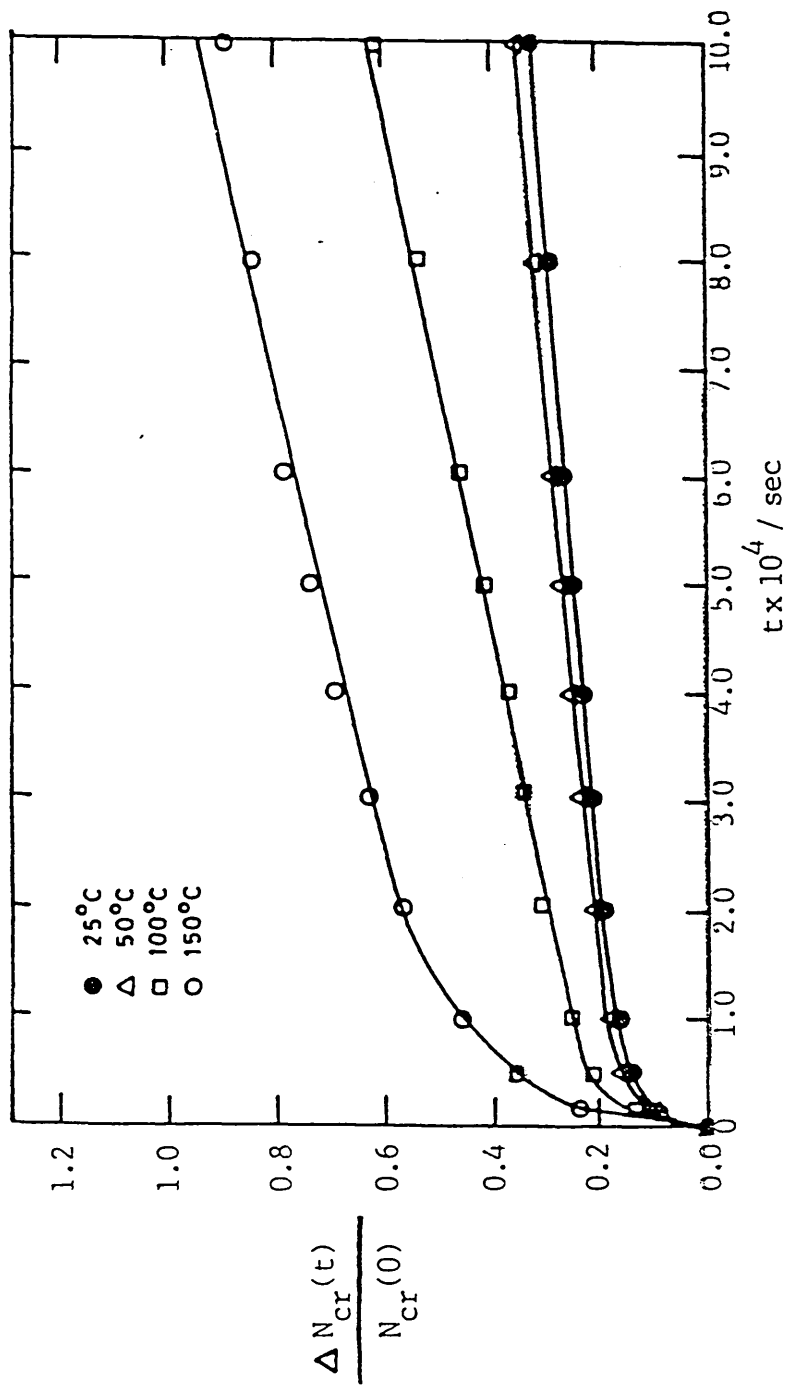


Fig 6.4.1.8. Variation in the fraction of crosslinks formed per unit volume with time in PDMS elastomer at various temperatures. ($N_{CR}(0) = 0.118 \times 10^{-6} \text{ mol. mm}^{-3}$.)

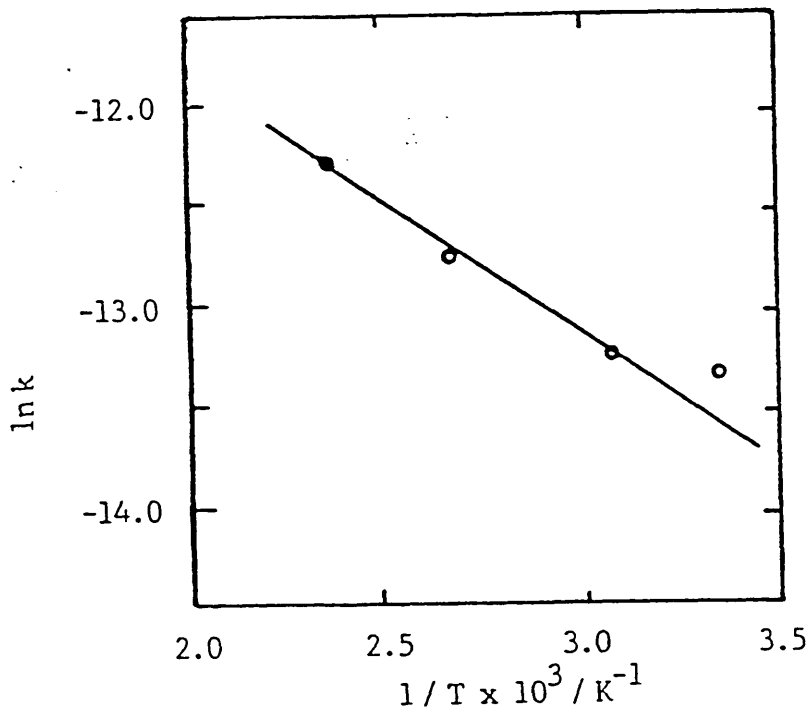


Fig 6.4.1.9. Arrhenius plot for the determination of the activation energy of the crosslink formation reaction occurring in PDMS elastomer. ($N_{cr_m}(0) = 0.118 \times 10^{-6} \text{ mol. mm}^{-3}$.)

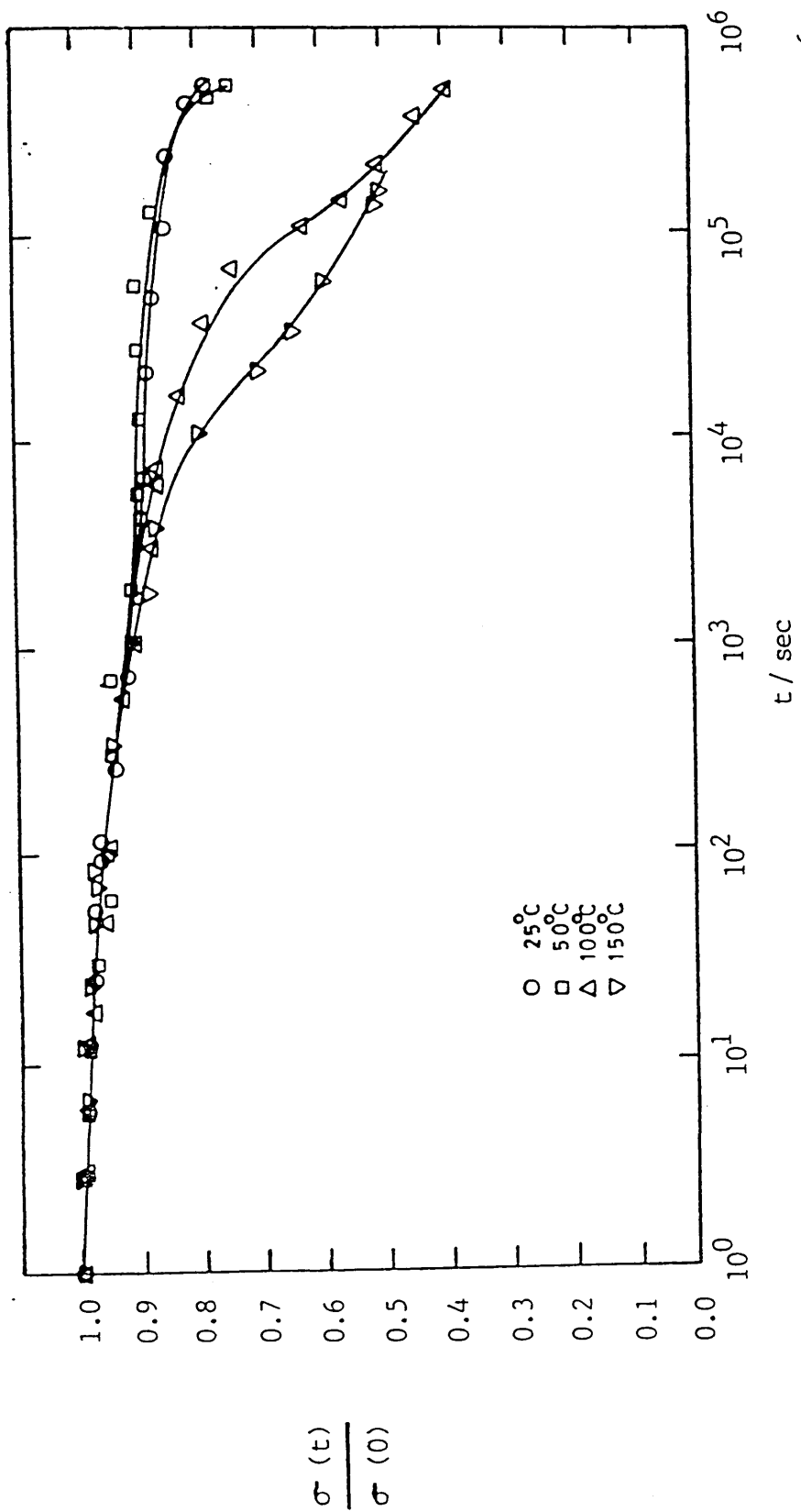


Fig 6.4.1.10. Stress relaxation of PDMS elastomer at various temperatures. ($N_{cr}(0) = 0.129 \times 10^{-6} \text{ mol} \cdot \text{mm}^{-3}$.)

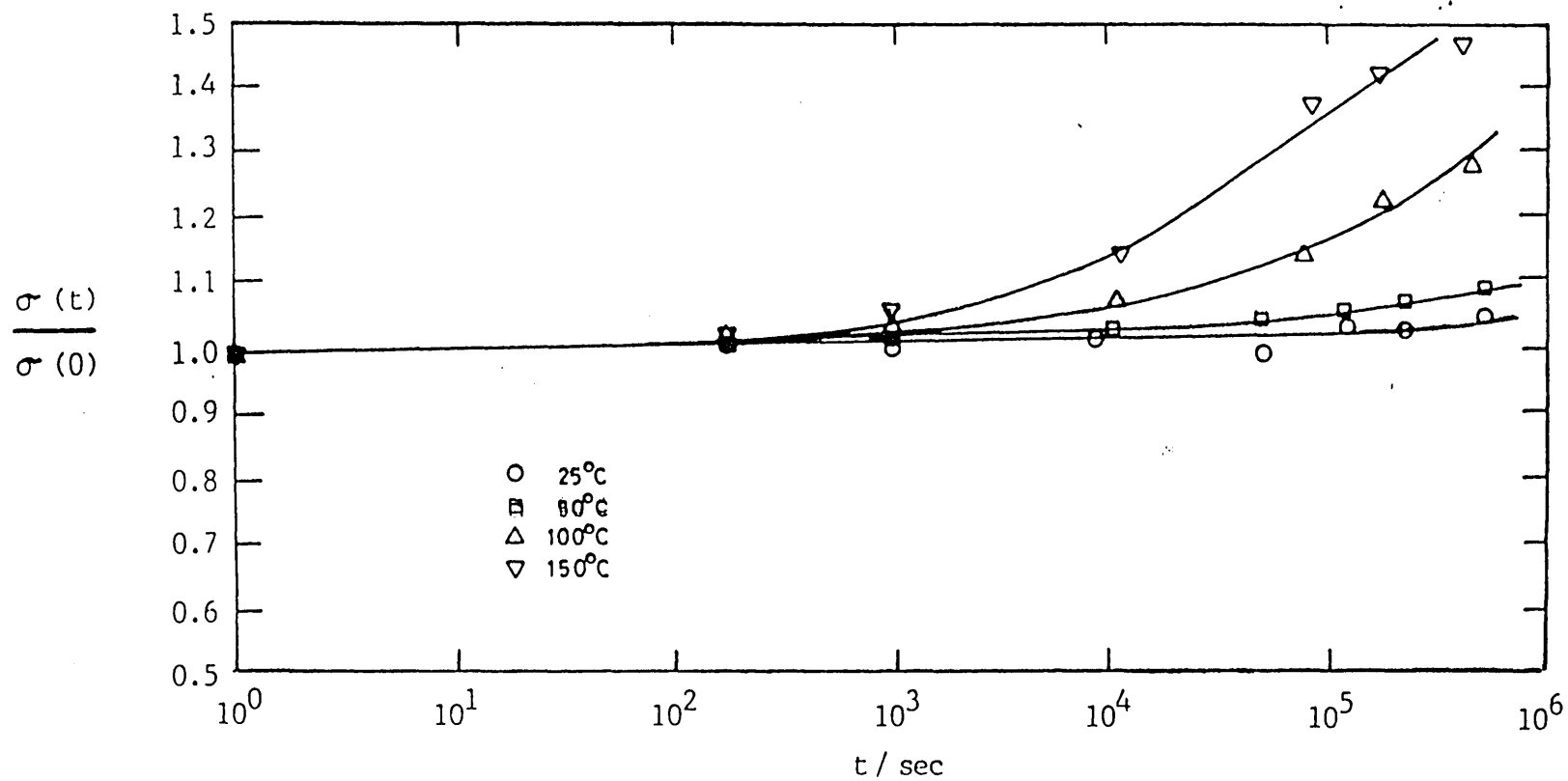
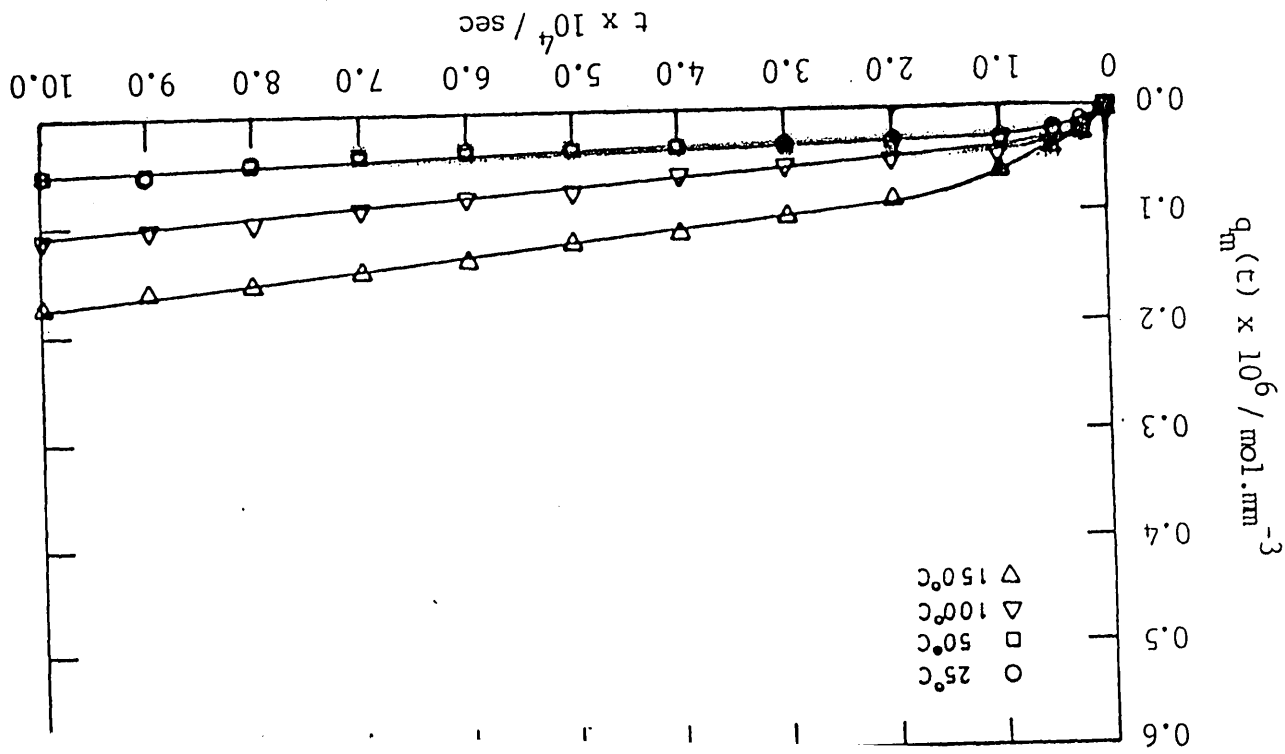
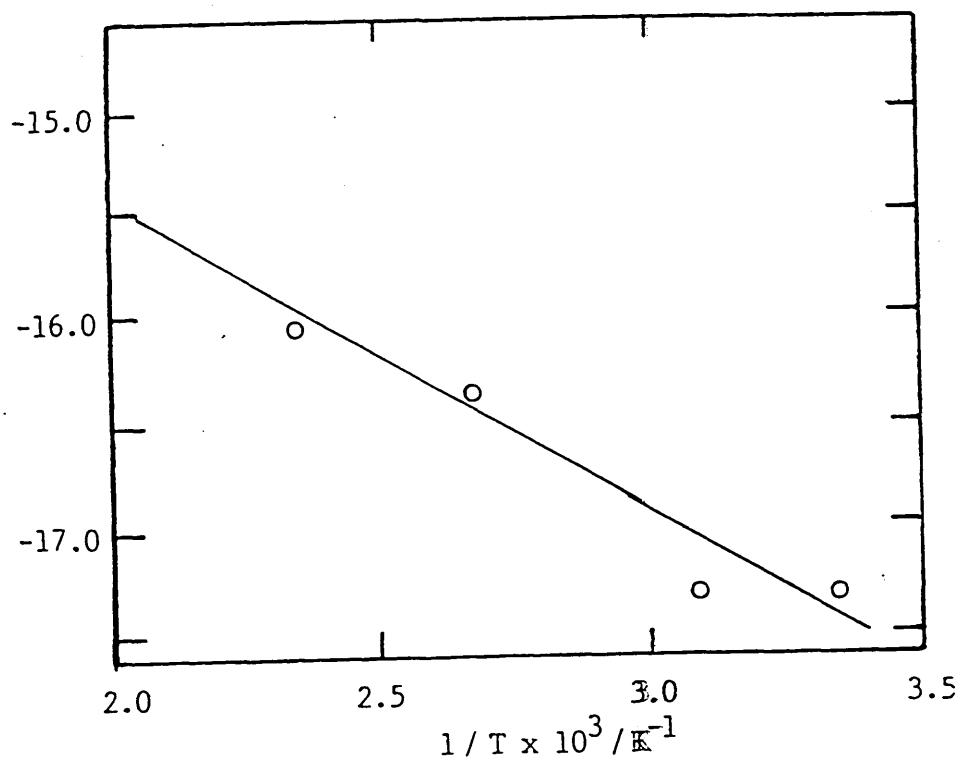


Fig 6.4.1.11. Intermittent stress relaxation of PDMS elastomer at various temperatures. ($N_{cr_m} = 0.129 \times 10^{-6} \text{ mol. mm}^{-3}$.)

Fig 6.4.1.12. Variation in the number of main chain scissions per unit volume with time occurring in PDMS elastomer at various temperatures. ($N_{cr}^m(0) = 0.129 \times 10^{-6} \text{ mol. mm}^{-3}$.)





4.1.13. Arrhenius plot for the determination of the activation energy of the main chain scission reaction occurring in PDMS elastomer. ($N_{cr_m}(0) = 0.129 \times 10^{-6} \text{ mol. mm}^{-3}$.)

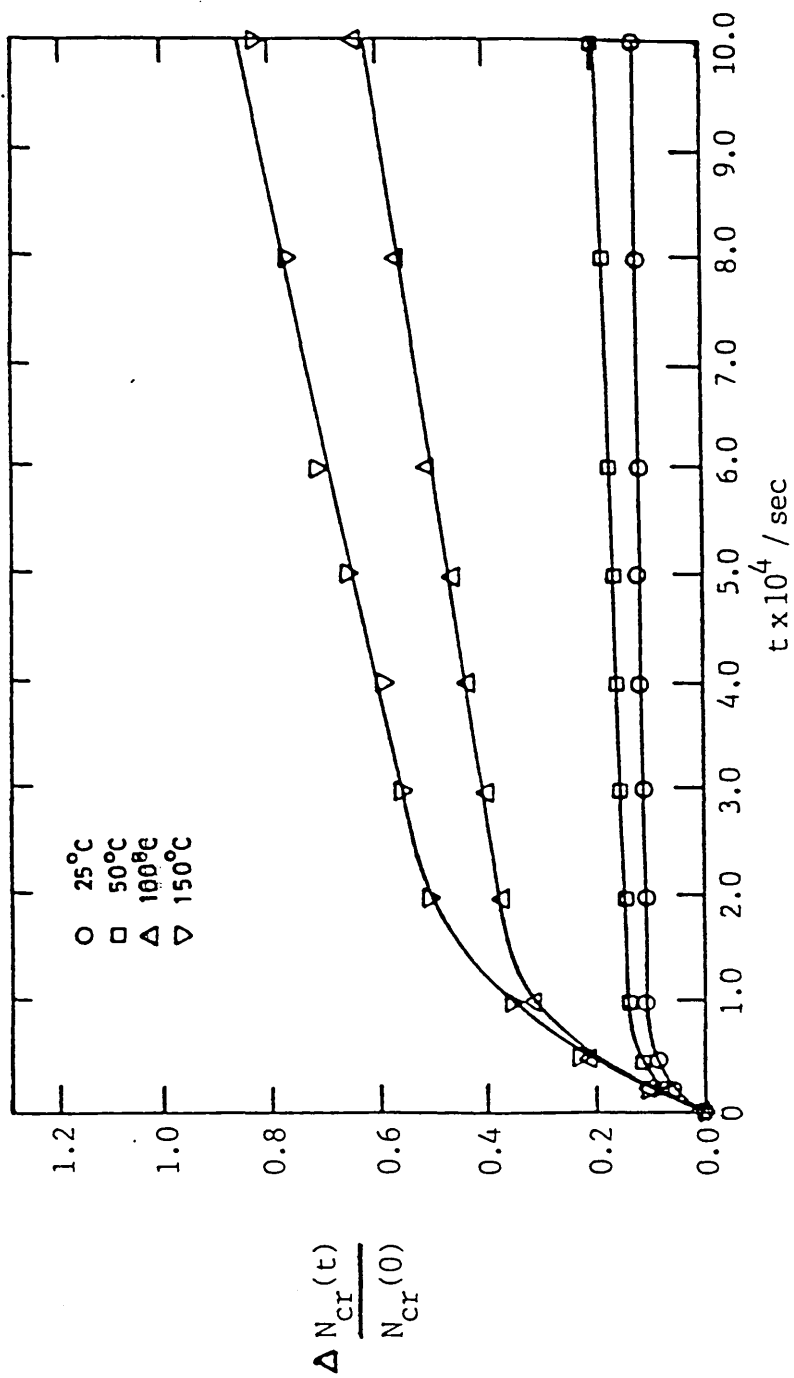
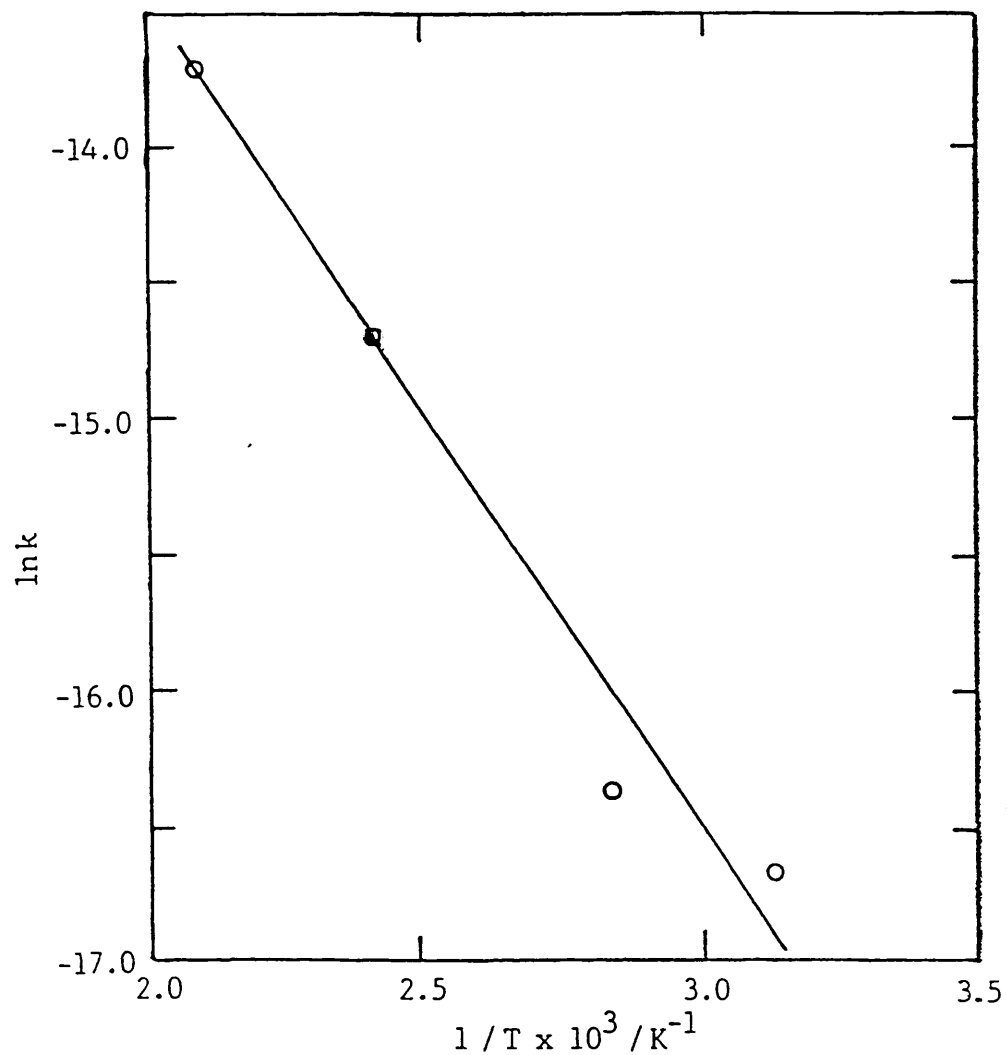


Fig 6.4.1.14. Variation in the fraction of crosslinks formed per unit volume with time in PDMS elastomer at various temperatures. ($N_{CR}(0) = 0.129 \times 10^{-6} \text{ mol. mm}^{-3}$.)



4.1.15. Arrhenius plot for the determination of the activation energy of the crosslink formation reaction in PDMS elastomer. ($N_{cr_m}(0) = 0.12 \times 10^{-6} \text{ mol. mm}^{-3}$.)

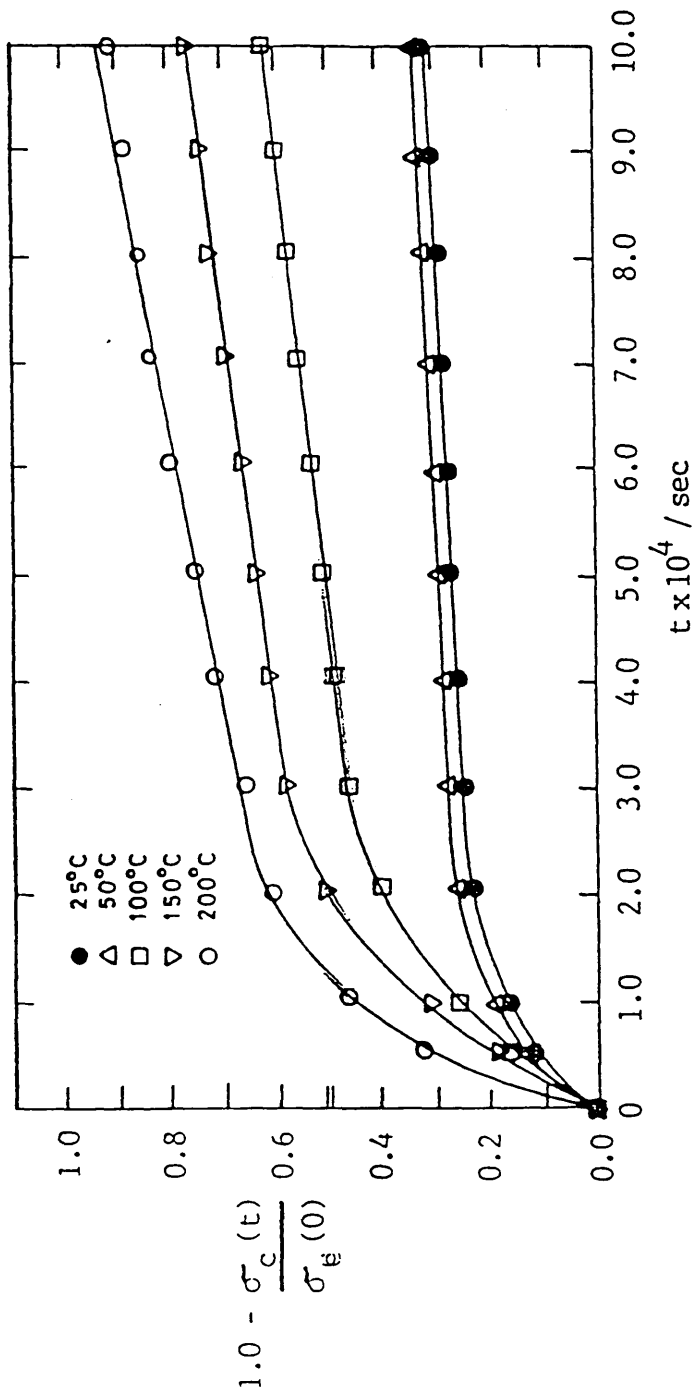
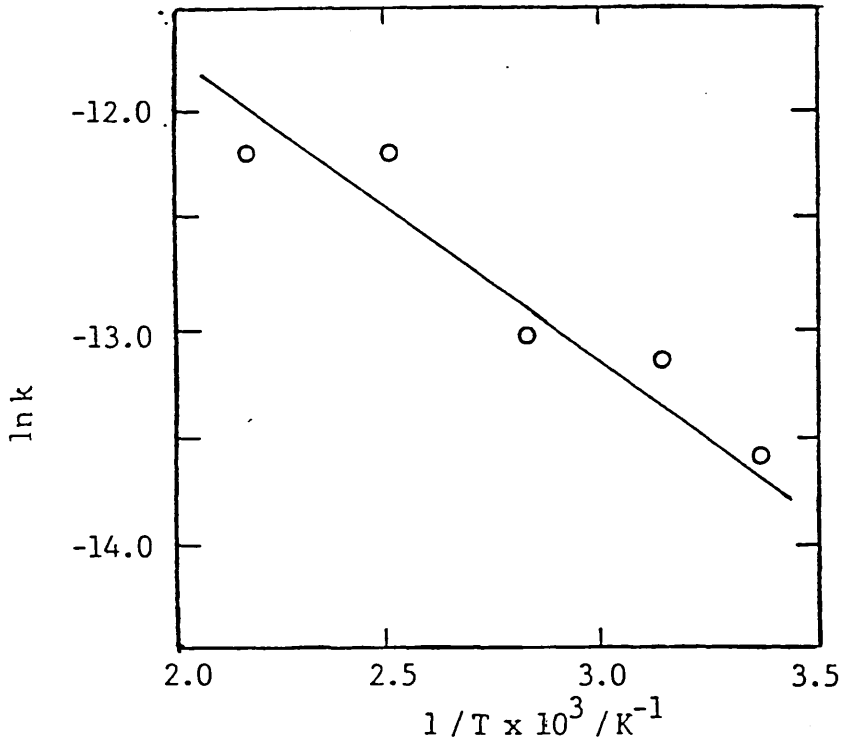


Fig 6.4.1.16. Variation in the fraction of crosslinks formed per unit volume with time in PDMS elastomer that are attributed to the reformation of chains cleaved during the stress relaxation test. ($N_{Cr_m}(0) = 0.118 \times 10^{-6} \text{ mol} \cdot \text{mm}^{-3}$.)



6.4.1.17. Arrhenius plot for the determination of the activation energy of the reaction associated with the reformation of chains cleaved during the stress relaxation test.

($N_{cr_m}(0) = 0.118 \times 10^{-6} \text{ mol. mm}^{-3}$.)

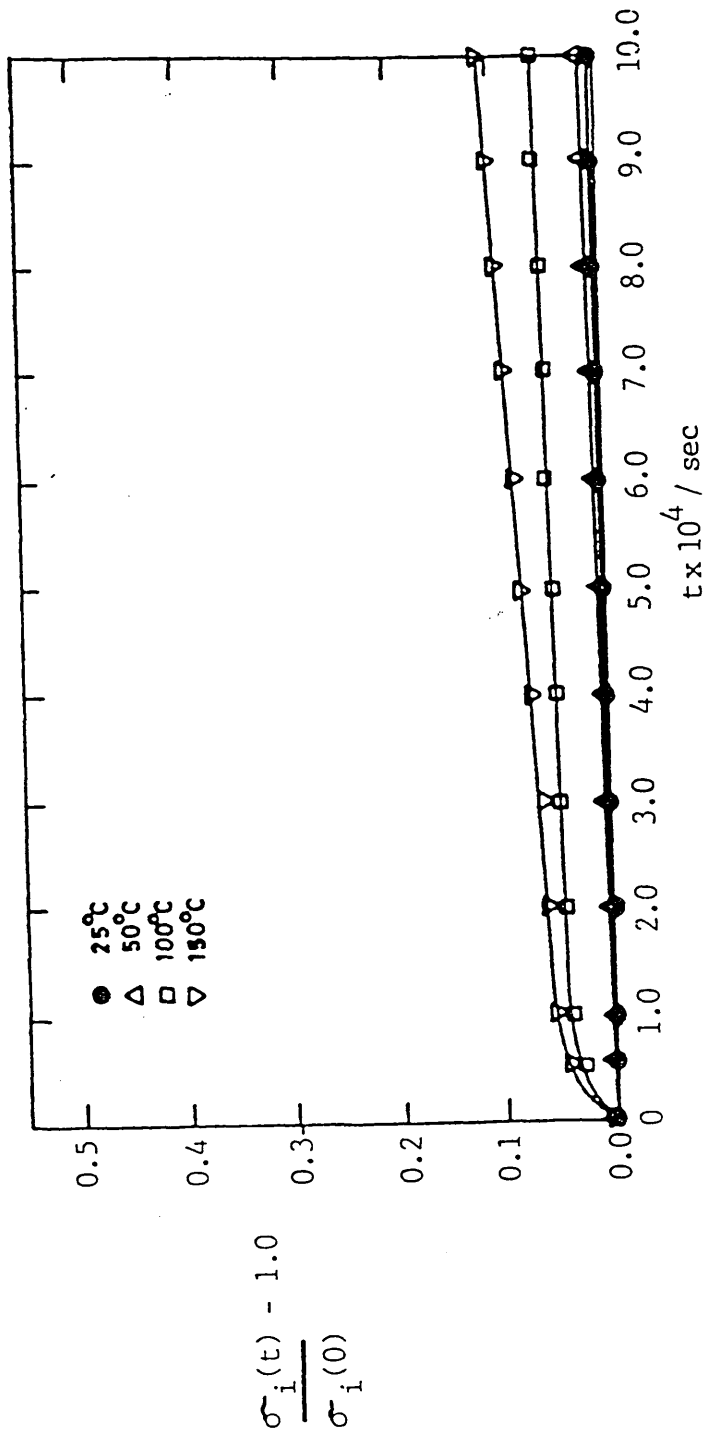


Fig 6.4.1.18. Variation in the fraction of crosslinks formed per unit volume with time that are attributed to the reformation of chains cleaved prior to the onset of the stress relaxation test. ($N_{cr}(0) = 0.118 \times 10^{-4} \text{ mol} \cdot \text{mm}^{-3}$)

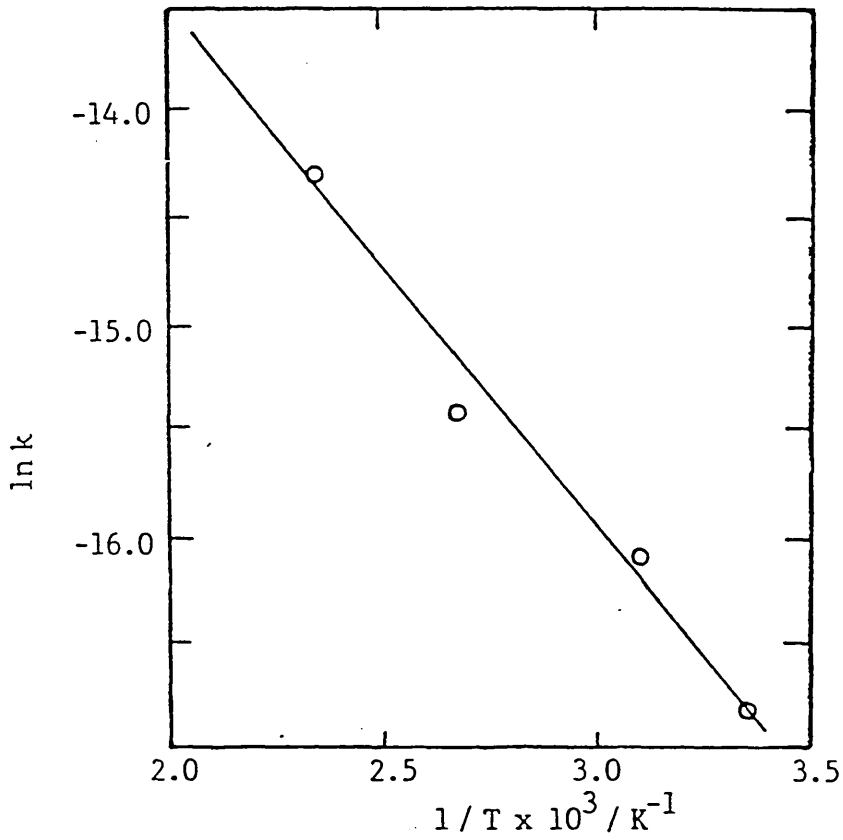


Fig 6.4.1.19. Arrhenius plot for the determination of the activation energy of the reaction associated with the reformation of chains cleaved prior to the onset of the stress relaxation test. ($N_{cr_m}(0) = 0.118 \times 10^{-6} \text{ mol. mm}^{-3}$.)

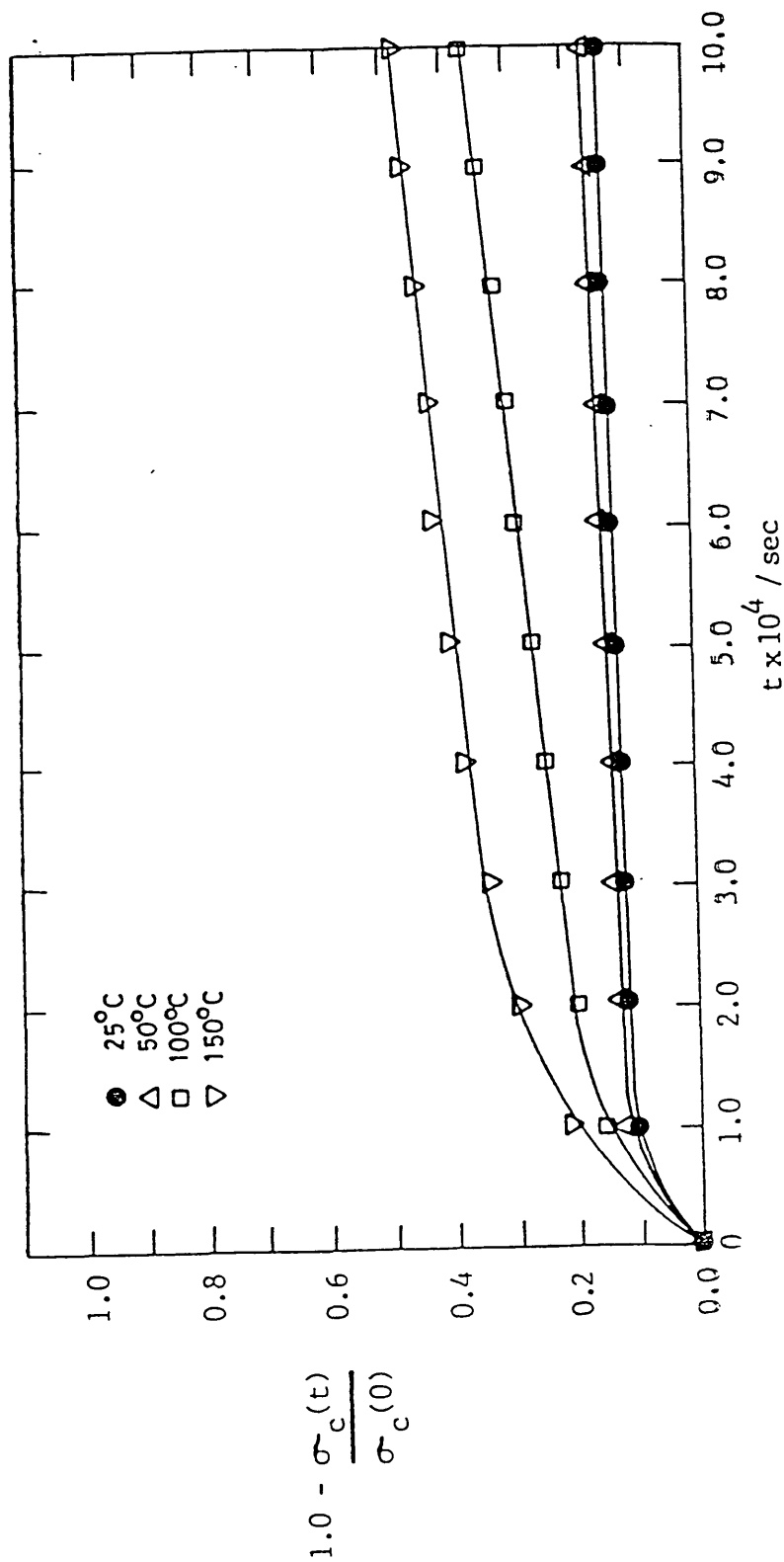
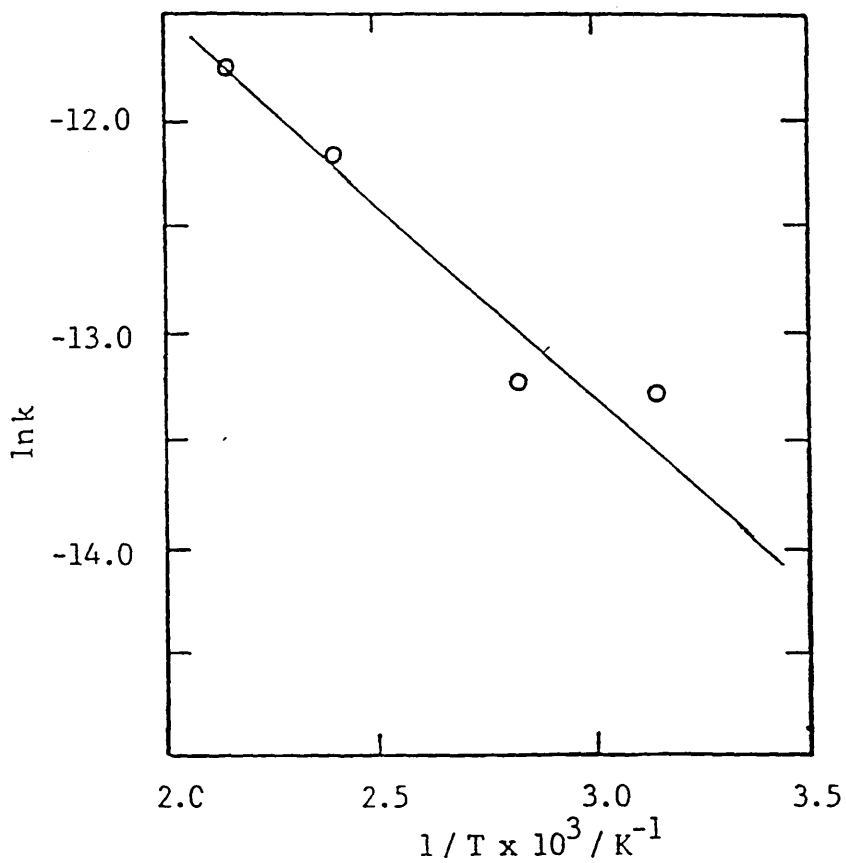


Fig 6.4.1.20. Variation in the fraction of crosslinkages formed per unit volume with time in PDMS elastomer that are attributed to the reformation of chains cleaved during the stress relaxation test. ($N_{cr_m}(0) = 0,129 \times 10^{-6} \text{ mol. mm}^{-3}$.)



6.4.1.21. Arrhenius plot for the determination of the activation energy of the reaction associated with the reformation of chains cleaved during the stress relaxation test.

($N_{cr_m}(0) = 0.129 \times 10^{-6} \text{ mol. mm}^{-3}$.)

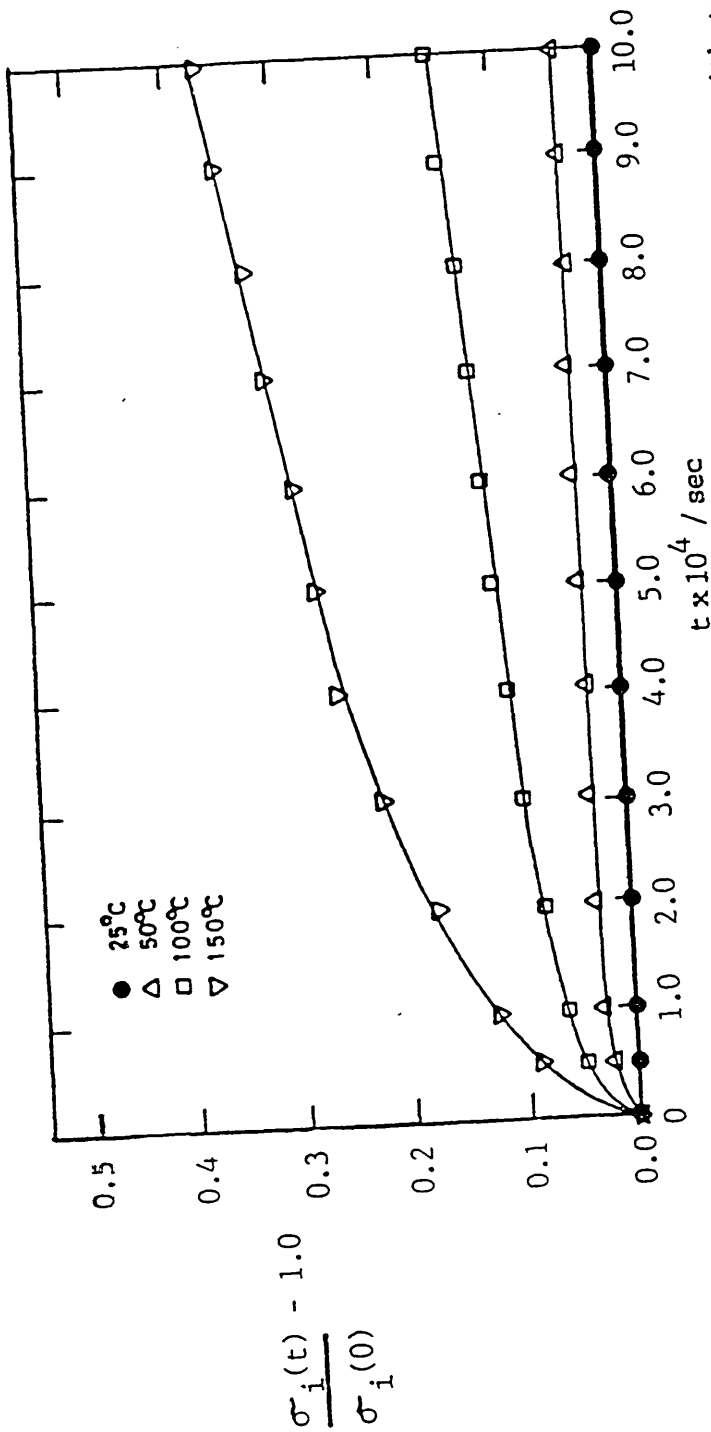


Fig 6.4.1.22. variation in the fraction of crosslinks formed per unit volume with time that are attributed to the reformation of chains cleaved prior to the onset of the stress relaxation test. ($N_{cr_m}(0) = 0.129 \times 10^{-6} \text{ mol. mm}^{-3}$.)

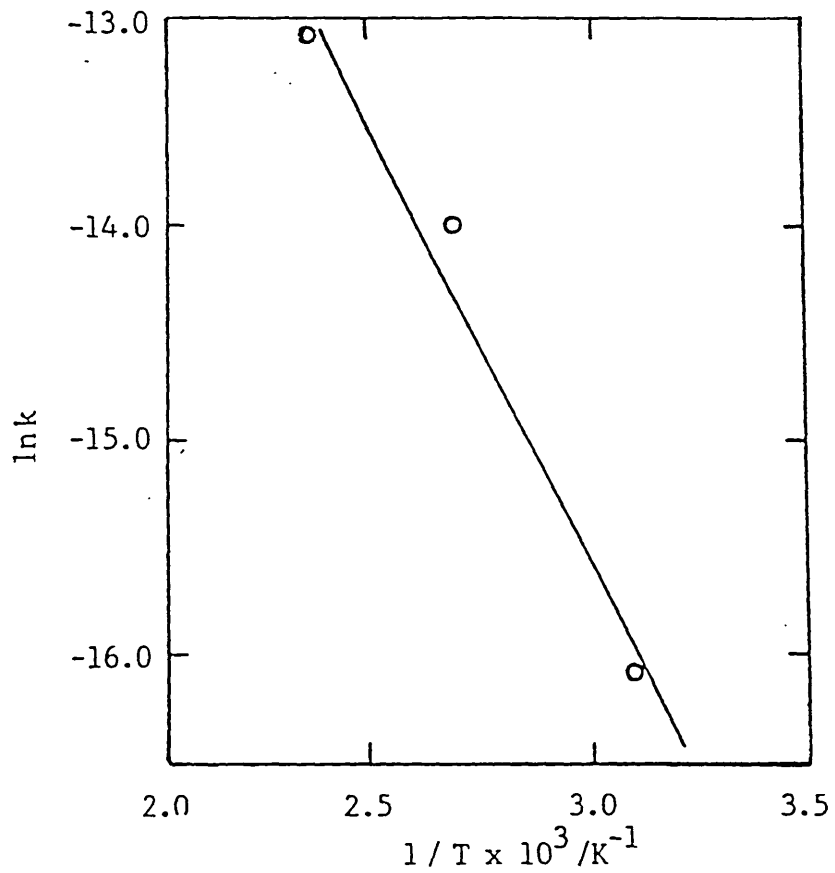


Fig 6.4.1.23. Arrhenius plot for the determination of the activation energy of the reaction associated with the reformation of chains cleaved prior to the onset of the stress relaxation test. ($N_{cr_m}(0) = 0.129 \times 10^{-6} \text{ mol. mm}^{-3}$.)

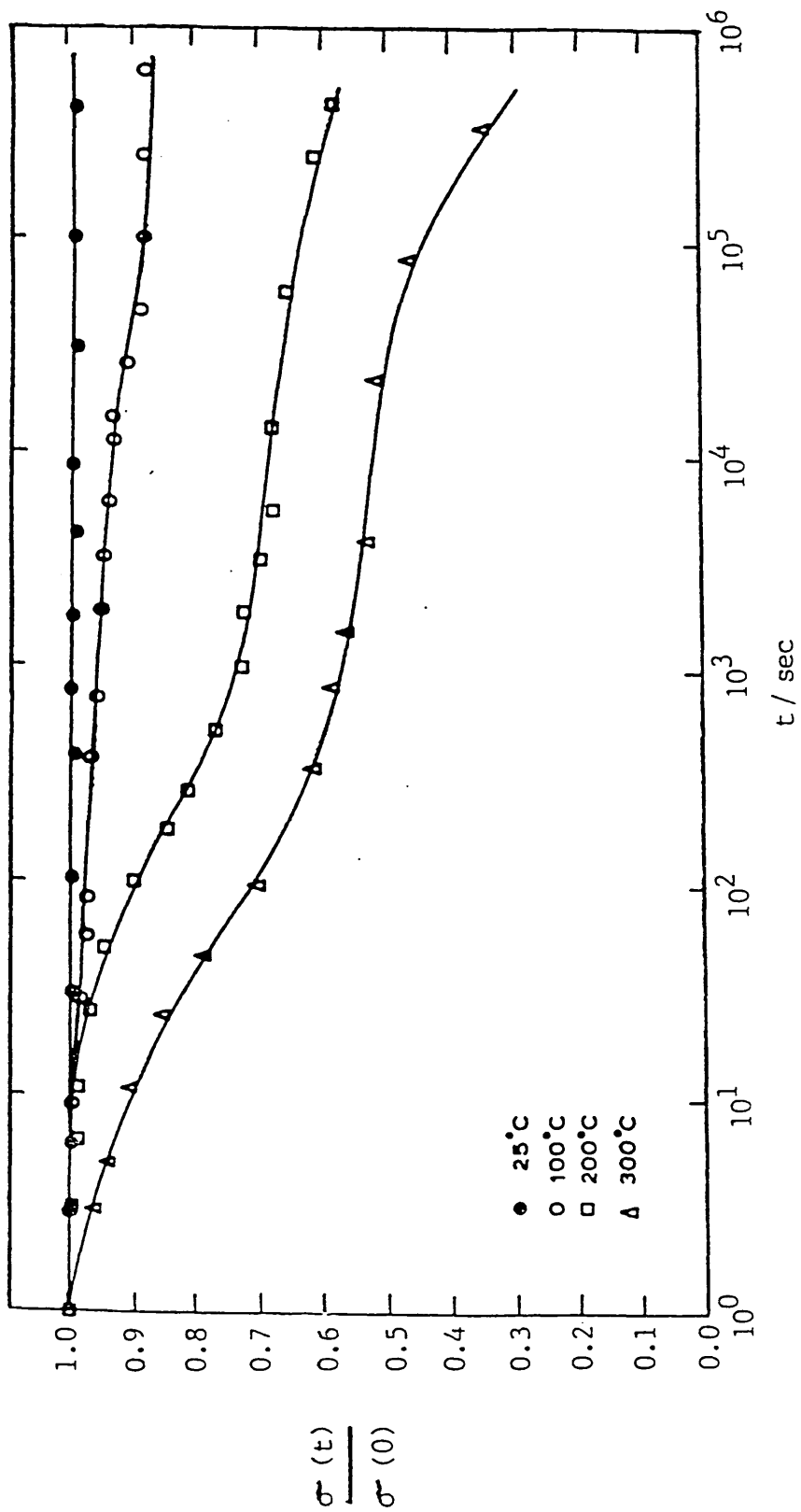


Fig 6.4.2.1. Stress relaxation of Viton E60-C elastomer at various temperatures.

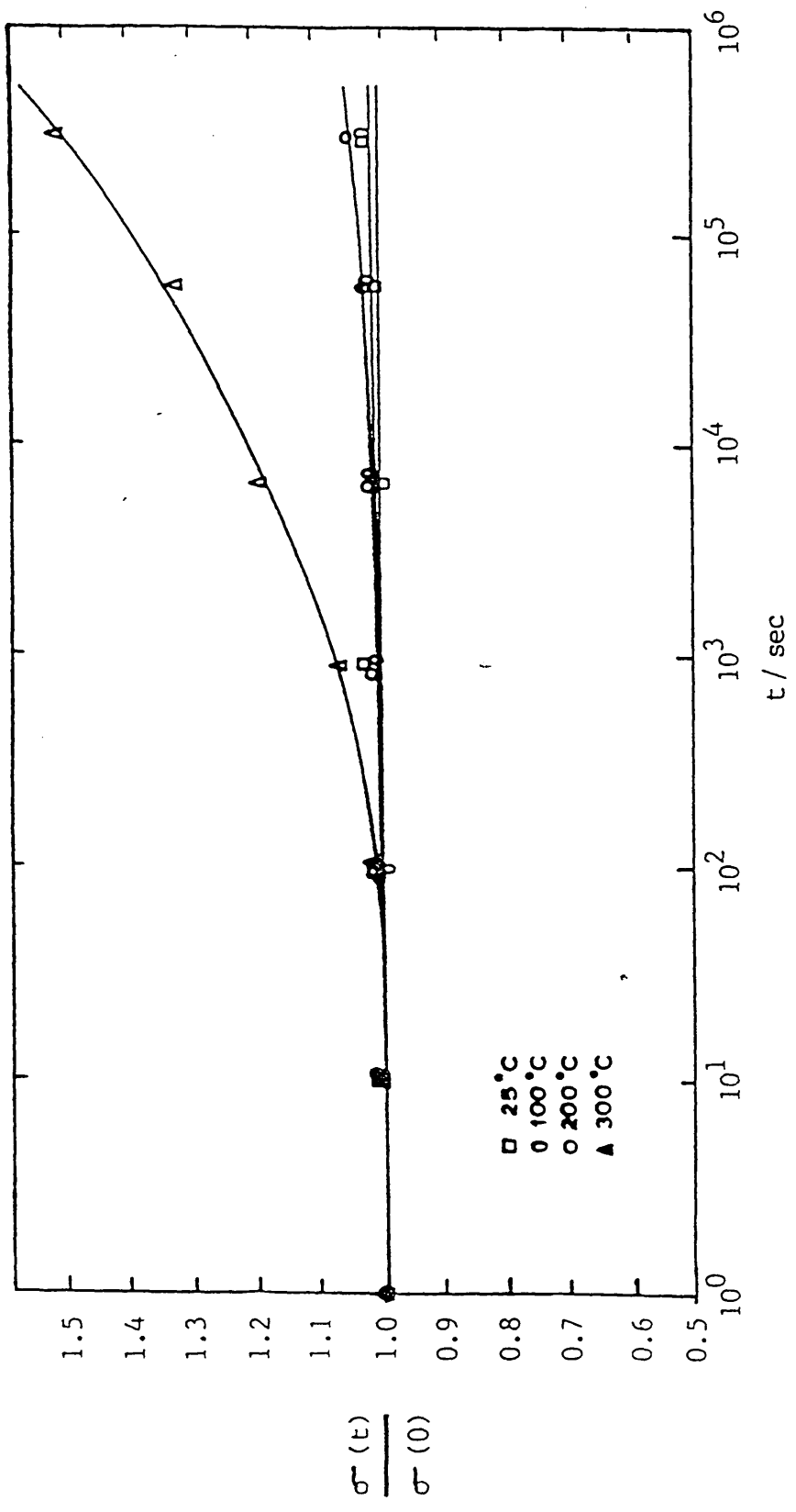


Fig 6.4.2.2. Intermittent stress relaxation of Viton E60-C elastomer at various temperatures.

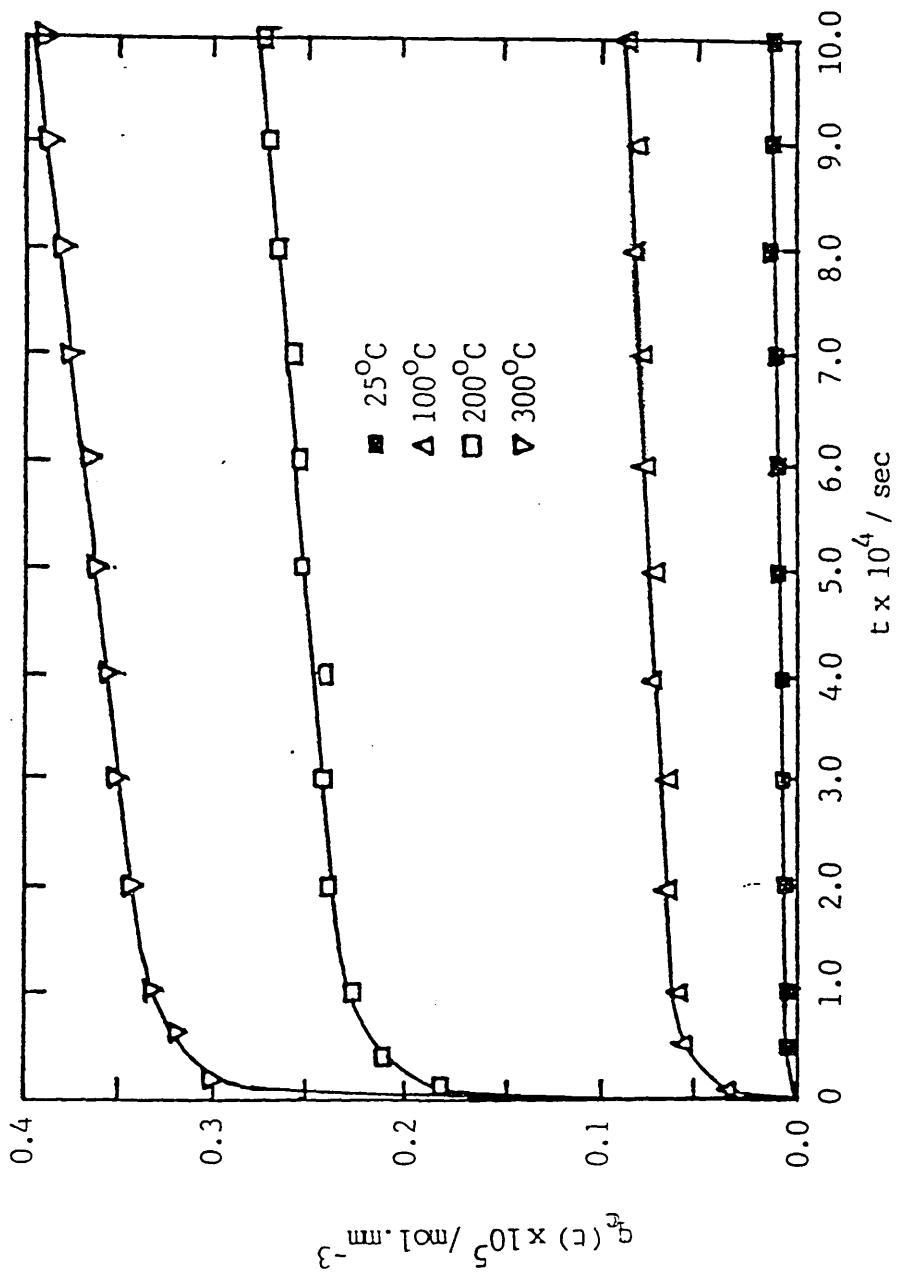
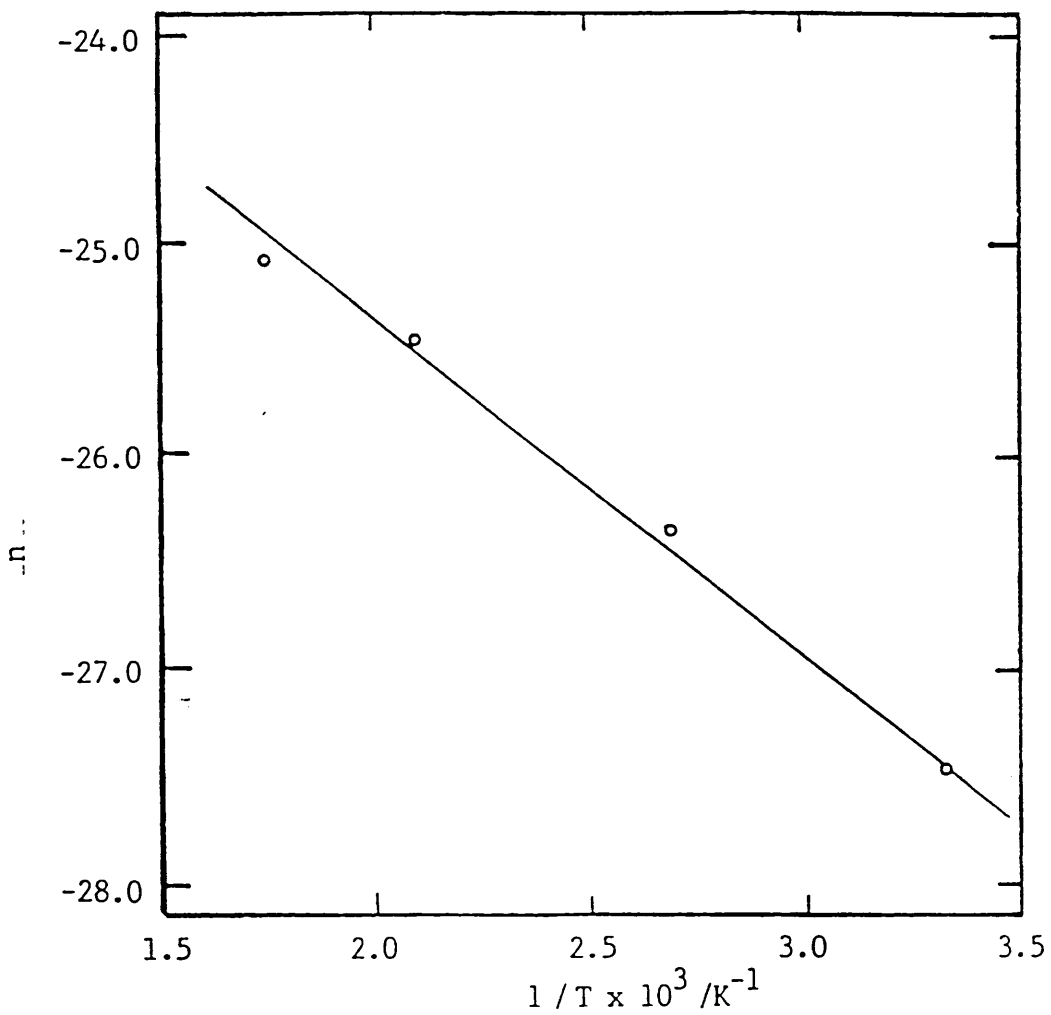


Fig 6.4.2.3. Variation in the number of crosslink scissions per unit volume with time occurring in Viton E60-C elastomer at various temperatures.



6.4.2.4. Arrhenius plot for the determination of the activation energy of the crosslink scission reaction occurring in Viton E60-C elastomer.

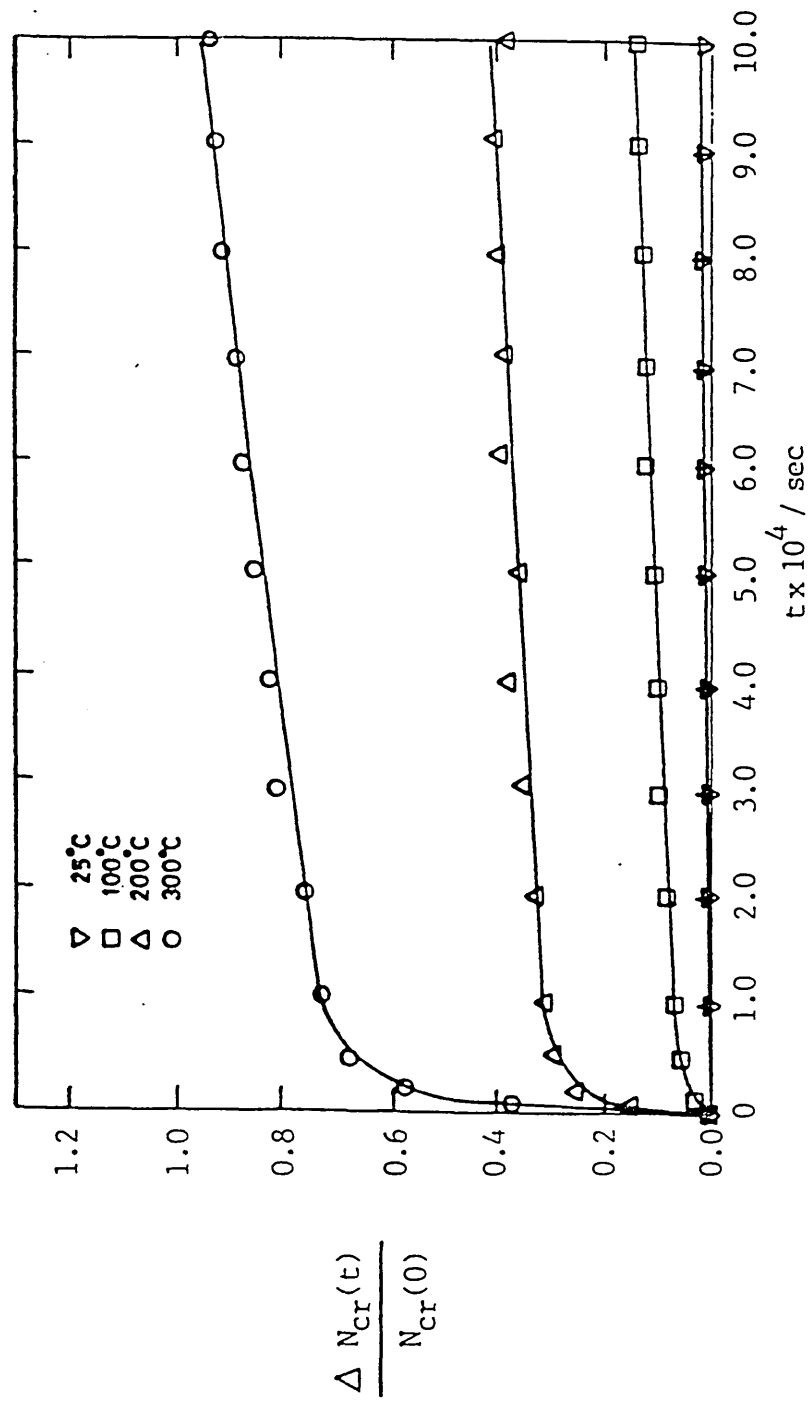
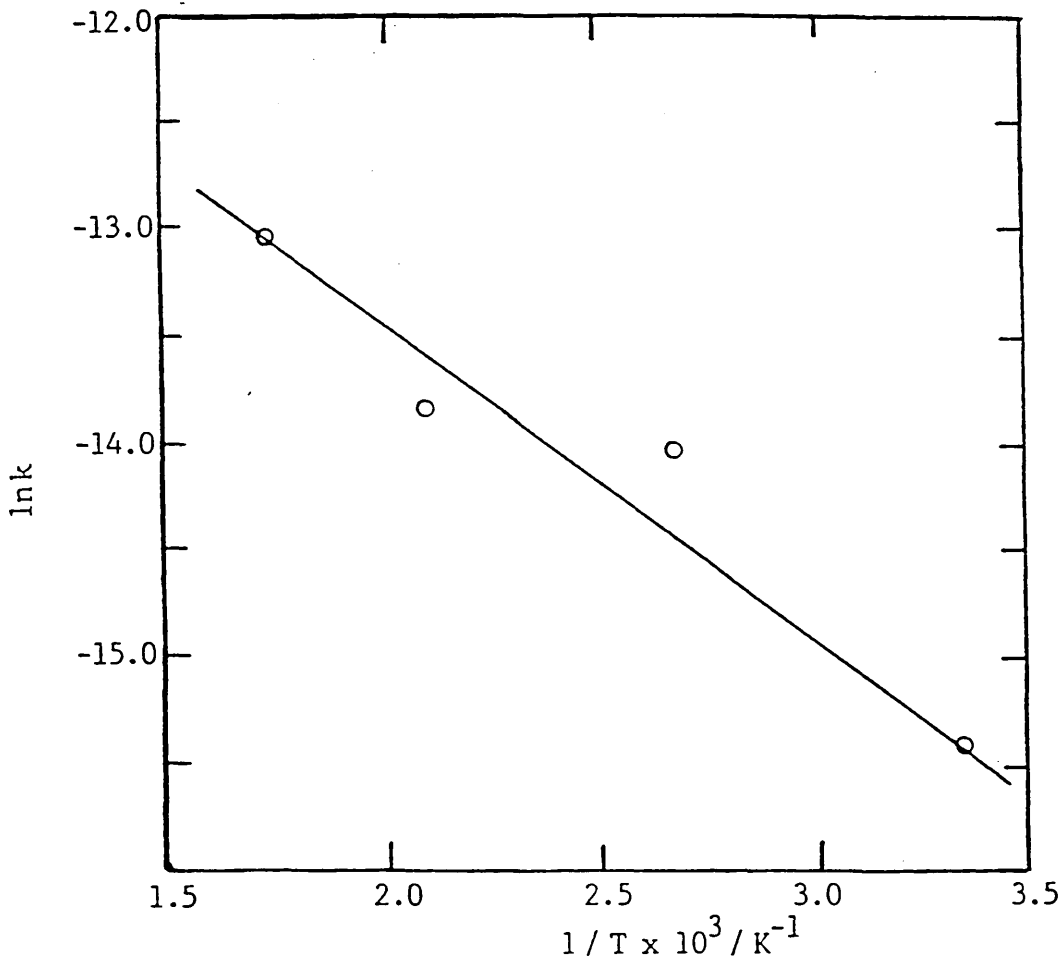


Fig 6.4.2.5. Variation in the fraction of crosslinks formed per unit volume with time in Viton E60-C elastomer at various temperatures.



6.4.2.6. Arrhenius plot for the determination of the activation energy of the crosslink formation reaction occurring in Viton E60-C elastomer.

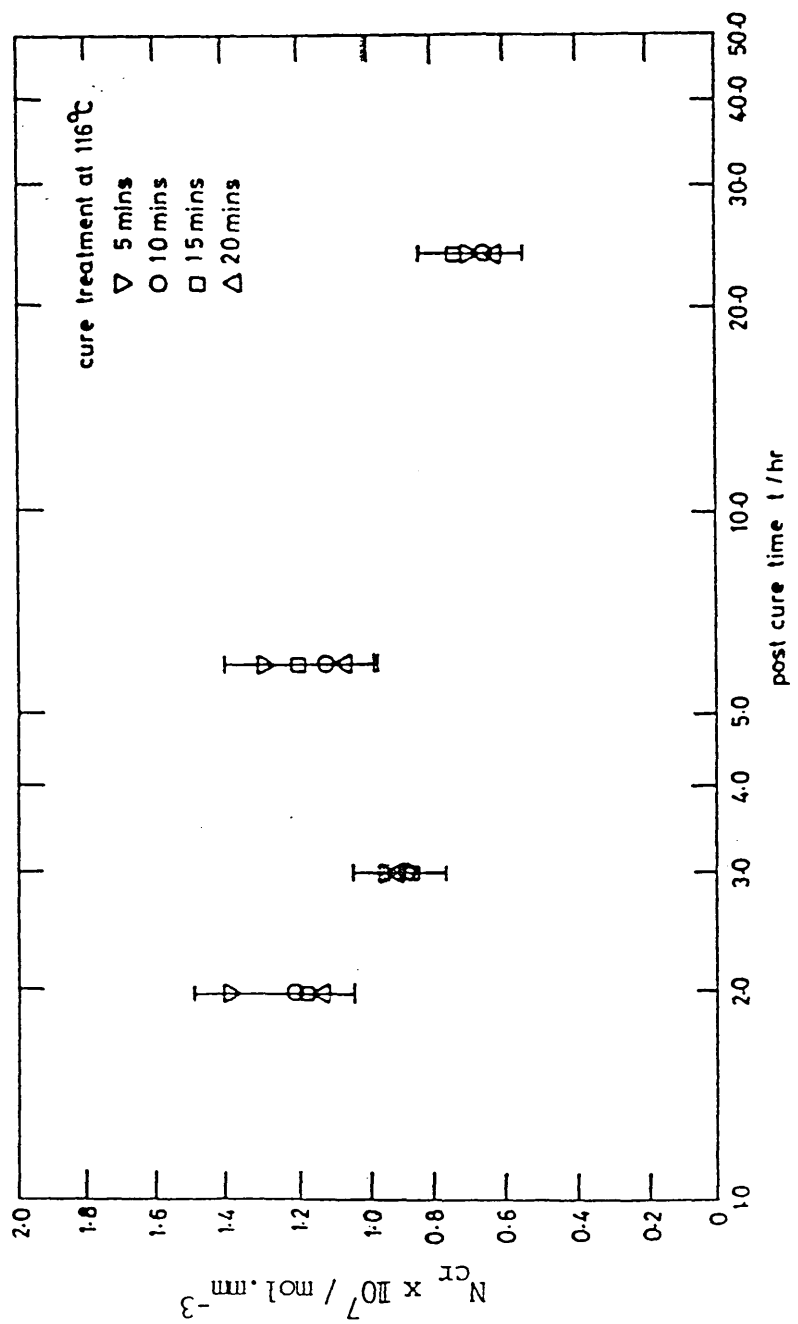


Fig 6.4.3.1.1. Variation in crosslink density during post curing after various cure treatments.
 (polydimethylsiloxane elastomer containing 1.00wt% 2,4-DCBP paste)

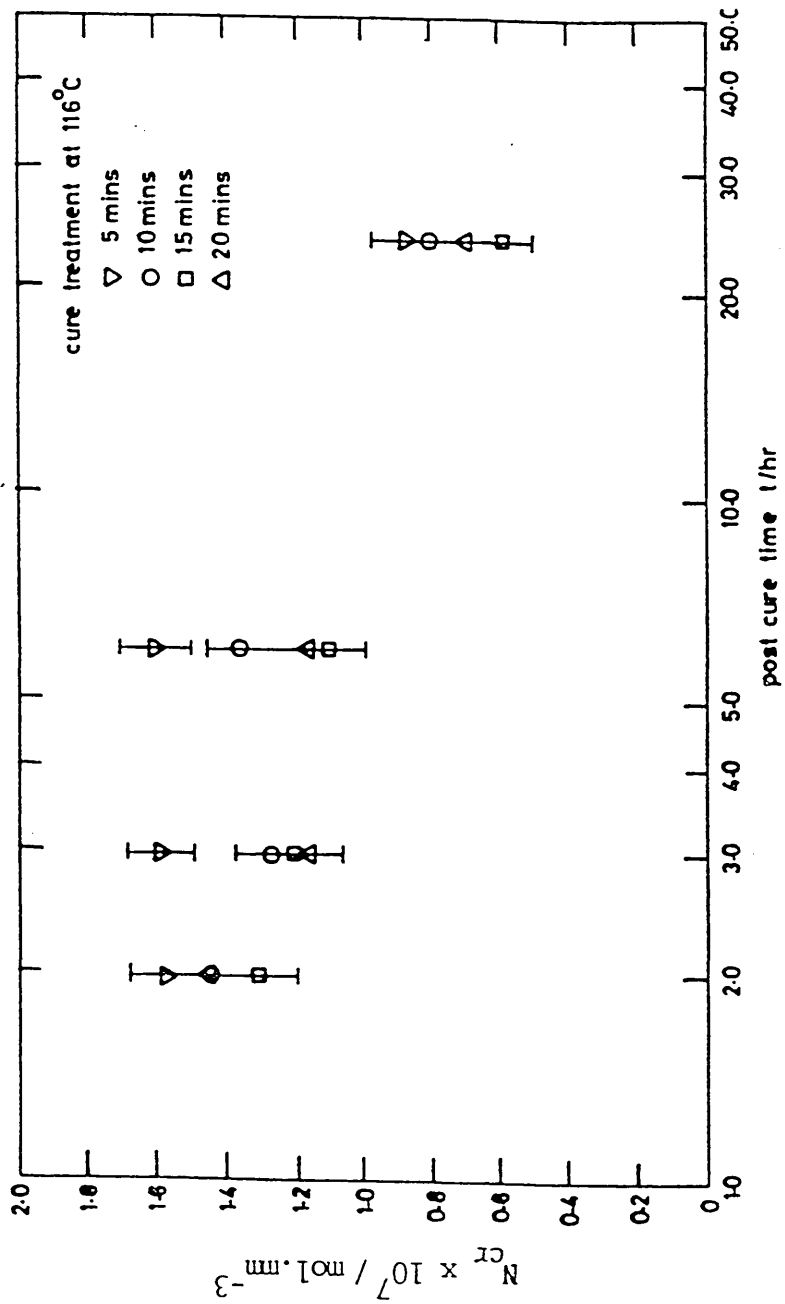


Fig 6.4.3.2. Variation in crosslink density during post curing after various cure treatments. (polydimethylsiloxane elastomer containing 1.25wt% 2,4-DCBP paste)

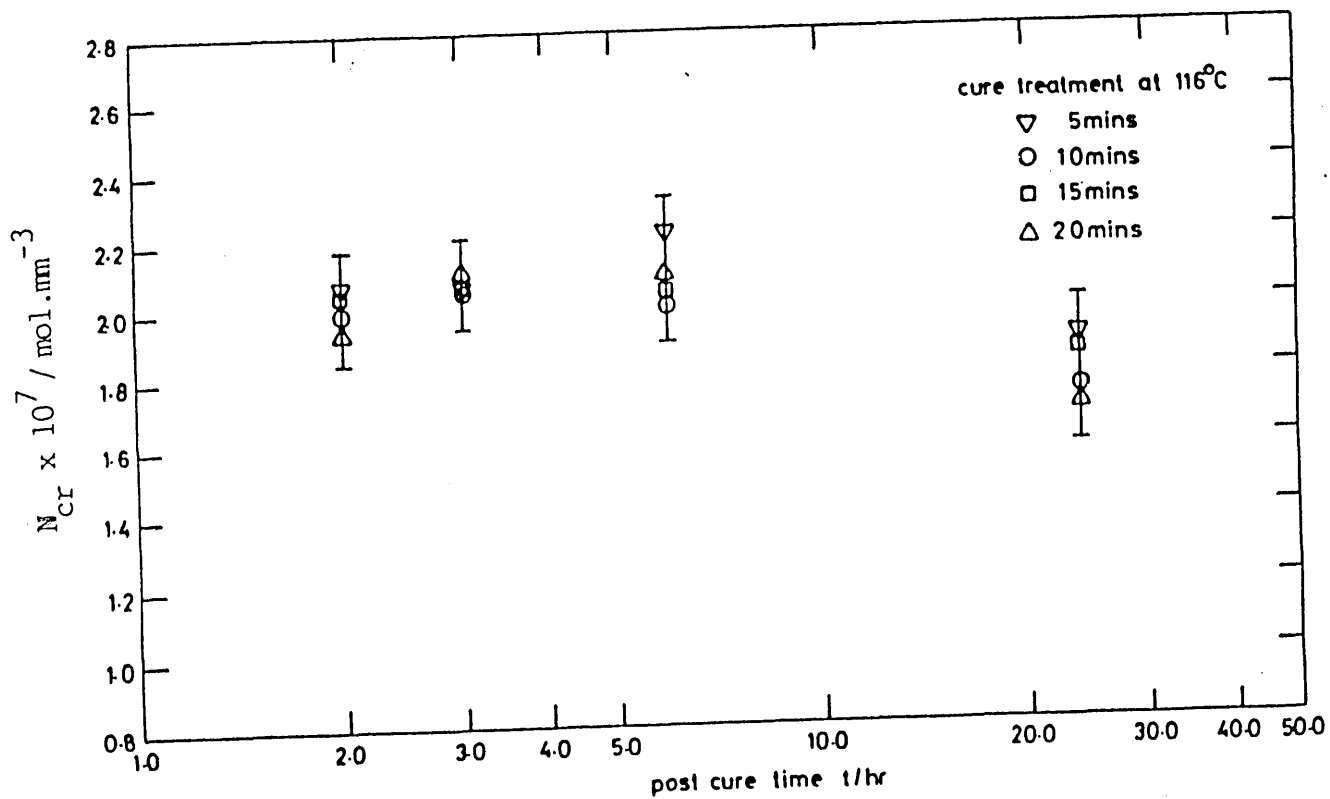


Fig 6.4.3.3. Variation in crosslink density during post curing after various cure treatments. (polydimethylsiloxane elastomer containing 1.50wt% 2,4-DCBP paste)

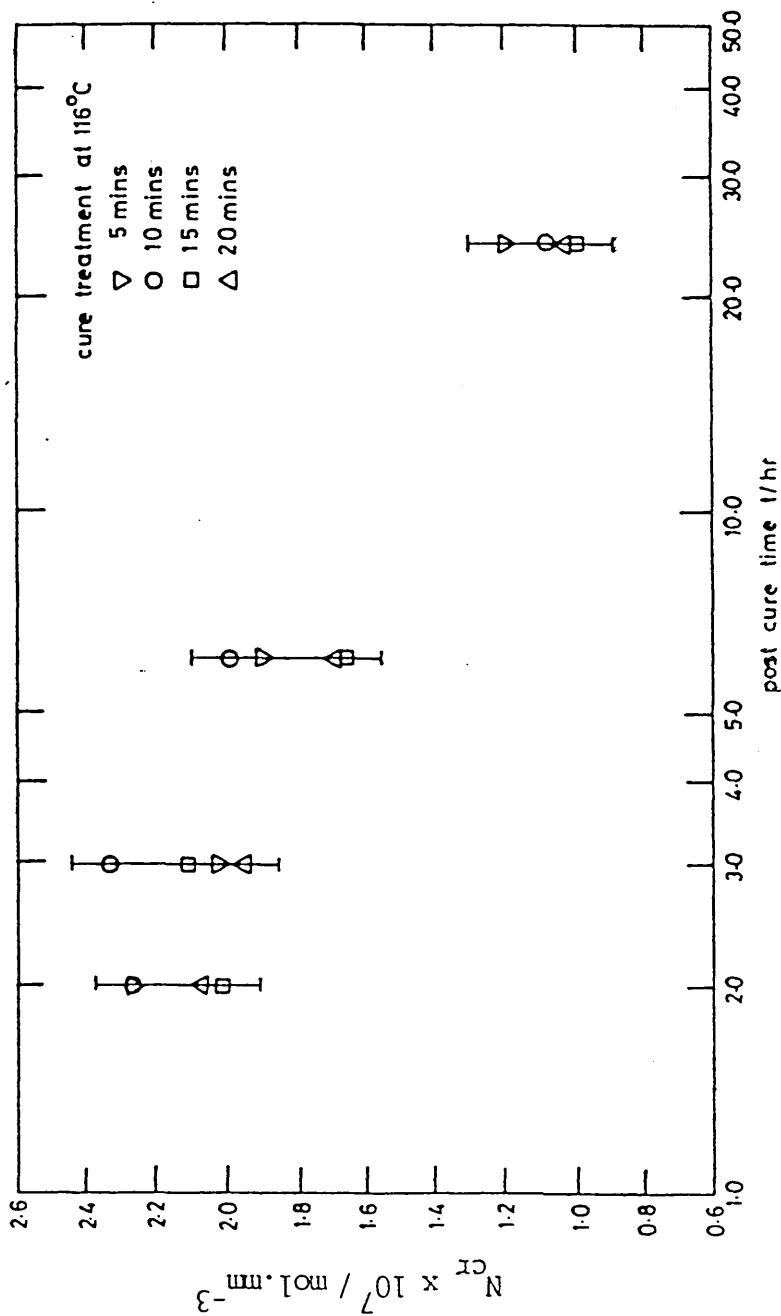


Fig 6.4.3.4. Variation in crosslink density during post curing after various cure treatments.
 (polydimethylsiloxane elastomer containing 2.00wt% 2,4-DCBP paste)

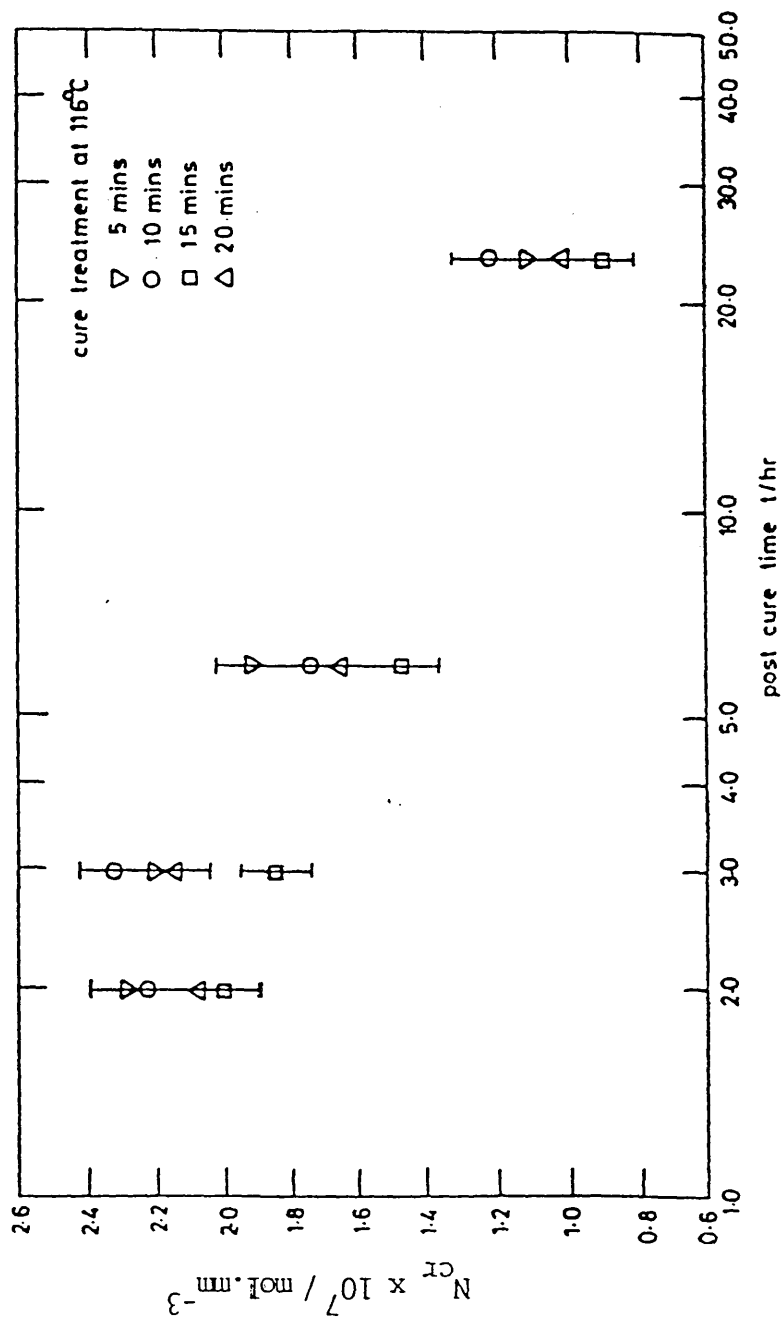


Fig 6.4.3.5. Variation in crosslink density during post curing after various cure treatments. (polydimethylsiloxane elastomer containing 3.00 wt% 2,4-DCBP paste)

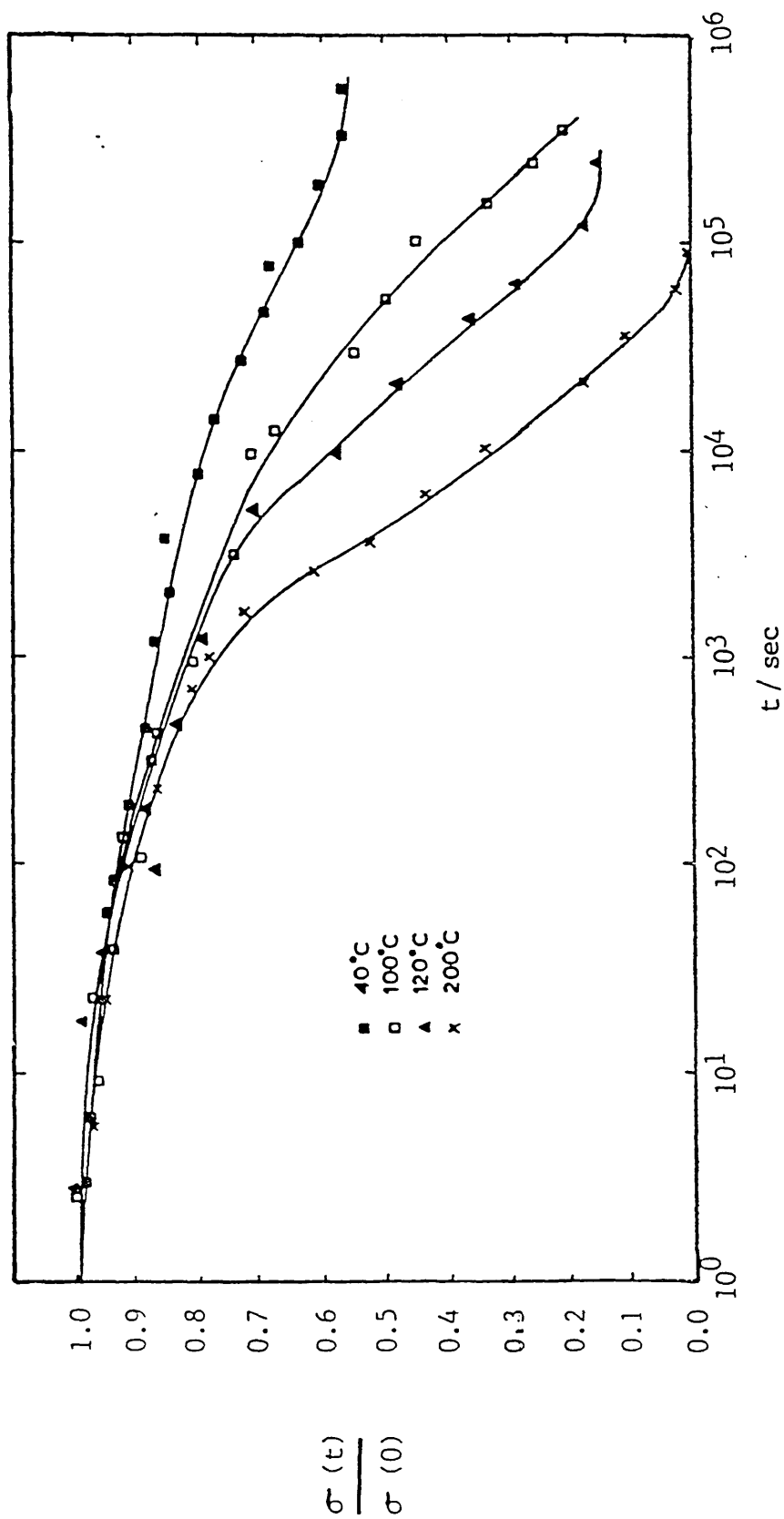


Fig 6.5.1.1. Stress relaxation of PMS elastomer during γ -irradiation at various temperatures.
 ($N_{Cr_m}(0) = 0.118 \times 10^{-6} \text{ mol. mm}^{-3}$.)

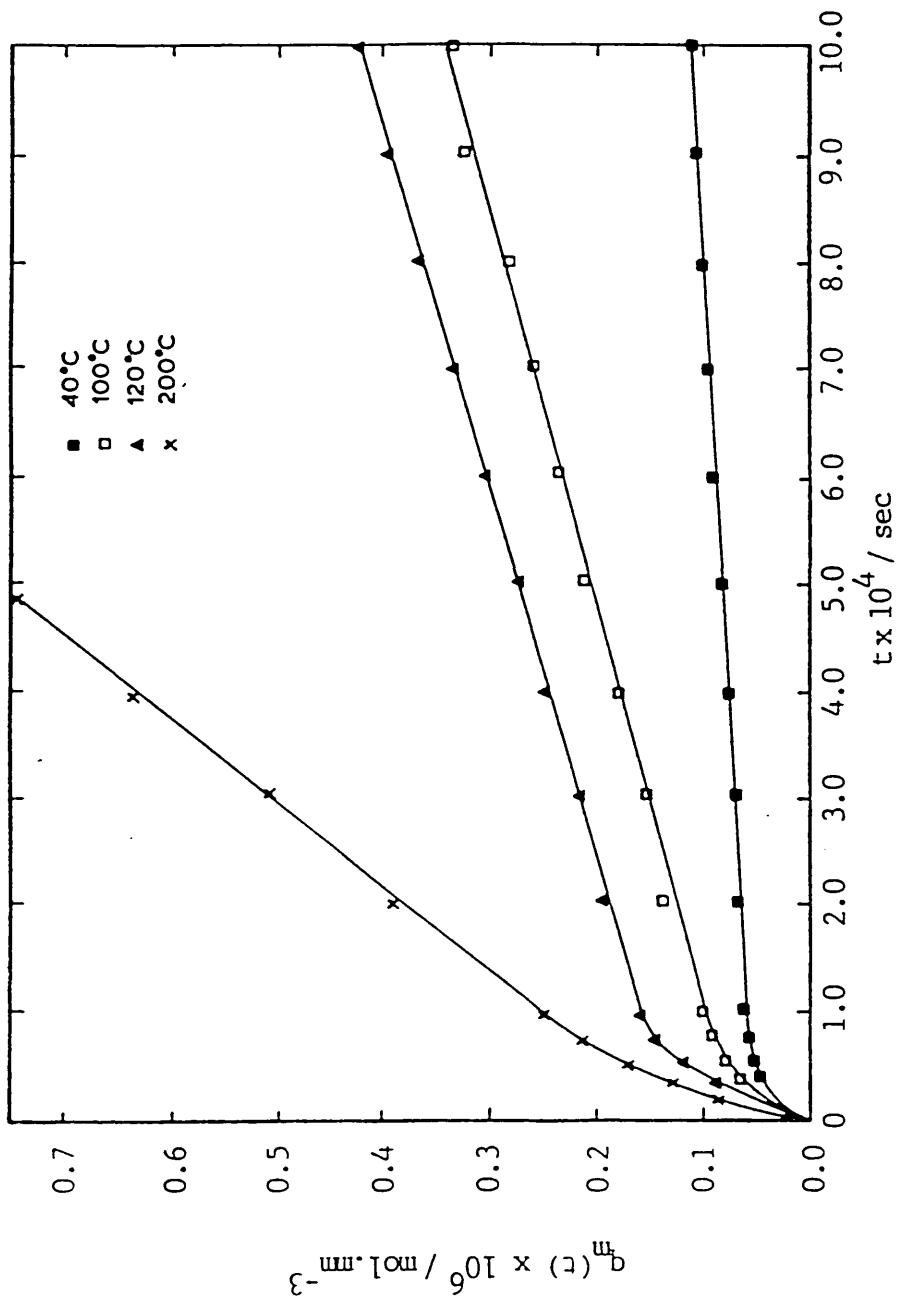


Fig 6.5.1.2. Variation in the number of main chain scissions per unit volume with time occurring in PDMS elastomer during γ -irradiation at various temperatures. ($N_{cr_m}(0) = 0.118 \times 10^{-6} \text{ mol.mm}^{-3}$.)

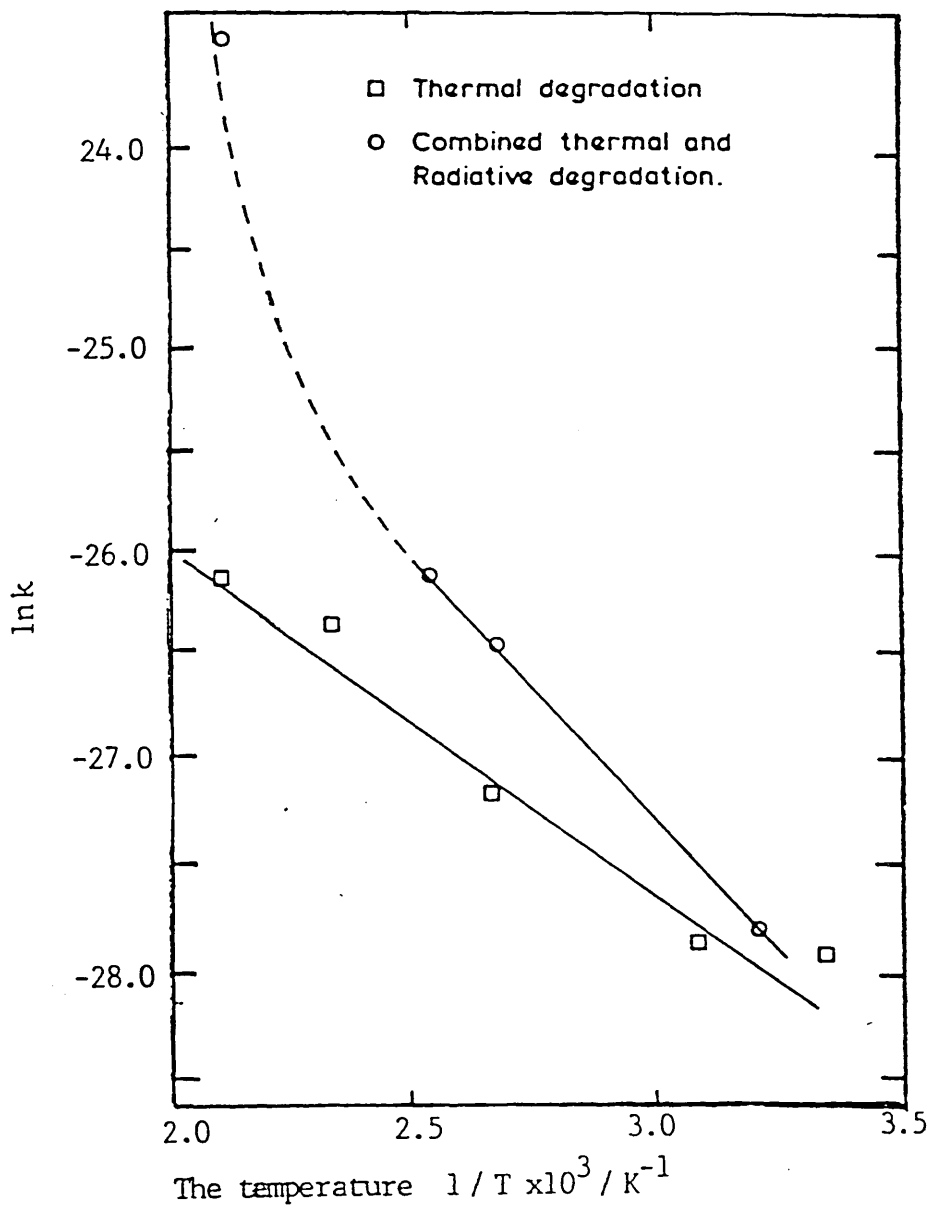


Fig 6.5.1.3. The temperature dependence of the chain scission rate observed in PDMS elastomer during γ -irradiation. ($N_{cr_m}(0) = 0.118 \times 10^{-6} \text{ mol. mm}^{-3}$.)

* data of Fig 6.4.1.5. is included for comparison

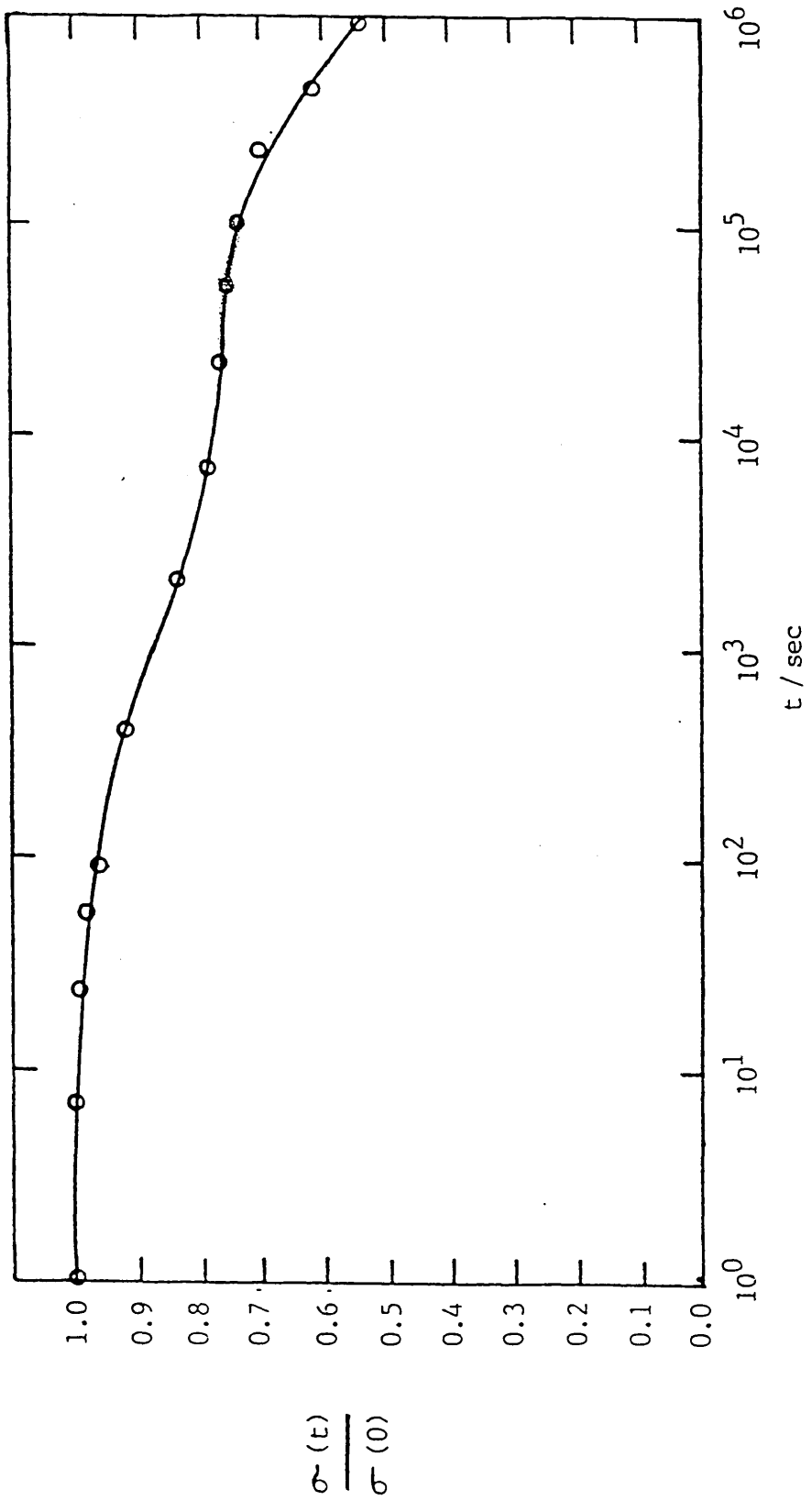


Fig 6.5.2.1. Stress relaxation of Viton E60-C elastomer during γ -irradiation at 40°C.

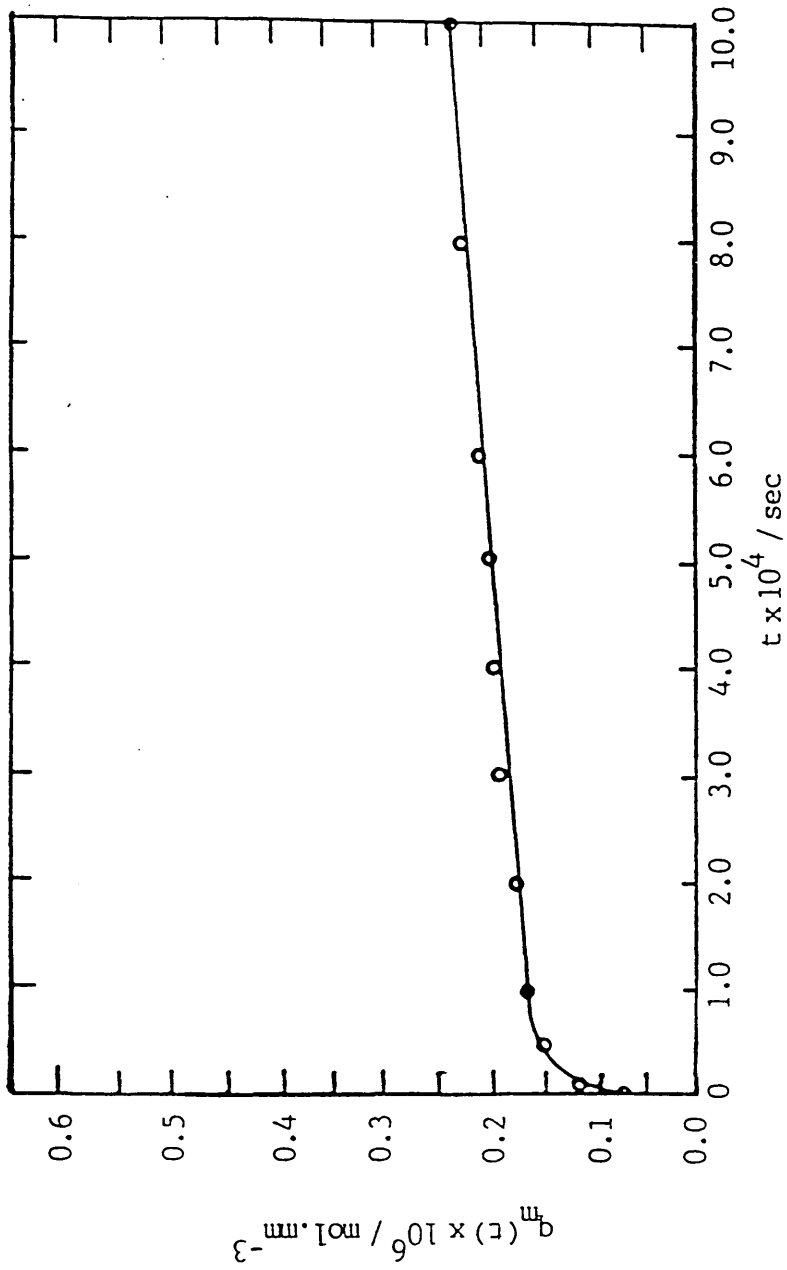


Fig 6.5.2.2. Variation in the number of main chain scissions per unit volume with time occurring in Viton E60-C elastomer during γ -irradiation at 40°C.

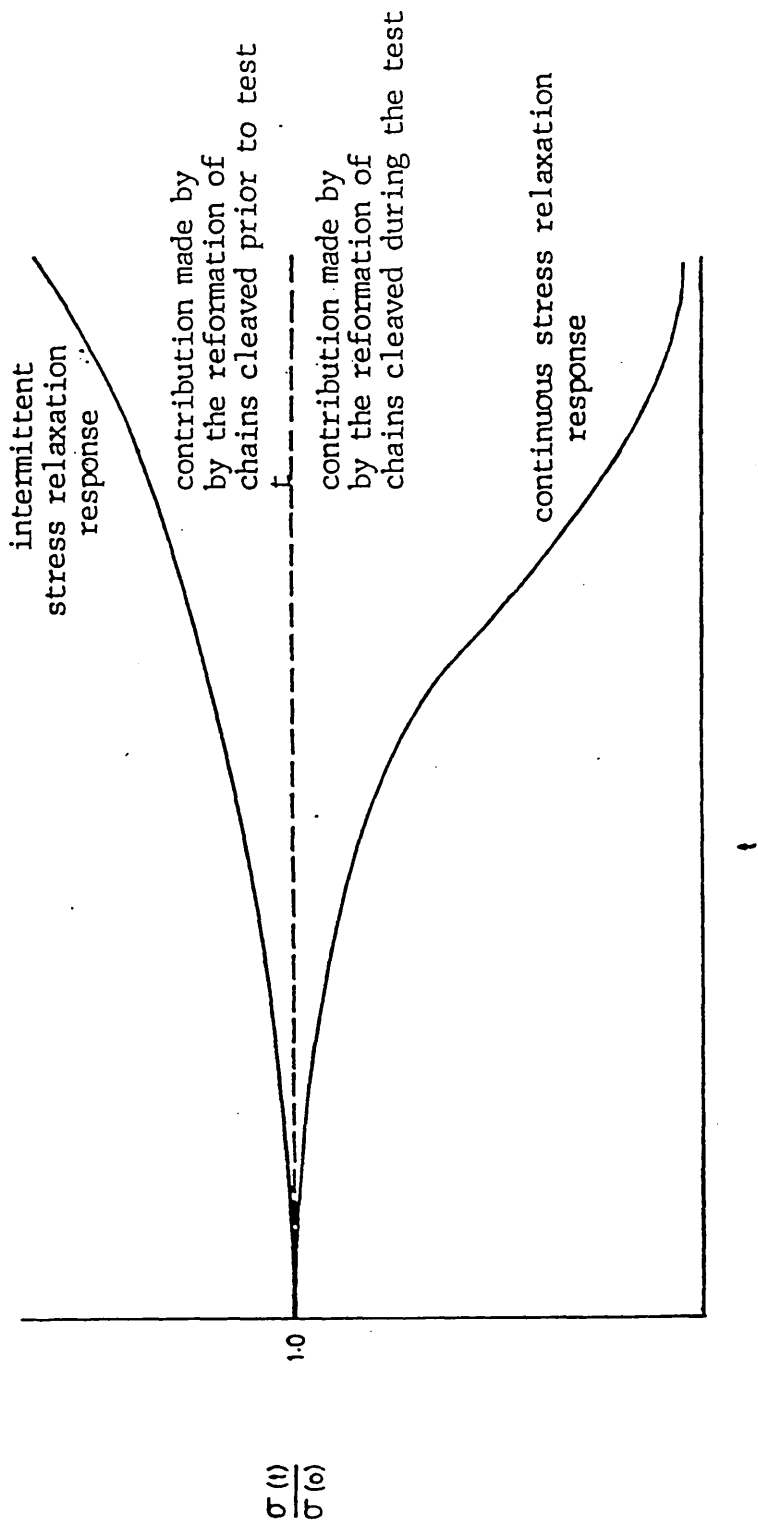


Fig 7.4.1.1. Representation of the model used to rationalise the observed chain reformation response encountered during the thermal degradation of polydimethylsiloxane elastomer.

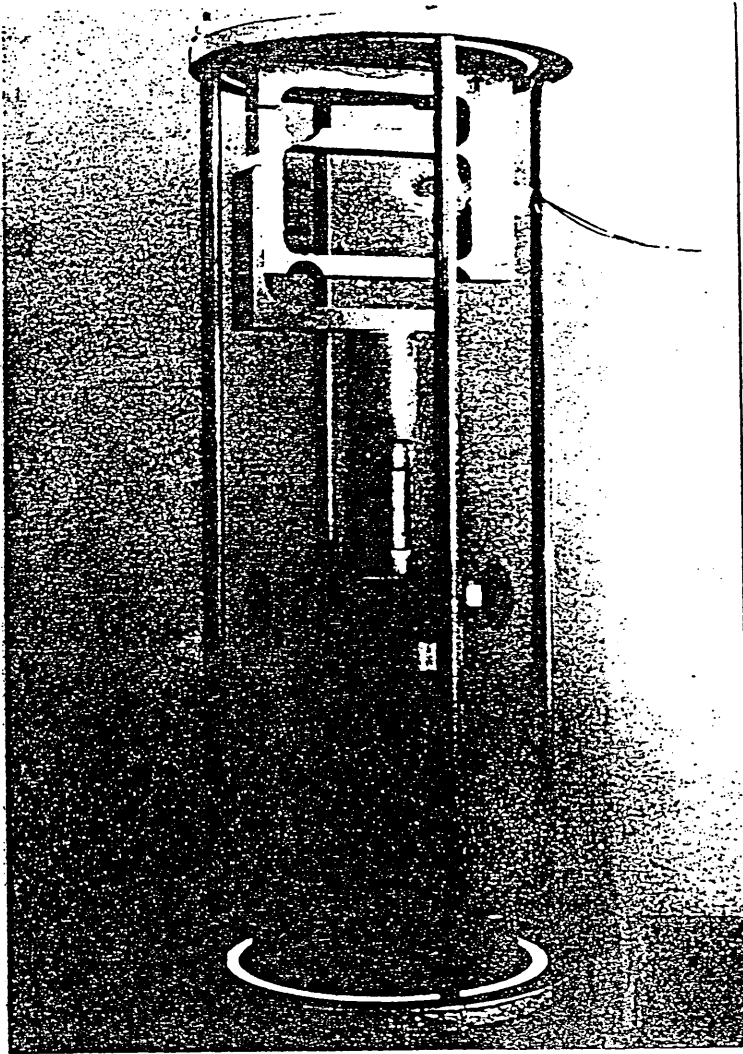


Plate 5.1. Stress relaxation rig employed in the thermal / radiative degradation studies.

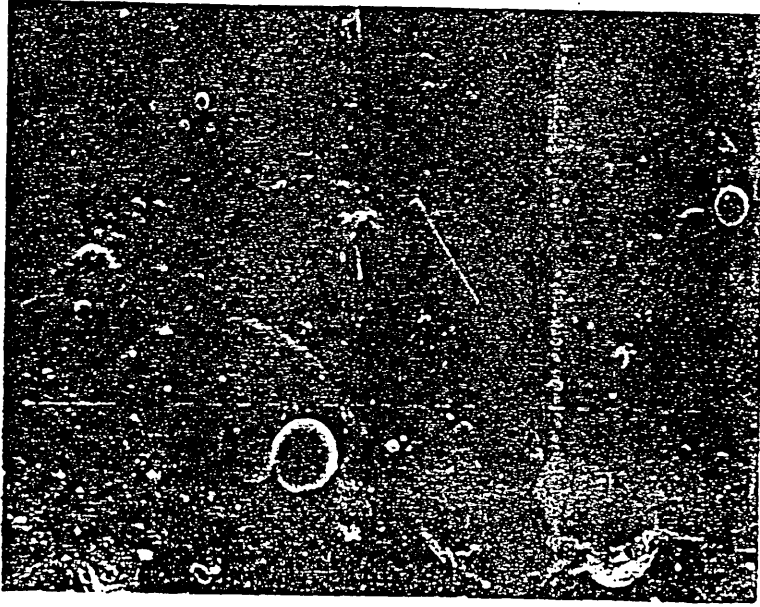


Plate 6.2.1. Scanning electron micrograph of the fracture surface of a polydimethylsiloxane elastomer containing 1.0wt% polystyrene. (X400)

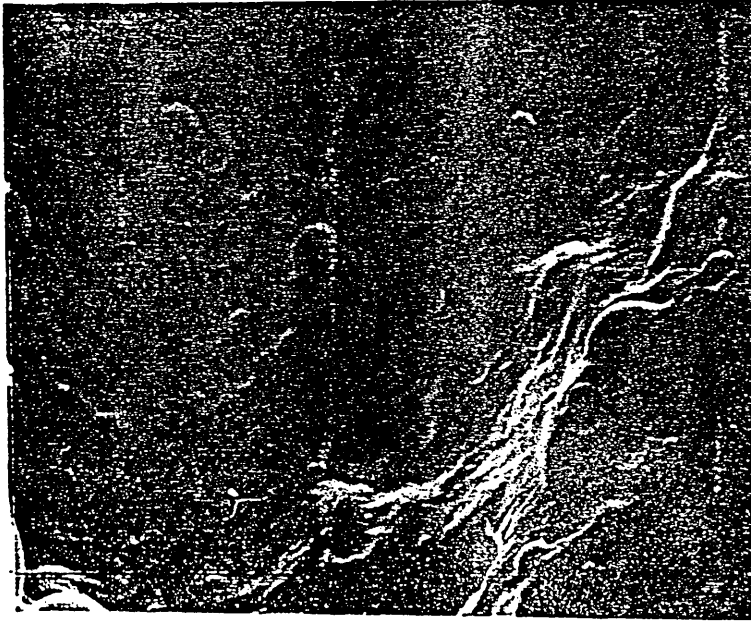


Plate 6.2.2. Scanning electron micrograph of the fracture surface of a polydimethylsiloxane elastomer containing 2.0wt% polystyrene. (X800)

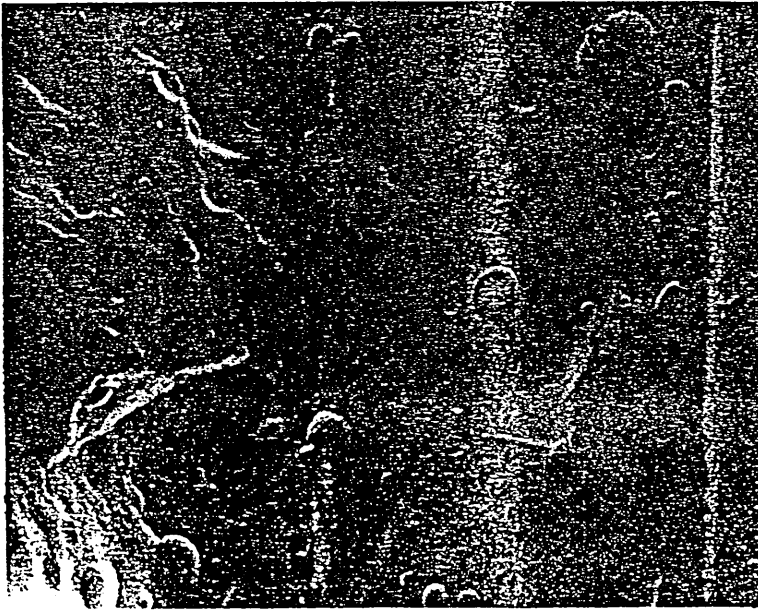


Plate 6.2.3. Scanning electron micrograph of the fracture surface of a polydimethylsiloxane elastomer containing 3.0wt% polystyrene. (X800)

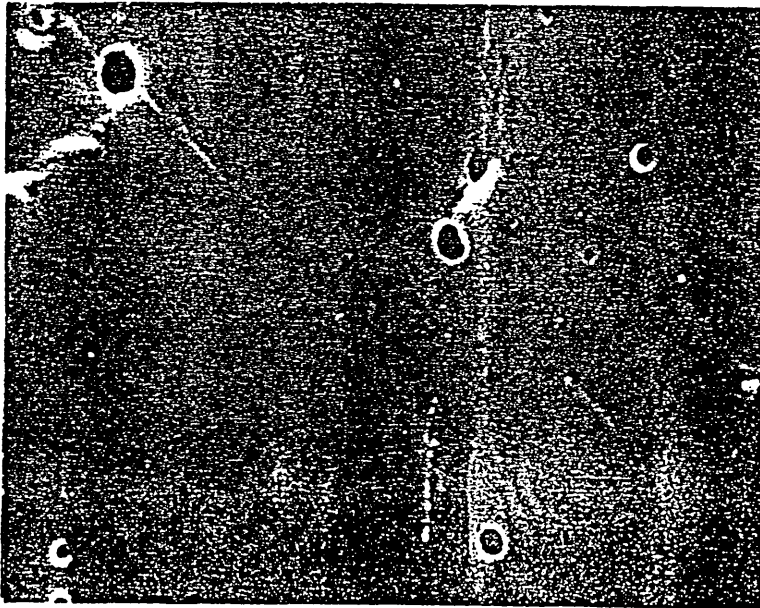


Plate 6.2.4. Scanning electron micrograph of the fracture surface of a polydimethylsiloxane elastomer containing 1.0wt% polystyrene after immersion in toluene for a period of 24 hours. (X400)